

Austrian Journal of Forest Science

Centralblatt
für das gesamte
Forstwesen

Geleitet von
P. Mayer und H. Hasenauer
Gegründet 1875



137. Jahrgang ♦ Heft 2 ♦ 2020
Seite 69–162

 AV-Medien
Der Lebensverlag.

Austrian Journal of Forest Science

Centralblatt
für das gesamte
Forstwesen

Gegründet im Jahre 1875
von den Forstinstituten der Universität
für Bodenkultur (BOKU) und des
Bundesforschungs- und Ausbildungszentrum
für Wald, Naturgefahren und Landschaft (BFW)

Ziel: Das Centralblatt für das gesamte Forstwesen veröffentlicht wissenschaftliche Arbeiten aus den Bereichen Wald- und Holzwissenschaften, Umwelt und Naturschutz, sowie der Waldökosystemforschung. Die Zeitschrift versteht sich als Bindeglied von Wissenschaftlern, Forstleuten und politischen Entscheidungsträgern. Daher sind wir auch gerne bereit, Überblicksbeiträge sowie Ergebnisse von Fallbeispielen sowie Sonderausgaben zu bestimmten aktuellen Themen zu veröffentlichen. Englische Beiträge sind grundsätzlich erwünscht. Jeder Beitrag geht durch ein international übliches Begutachtungsverfahren.

Aims and scope: The Austrian Journal of Forest Science publishes scientific papers related to forest and wood science, environmental science, natural protections as well as forest ecosystem research. An important scope of the journal is to bridge the gap between scientists, forest managers and policy decision makers. We are also interested in discussion papers, results of specific field studies and the publishing of special issues dealing with specific subjects. We are pleased to accept papers in both German and English. Every published article is peer-reviewed.

Herausgeber:

DI Dr. Peter Mayer
Bundesforschungs- und
Ausbildungszentrum für Wald, Na-
turgefahren und Landschaft (BFW)
Seckendorff-Gudent-Weg 8
A-1131 Wien

Editor-in-Chief:

Univ.-Prof. Dr. Hubert
Hasenauer
Institut für Waldbau
Universität für Bodenkultur
Peter-Jordan-Straße 82
A-1190 Wien

Managing Editor:

DI Dr. Mathias Neumann
Institut für Waldbau
Universität für Bodenkultur
Peter-Jordan-Straße 82
A-1190 Wien

Gründungsherausgeber: Rudolf Micklitz, 1875

Wissenschaftlicher Beirat:

Hrovje Marjanovic
Miglena Zhiyanski
Silvio Schüler

Croatian Forestry Research Institute, Jastrebarsko, Croatia
Forest Research Institute, Bulgarian Academy of Science, Sofia, Bulgaria
Bundesforschungs- und Ausbildungszentrum für Wald, Naturgefahren und
Landschaft (BFW), Vienna, Austria

Michal Zasada
Georg Kindermann:
Martin Braun
Barbara Fussli

Warsaw University of Life Sciences (SGGW), Warsaw, Poland
International Institute of Applied Systems Analysis (IIASA), Laxenburg, Austria
Universität für Bodenkultur Wien (BOKU), Wien, Austria
Bayerisches Amt für forstliche Saat- und Pflanzenzucht, Teisendorf, Germany

Internet: <http://www.boku.ac.at/cbl>

Gedruckt mit der Förderung des Bundesministeriums für Bildung, Wissenschaft
und Kultur in Wien.

Austrian Journal of Forest Science

Centralblatt für das gesamte Forstwesen

ORGAN DES DEPARTMENTS FÜR WALD- UND BODENWISSENSCHAFTEN DER UNIVERSITÄT FÜR
BODENKULTUR UND DES BUNDESAMT UND FORSCHUNGSZENTRUM FÜR WALD

Begründet 1875

137. JAHRGANG HEFT 2 April bis Juni 2020 Seite 69–162

Nachdruck, auch auszugsweise, nur mit Genehmigung des Verfassers und des Verlages gestattet.

INHALT DIESES HEFTES

- Paweł Przybylski:** Comparison of two methods for identifying alien genotypes in clonal seed orchards and consequences of misidentification; *Ein Vergleich zweier Methoden zur Identifizierung fremder Genotypen und die Konsequenzen deren Fehlerkennung* 69
- Guoming Qin, Rongsheng Li, Wentao Zou, Niu Yu, Jinchang Yang, Guangtian Yin, Zhihai Wang, Zhaoli Chen:** Estimating Biomass partitioning in *Mytilaria laosensis* Using Additive Models; *Schätzung der Biomasseverteilung in *Mytilaria laosensis* unter Verwendung additiver Modelle* 85
- Yu Zhang, Kangning Xiong, Yao Qin, Yanghua Yu, Tingling Li:** Stoichiometric characteristics of ecological-economic forests in karst rocky desertification areas of southern China; *Stöchiometrische Eigenschaften von verkarsteten Öko-ökonomischen Wäldern in Südchina* 109
- Shes Kanta Bhandari, Bir Bahadur Khanal Chhetri:** Individual-based modelling for predicting height and biomass of juveniles of *Shorea robusta*; *Einzelbaumbasierte Modellierung zur Abschätzung der Höhe und Biomasse von Jungbäumen von *Shorea robusta** 133

ÖSTERREICHISCHER AGRARVERLAG WIEN

Erscheinungsweise: jährlich 4 Hefte,
Jahresbezugspreise inkl. Postgebühr und 10% Mehrwertsteuer im Inland € 259,10, Einzelheft
€ 64,80; im Ausland € 264,20 (exkl. 10% Ust.). Das Abonnement gilt für ein weiteres Jahr als erneuert, falls
nicht 8 Wochen vor Ende des Bezugszeitraumes eine schriftliche Kündigung beim Verlag eintrifft. Alle Rechte
vorbehalten! Nachdruck und fotomechanische Wiedergabe, auch auszugsweise, nur mit Genehmigung des
Verlages; veröffentlichte Texte und Bilder gehen in das Eigentum des Verlages über, es kann daraus kein wie immer
gearteter Anspruch, ausgenommen allfälliger Honorare, abgeleitet werden! Printed in Austria. Die Herausgabe
dieser Zeitschrift erfolgt mit Förderung durch das Bundesministerium für Wissenschaft und Forschung.

Die Offenlegung gemäß §25 Mediengesetz ist unter www.agrarverlag.at/offenlegung ständig abrufbar.

Medieninhaber und Herausgeber:
Österreichischer Agrarverlag, Druck- und Verlagsges.m.b.H. Nfg. KG, Sturzgasse 1a, 1140 Wien.
DVR-Nr. 0024449, HRB-Nr.: FN 150499 y; UID-Nr.: ATU 41409203, ARA: 9890.
Abonnement-Verwaltung: Sturzgasse 1a, 1140 Wien,
Tel. +43 (0) 1/981 77-0, Fax +43 (0)1/981 77-130.
Internet: <http://www.forestscience.at>. Layout: Markus Reithofer.

137. Jahrgang (2020), Heft 2, S. 69-84

**Austrian Journal of
Forest Science**
Centralblatt
für das gesamte
Forstwesen

Comparison of two methods for identifying alien genotypes in clonal seed orchards and consequences of misidentification

Ein Vergleich zweier Methoden zur Identifizierung fremder Genotypen und die Konsequenzen deren Fehlerkennung

Paweł Przybylski*

Keywords: *Breeding, Pinus sylvestris, seed orchard, molecular markers, genetic improvement*

Schlüsselbegriffe: *Züchtung, Pinus sylvestris, Samenplantage, molekulare Marker, genetische Verbesserung*

Abstract

Genetic gains in forestry are often implemented by producing improved forest seeds in seed orchards. However, unwanted alien genotypes are often accidentally introduced into seed orchards, or genotypes are planted in incorrect locations, both of which can reduce genetic gains. Such errors can be detected using markers, mainly isoenzymatic proteins and microsatellite DNA. These markers differ in their sensitivity, meaning that they can yield different assessments of seed orchard genetic material even when plant material is identical. The main objective of this paper was to compare these two verification methods and their consequences for genetic improvement. Two uneven-aged Scots pine clonal seed orchards were analysed using sets of isoenzymatic and microsatellite loci identified in other studies. The statistical analysis allowed comparison of the actual architecture of seed orchards to the planned layout. The number of clones was also compared to the effective number of clones.

¹ Forest Research Institute, Department of Silviculture and Forest Tree Genetics.

*Corresponding author: Paweł Przybylski, p.przybylski@ibles.waw.pl

The results of microsatellite DNA analysis indicate that misplaced ramets are present from 12.29% to 30.89% of the time. Errors had an impact on breeding efficiency by reducing the relative effective number of clones. Isoenzyme and microsatellite methods had different discriminatory powers, which affected the results of the study. This study indicates that seed orchards can contain large numbers of incorrectly identified individuals. Microsatellite DNA analysis is recommended over isoenzyme analysis for detecting such errors, as the former is a more sensitive analytical method.

Zusammenfassung

Der Züchtungsfortschritt im Forstwesen wird meistens durch die Verwendung von verbessertem Material aus Samenplantagen erreicht. Züchtungsprogramme der Forstbäume führen in der Praxis oft zum Auftreten fremder Genotypen in Samenplantagen, welche den Erfolg des Züchtungsfortschritts reduzieren. Molekulare Marker wie Isoenzyme und DNA-Mikrostelliten eignen sich, um solche Fehler festzustellen. Diese Methoden unterscheiden sich hinsichtlich ihrer Genauigkeit des Ergebnisses. Daher ist es möglich, für identisches Pflanzenmaterial zu unterschiedlichen Ergebnissen zu kommen. Der Vergleich dieser Überprüfungsmethoden und die Konsequenzen der getroffenen Entscheidung ist das Ziel dieser Arbeit. Die Analysen wurden auf zwei nicht-gleichaltrigen Klonsamenplantagen unter Anwendung von Isoenzym- sowie Mikrostellitenmarkersets durchgeführt. Eine statistische Analyse ist erfolgt. Sie ermöglichte sowohl den Vergleich zwischen dem Plan und der tatsächlichen Anordnung der Klone als auch eine Schätzung der effektiven Anzahl der Klone. Die Ergebnisse basierend auf Mikrostellitenmarkern beweisen das Auftreten von fremden Genotypen in einer Häufigkeit zwischen 12.29 % und 30.89 %. Die Fehler beeinflussten die Züchtungseffizienz negativ dadurch, dass die effektive Anzahl der Klone reduziert war. Unterschiede bei der Aussagekraft der beiden Ansätze hatten einen Einfluss auf die Ergebnisse. Die vorliegende Studie unterstreicht den Nutzen von Klontifikationsanalysen in Samenplantagen. Es empfiehlt sich, auf Mikrostelliten-DNS als die sensitivere analytische Methode zurückzugreifen.

Introduction

Modern forest management can benefit from advances in scientific knowledge, everywhere from seed production to felling technology. In many countries, seed production is based on forest tree breeding. In practice, this means that seeds obtained from clonal seed orchards account for an increased share of the seeds used in forest regeneration (Przybylski et al. 2015). Gains from forest tree breeding are based on phenotypic selection of forest trees displaying desirable traits. Clones of selected individuals are then reproduced within seed orchards (Chałupka et al. 2011). For maximum genetic gains, it is necessary to avoid errors when establishing orchards, because mistakes cause undesirable genotypes to be present in an orchard's genetic pool (Kaya & Isik 2009). Genotypes not from a plus tree ramet may be accidentally introduced into clonal seed orchards, displacing a plus tree from the gene pool of

the orchard. This phenomenon was mentioned by Paule (1991), Burczyk et al. (2000), Gömöry et al. (2003) and Kaya & Isik (2009). Two categories of errors in Polish seed orchard establishment were described by Odrzykoski (2007). Category I errors are caused by mistakes in the spatial architecture of the seed orchard, due to planting ramets in the wrong place but using clones that are a part of the seed orchard design. Category II errors arise from misidentification, which place individuals that are not part of the breeding population into the orchard (Odrzykoski 2007).

Detection of alien genotypes in seed orchards can be done using molecular markers, which help identify planting errors. Markers can be divided into three groups: morphological markers, biochemical markers and DNA markers (Dzialuk and Burczyk, 2001). This paper focuses on the use of biochemical and DNA markers.

Until recently, the analysis of morphological features was the primary method of describing tree population genetic variability. However, plant phenotype is of limited value because morphological variability among genotypes can be low and the number of useful phenotypic features is limited. Therefore, the probability of committing an error using morphological markers is high. In addition, determining the inheritance of traits and environmental effects on overall morphological variability is not possible, and therefore morphological features are of limited value beyond the initial stages of clone identification (Dzialuk and Burczyk, 2001).

The application of biochemical marker analyses was a breakthrough in population genetics. These approaches were used by a number of researchers investigating graft errors in seed orchards, such as Breitenbach-Dorfer et al. (1992), Burczyk et al. (2000), Gömöry et al. (2003), and Przybylski et al. (2019). One of the newer techniques for identifying individuals is microsatellite DNA markers (Simple Sequence Repeats; SSR), used in criminal trials for alleged theft of wood (White et al. 2000). They are widely used in affinity relatedness and to obtain unique genetic profiles to identify individuals (Burczyk 2006; Dzialuk, 2009). Unfortunately, SSR markers have some disadvantages, such as the presence of null alleles and high costs of testing.

Comparative tests using molecular markers involve developing a set of markers that will provide the maximum chance to detect differences between genotypes, with minimal financial outlay. In the human population, the discriminatory power of an 11 SSR marker set reaches 0.949156 (94.91%), which is accepted for identification of individuals in cases of criminology and contested paternity (Konarzewska et al. 2006). The highest discriminatory power of DNA markers obtained in tests reach 0.99999 (99.99%) (Wysocka et al. 2008). Recent studies of plant populations have achieved high discriminatory power using SSR markers (de Barba et al. 2016).

A review of literature showed that two biochemical testing tools, isoenzymatic markers and microsatellite DNA, may be used to verify seed orchard identities. However, these methods differ in discriminatory power. The main objective of the present

study was, therefore, to evaluate the discriminatory power of systems based on isoenzymatic proteins and DNA and to evaluate the consequences of applying these methods on estimates of breeding efficiency.

Methods

Plant material

The study consisted of the molecular verification of individuals in two scots pine clonal seed orchards. The Susz District seed orchard (N53°45'21", E19°12'16") was established in 1977-1978 and Pniewy District seed orchard (N52°30'32", E16°15'24") was established in 1993 (Figure 1). These are first generation seed orchards, and as a result the genetic value (breeding value) of cloned plus trees planted in these orchards is unknown. In the Susz seed orchard, 9 838 ramets were planted from 50 plus tree clones, and in Pniewy, 1 733 ramets were planted from clones of 53 plus trees. Material from 138 ramets at Susz and 131 ramets at Pniewy was collected for molecular analyses. Samples were collected from two blocks within each analysed seed orchard from all trees that remained after the most recent systematic thinning.

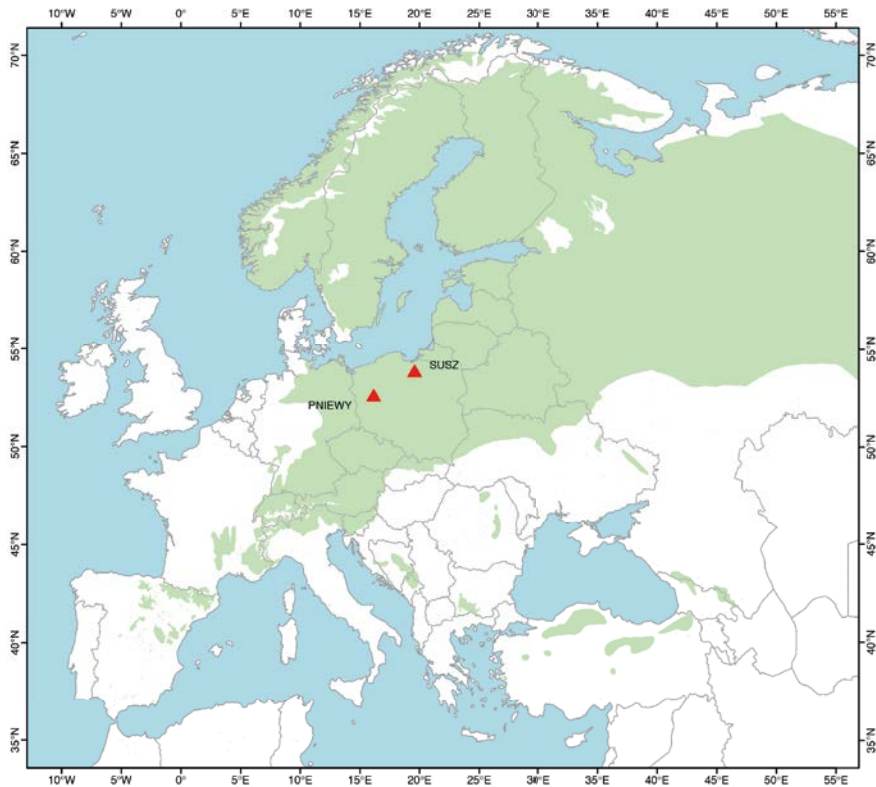


Figure 1: *Pinus sylvestris* (L.) occurrence range (source IUFRO) and location analyzed seed orchards in Poland.

Abbildung 1: Vorkommensbereich von *Pinus sylvestris* (L.) (Quelle IUFRO) und Lage der untersuchten Samenplantagen in Polen.

The reference samples for the Susz seed orchards came from the original parental plus trees. When it was not possible to collect reference material in this way, because plus trees were dead, a repeated set of 4 ramets from the tested seed orchard constituted the reference sample. For the Pniewy orchard, the reference samples were obtained from a clonal archive outside of the seed orchard.

Genotype analysis

Isoenzymatic proteins (IZO)

Variation was examined in eight enzymatic proteins (Table 1) extracted separately

from winter buds. Protein extraction was conducted using a 150- μ l extraction buffer (Odrzykoski, 2002). After filtering through Miracloth filter paper, the resulting solutions were used to moisten pieces of Whatman 3ET filter paper, which were subsequently placed onto electrophoresis gel. Using two buffer systems (Odrzykoski, 2007), the electrophoresis was conducted in 13% starch gel (Starch-Art). Following electrophoresis, gels were cut into 1.5-mm slices, which were individually used to visualise the phenotype of the analysed proteins. Location of individual bands was determined using the methods of Conkle et al. (1982), with a modification comprising the use of an overlay procedure with 2% agar, excluding *EstB* and *Got*. Identification of the loci and interpretation of the obtained zymograms were carried out using the approach described by Odrzykoski (2002).

Table 1: List of buffer systems (A, C), enzymes with European Community numbers (E.C.), and enzyme loci used in this study.

Tabelle 1: Liste der Puffersysteme (A, C), Enzyme (mit E.C. Nummern) und Enzymort, die in dieser Studie verwendet wurden.

System	Enzyme	No. E.C.	Locus
A	Esterase	3.1.1.2	<i>EstB</i>
	Glutamate-oxaloacetate transaminase	2.6.1.1	<i>GotA</i>
			<i>GotB</i>
			<i>GotC</i>
NADH-diaphorase	1.8.1.4	<i>DiaC</i>	
Glutamate dehydrogenase	1.4.1.2	<i>Gdh</i>	
C	6-phosphogluconate dehydrogenase	1.1.1.44	<i>PgdA</i>
	Shikimate dehydrogenase	1.1.1.25	<i>SdhA</i>
			<i>SdhB</i>
	NAD-dependent malate dehydrogenase	1.1.1.37	<i>MdhA</i>
<i>MdhC</i>			
Alcohol dehydrogenase	1.1.1.1	<i>AdhA</i>	
		<i>AdhB</i>	

Microsatellite DNA (SSR)

DNA was isolated with a commercially available set of microsatellite markers (Marchel-Nagel – Nucleo Spin Plant II) after extraction from 3-4 needles from each graft. Needles were ground in a mortar using liquid nitrogen, until obtaining about 20 mg

of dry powdered mass. The yield of DNA extracted for each sample was evaluated by measuring absorbance at wavelengths of 260 and 280 nm. (Quawell Q500). An average absorbance for wavelengths of 260/280 nm was 1.80, at which the samples produced 80 ng DNA/ μ l, which was diluted to 20 ng DNA/ μ l. Four microsatellite loci were used in testing: Spac11.6, Spag7.14 (Soranzo et al. 1998), and PtTX3107, PtTX4001 (Elsik and Williams 2001), which differ in the type of repeating motif and the length of alleles. A multiplex PCR was used for loci Spac11.6, PtTX3107 and PtTX4001. A separate reaction was used for locus Spag7.14. In all cases, reactions were performed with 25 μ l of a solution composed of ultrapure water, Taq DNA polymerase (0.1 U/ μ l), MgCl₂ (4mM), dNTPs (0.5mM), primers and matrix DNA. The optimised thermal profile of the reaction is provided in Table 2. For locus Spac11.6, the touchdown PCR method was used (Balletti et al. 2012). The mixture of all PCR products was separated in a Beckman Coulter sequencer, in the polymer LPA I, using the Frag I length standard (as recommended by the manufacturer). The results obtained were analysed with CEQ™800 software, which provided chromatograms that then were used to determine the lengths of individual alleles.

Table 2: Thermal profile of PCR used in this study.

Tabelle 2: Thermisches Profil der verwendeten PCR.

Step	Temperature (°C)	Time (minutes)	
First denaturation	94	5	
Denaturation	92	1	40 cycle's
Annealing	58 - 60	1	
Elongation	72	1	
Finish elongation	70	7	

Deficiency of heterozygotes may prove the presence of null alleles, which may not be detected in the sample directly. Therefore, an analysis was carried out to determine their presence and frequency, using the methods of Chakraborty et al. (1992), Brookfield (1996) and van Oosterhout et al. (2004). Analyses were performed by Micro Checker v2.2.3. (van Oosterhout et al. 2004).

Statistical analyses

To determine the discrimination power of the clonal verification system, the cumulative probability of obtaining identical genotypes (P_{ID}) for two different clones was calculated as:

$$P_{ID} = 2 ((\sum p_i^2)^2 - \sum p_i^4)$$

where p_i = the mean allele frequency (i^{th} alleles) in the sample of grafts from the two tested seed orchards combined (Taberlet & Luikart, 1999). Calculations were performed using GeneAEx 6.5 software (Peakall & Smouse, 2006). The genotypes obtained were used to estimate the rates of category I and II errors in seed orchards. In order to assess the impact of errors on genetic variability, the actual composition of genotypes and their spatial arrangement (W_1) was compared with the originally designed seed orchard population (W_0). For W_0 , it is assumed that no errors were made and all ramets were planted as specified in the planting plan. For both W_0 and W_1 , the effective numbers of clones (N_c) was calculated based on Kang & Lindgren (1999) and Kang et al. (2001):

$$N_c = \frac{Ng}{\left(\frac{CV\%}{100}\right)^2 + 1}$$

where: Ng = corrected census number of genotypes after molecular verification and $CV\%$ = coefficient of variation for the number of ramets. The relative effective number of clones was calculated as $N_r = N_c/N$ (Kang et al. 2001).

Results

Null alleles were not relevant for the interpretation of the results. Based on the data obtained, null alleles were proven to be present for the locus Spac11.6 in Susz and for loci PtTX3107 and Spag7.14 in Pniewy. The null allele frequency ranged from 0.09 to 0.14 (Table 3).

Table 3: Seed orchards and loci, in which null alleles were detected using Micro Checker software. Allele frequency was estimated by four software methods: p1 – Chakraborty et al. (1992), p2 – Brookfield (1996), p3 – modified Brookfield method (1996), and p4 – Oosterhout et al. (2004).

Tabelle 3: Samenplantagen und Enzymort (Locus), in denen mit der Micro-Checker-Software Null-Allele nachgewiesen wurden. Die Allelfrequenz wurde mit vier Softwaremethoden geschätzt: p1 – Chaakraborty et al. (1992), p2 – Brookfield (1996), p3 – modifizierte Brookfield-Methode (1996) und p4 – Oosterhout et al. (2004).

Seed orchards	Locus	p1	p2	p3	p4	Means
Susz	Spac 11.6	0.11	0.09	0.07	0.09	0.09
Pniewy	PtTX3107	0.13	0.17	0.13	0.12	0.14
Pniewy	Spag7.14	0.09	0.10	0.07	0.08	0.09

The discriminatory power of markers varied. Using four microsatellite DNA loci, discriminatory power was 4×10^{-6} , while the use of thirteen isoenzymatic loci resulted in a sensitivity of 8×10^{-5} , which is one order of magnitude less (Table 4). It should be noted that any of the proposed marker systems can be used to verify identity in clonal seed orchards.

Table 4: Comparison of the individual and accumulated probability of obtaining identical genotypes (P_{ID}) for unrelated ramets in clones from two seed orchards combined. Loci were added in the order given in column one.

Tabelle 4: Vergleich der individuellen und kumulativen Wahrscheinlichkeit, um identische Genotypen (P_{ID}) für nicht verwandte Ramete in Klonen aus zwei kombinierten Samenplantagen zu erhalten. Loci wurden in der angegebenen Reihenfolge hinzugefügt.

Locus	Loci SSR	P_{ID} (by locus)	P_{ID} (locus combination)	Loci IZO 13	P_{ID} (by locus)	P_{ID} (locus combination)
1	Spac11.6	0.46	0.46	EstB	0.41	0.41
2	PtTX3107	0.03	0.01	PgdB	0.39	0.1637
3	PtTX4001	0.06	0.0009	SdhA	0.52	0.0858
4	Spac7.14	0.005	0.000004	SdhB	0.82	0.0708
5				MdhA	0.82	0.0581
6				MdhC	0.41	0.0238
7				Gdh	0.39	0.0093
8				DiaC	0.54	0.0051
9				GotA	0.91	0.0047
10				GotB	0.31	0.0014
11				GotC	0.37	0.005
12				AdhA	0.41	0.0002
13				AdhB	0.38	0.00008

The presence of category I and category II errors was proven in both seed orchards. The error rates differed depending on verification method. A category II error was found using SSR, while the IZO verification system for the same ramets either did not detect an error or indicated a category I error. The SSR and IZO methods gave

different results for 11 ramets from the Susz seed orchard and for 3 ramets from the Pniewy seed orchard. In addition, for SSR analyses, due to the poor quality of extracted DNA, genotype was not determined for 15 ramets from Susz and 9 ramets from Pniewy. Due to differences between analytical methods, the error rate in seed orchards is interpreted as a percentage ratio between false ramets and all ramets analysed in a seed orchard. A detailed summary of false ramets is given in Table 5. On the basis of IZO, the category I error rate ranged from 10.69% in the Pniewy orchard to 13.04% in Susz orchard. For SSR analyses, category I error rate was 5.69% in Susz and 8.20% in Pniewy. The number of category II errors for IZO ranged from 9.16% in the Pniewy orchard to 24.64% in Susz and for SSR it ranged from 12.29% in Pniewy to 30.89% in Susz.

Table 5: Summary information on the two seed orchards used in this study, and the number of ramets that were in correct and incorrect locations and that were alien genotypes.

Tabelle 5: Informationen zu den beiden Samenplantagen dieser Studie, die Anzahl der Rameten, die richtig bzw. falsch lokalisiert wurde sowie die fremden Genotypen.

	Susz	Pniewy
Year of establishment	1977-78	1993
Number of clones	50	53
Number of ramets in seed orchards	9 838	1 733
Number of studied ramets	138 IZO 123 SSR	131 IZO 122 SSR
Number of correctly located ramets	86 IZO 78 SSR	105 IZO 97 SSR
Number of incorrectly located ramets – Category I error	18 IZO 7 SSR	14 IZO 10 SSR
Number of ramets of alien genotypes – Category II error	34 IZO 38 SSR	12 IZO 15 SSR

Error rates affected seed orchard parameters. The results showed that the planned number of genotypes was lower than the actual number of genotypes in orchards, where the latter increased from 10 to 13 genotypes per orchard for SSR analyses (Table 6). This indicates an average increase in the number of orchard genotypes by 0.22. The SSR method allowed reporting of the increased number of additional genotypes, with 1 to 3 additional genotypes, depending on orchard (Table 6). Additional genotypes affected the effective and relative effective number of clones. In summary, in

each case, alien genotypes decreased the relative effective number of clones, from 0.14 for the Susz seed orchard to 0.04 for Pniewy using SSR analyses (Table 6).

Table 6: Corrected number of genotypes after molecular verification (N_g), the mean number of ramets per genotype (N_{sg}) and effective (N_c) and relative effective (N_r) number of clones in seed orchards. Results show in two variants analysis: W0, originally planned composition of the seed orchards; W1, both seed orchards after molecular verification.

Tabelle 6: Korrigierte Anzahl der Genotypen nach molekularer Identifikation (N_g), mittlere Anzahl der Rameten pro Genotyp (N_{sg}) sowie effektive (N_c) und relative effektive Anzahl (N_r) der Klone in den Samenplantagen: W0, ursprünglich geplante Zusammensetzung der Samenplantagen; W1, beide Samenplantagen nach molekularer Identifikation.

	Susz		Pniewy	
SSR	W0	W1	W0	W1
N_g	50	60	53	66
N_{sg}	2.46	2,05	2,30	1,85
N_c	38.12	43.28	42.88	51.42
N_r	0.86	0.72	0.81	0.77
IZO	W0	W1	W0	W1
N_g	50	57	53	65
N_{sg}	2.76	2.42	2.47	2.01
N_c	43.28	41.13	44.81	50.92
N_r	0.87	0.72	0.84	0.78

Discussion

In most clonal seed orchards that have been verified, errors involving incorrect graft assignment were identified (Burczyk et al. 2000, Działuk 2009, Gömöry et al. 2003). Alien genotypes are introduced when errors occur during the complex procedures of establishment and maintenance of seed orchards. Errors have various causes, but since they are all due to human mistakes, with care they can be eliminated. The main causes of errors include: misidentification when collecting plant material; errors made during work in a forest nursery; poor legibility of labels or label removal during ramet transport; errors when manually copying seed orchard designs; and cases where the rootstock outgrows the scion. It appears that errors during the establishment of orchards are not large (Suchowera and Chelmiński 2009). Regardless of the cause of an error, the impact of each type of error is different. Category I errors do not alter

the gene pool of a seed orchard. However, they can increase the risk of self-pollination. In contrast, Category II errors modify the gene pool by introducing alien pollen, which reduces breeding efficiency (Kaya et al. 2006). Alien genotypes may also modify the basic genetic characteristics of seed orchards, influencing heterozygosity and introducing unwanted alleles into the gene pool of seed orchard progeny (Stoehr et al. 2004).

The discriminatory power of a microsatellite DNA marker set can be evaluated by calculating the probability that two different individuals in a population have identical genotypes (P_{ID}) for the marker set. Dzialuk and Burczyk (2005) used P_{ID} to evaluate the discriminatory power of a set of 7 microsatellite loci (5 chloroplast loci and 2 nuclear loci), which can be used to identify stolen trees. A probability of P_{ID} from 10^{-3} to 10^{-4} is usually accepted as sufficient to identify individuals (Waits et al., 2001). Similar values could be adopted to identify Scots pine plus trees in Poland. The calculation of P_{ID} requires data on allele frequency in a reference population. Where ramets are identified in seed orchards, a reference population should consist of all Scots pine plus trees. Unfortunately, no such data exist for loci used in the present study. For the current analysis, material from 245 Scots pine plus trees was available. Polish populations of Scots pine are distinctive, with low interpopulation diversity, as determined using microsatellite loci, with $F_{ST} = 0.033$ (Nowakowska, 2007). This feature is common in various *Pinus* species (e.g. Marquardt and Epperson, 2004). Considering this, it can be assumed that allele frequencies in the 245 plus trees in this study provides a reliable estimate of allele frequency in the entire population of Scots pine plus trees in Poland.

An important result obtained here is that the discriminatory power of microsatellite markers is higher than that of isoenzymatic loci. This is consistent with other studies (Cieślewicz 2009). In the present study, a higher value of P_{ID} obtained for microsatellite DNA markers allowed category II errors to be identified, which has not been observed in isoenzymatic analyses. On the other hand, although isoenzymatic analyses are an older analytical technique than molecular biology, their effectiveness in verifying seed orchard identities remains high. The usability of isoenzymatic techniques is confirmed by the values of P_{ID} obtained using it. Przybylski et al. (2019) found P_{ID} of 0.0001, while Dzialuk & Burczyk (2005) report a P_{ID} of 0.004. Thus, given there are around 3,650 plus trees in Poland (unpublished data from the Forestry Research Institute), it is possible to assign an individual genotype to each ortet in seed orchards throughout Poland. It should be added that isoenzymatic tests are cheaper than microsatellite DNA analysis, the issue being that many steps in microsatellite cannot yet be automated.

Markers selected in this study were used previously for verification of ramets in seed orchards. Breitenbach-Dorfer et al. (1992), in studying a polymorphism of four enzymatic loci in *Abies alba*, demonstrated the usefulness of these loci for identifying individual clones. Burczyk et al. (2000), in analysing the variability of 14 isoenzymatic

loci, detected errors in the distribution of plus tree grafts in one plot of the Gniewkowo seed orchard. Gömöry et al. (2003) used 12 isoenzymatic loci to verify the identity of clones in three seed orchards, detecting errors of from 27% to 49% in graft assignment. In turn, Lewandowski (2006) describes using eleven isoenzymatic loci to identify grafts in a seed orchard. The analysis of 10 microsatellite loci from chloroplast DNA enabled the identification of erroneously distributed grafts in one plot of a seed orchard in the Gniewkowo forest district (Burczyk et al., 2000). Slavov et al. (2004), using three microsatellite loci, verified 152 ramets representing genotypes of 59 trees in a Douglas spruce orchard.

The presence of alien genotypes should be considered in terms of their effects on genetic gain in clonal seed orchards. Genetic gain refers to the capacity to pass genetic information on to the next generation (Trojankiewicz and Burczyk 2005). One important factor determining the high genetic gain of clonal seed orchards is the uniform distribution of unrelated clones in an orchard, which determines the maximum distance between ramets of the same clone. The lack of quantitative balance and the non-synchronised phenology of flowering between individual clones can lead to mating of related individuals (Burczyk 1998). This study has shown the negative effects of unwanted genotypes on the relative effective number of clones, which was reduced by 0.14. Moreover, errors in identification increased the number of genotypes by 0.22, thus reducing the efficiency of spatial arrangements in seed orchards.

Production seed orchards are created by planting a limited number of individuals. The main purpose of production orchards is to produce seeds that transfer desirable genetic traits to the progeny. For this reason, special attention should be paid to establishing an orchard correctly, arranging it with optimal clone spacing and ensuring a balanced representation of clones. Since errors in establishment of clonal orchards are common, clones in existing orchards should be verified. The best tool for verifying seed orchard clonal identities is microsatellite DNA markers, which possess high discriminatory power. The lower accuracy of isoenzymatic markers, as with morphological markers, makes them more appropriate for earlier stages of verification.

Acknowledgments

This project was funded by the Ministry of Science and Higher Education within the statutory activity of the IBL (240233)

References

- De Barba A., Miquel C., Lobreaux S., Quenette P.Y., Swenson J.E., Taberlet P. 2016. High-throughput microsatellite genotyping in ecology: improved accuracy, efficiency, standardization and success with low-quantity and degraded DNA. *Mol. Ecol.* Vol. 17, Issue 3, pp. 492-507. 10.1111/1755-0998.12594
- Balletti P., Ferrazzini D., Piotti A., Monteleone I., Ducci F. 2012. Genetic variation and di-

- vergence in Scots pine (*Pinus sylvestris* L.) within natural range in Italy. *Eur. J. Forest Res.* 131:1127-1138.
- Breitenbach-Dorfer M., Pinsker W., Hacker R., Müller F. 1992. Clone identification and clinal allozyme variation in populations of *Abies alba* from the eastern Alps (Austria). *Plant System Evolution* 181: 109-120.
- Brookfield J.F.Y. 1996. A simple new method for estimating null alleles frequency from heterozygote deficiency. *Mol. Ecol.* 5: 453-455.
- Burczyk J., Działuk A., Lewandowski A. 2000. Zmienność genetyczna sosny zwyczajnej (*Pinus sylvestris* L.) na klonowej plantacji nasiennej w Gniewkowie. *Sylwan* 2000(4): 65-47.
- Burczyk J. 1998. Mating system variation in a Scots pine clonal seed orchard. *Silvae Genetica* 47: 155-158.
- Burczyk J., Adams W.T., Birkes D.S., Chybicki I.J. 2006. Using genetic markers to directly estimate gene flow and reproductive success parameters in plants based on naturally regenerated seedlings. *Genetics* 173: 363-372.
- Chakraborty R., De Andrade M., Daiger S.P., Budowle B. 1992. Apparent heterozygote deficiencies observed in DNA typing data and their implications in forensic applications. *Annals of Human Genetics* 56: 45-57.
- Chałupka W., Matras J., Barzdajn W., Burczyk J., Tarasiuk S., Sabor S., Kawalczyk J., Fonder W., T. Grądzki, P. Kacprzak, Cz. Kozioł, Z. Rzońca, T. Pytko, Z. Szeląg, Z. Gryzo, S. Blonkowski 2010. Program zachowania leśnych zasobów genowych i hodowli selekcyjnej drzew leśnych w Polsce na lata 2010–2035. CILP, Warszawa, 142 p. ISBN: 978-83-61633-60-0
- Cieślewicz A. 2009. Charakterystyka wybranych loci mikrosatelitarnych u sosny zwyczajnej i ich wykorzystanie do identyfikacji szczepów drzew matecznych. UAM w Poznaniu, maszynopis rozprawy doktorskiej pp. 118.
- Conkle M.T., Hodgskiss P.D., Nunnally L.B., Hunter S. C. 1982. Starch Gel Electrophoresis of Conifer Seeds: a laboratory manual. USDA Forest Service. Pacific Southwest Forest and Range Experimental Station. General Technical Report PSW-64: 18.
- Działuk A., Burczyk J. 2005 Zmiany struktury genetycznej pomiędzy populacją rodzicielską a potomną w drzewostanie nasiennym sosny zwyczajnej (*Pinus sylvestris* L.). *Sylwan* vol. 10:30-38.
- Działuk A. 2009. Zmienność sosny zwyczajnej w: Opracowanie i wdrożenie do praktyki leśnej metod identyfikacji i wczesnej oceny leśnego materiału rozmnożeniowego w oparciu o markery molekularne. Maszynopis, sprawozdanie końcowe.
- Działuk A., Burczyk J. 2001. Molekularne markery DNA jako narzędzie badawcze genetyki drzew leśnych. *Sylwan* 8: 67-83.
- Gömory D., Bruchanik R., Longauer R. 2003. Fertility variation and flowering asynchrony in *Pinus sylvestris*: consequences for the genetic structure of progeny in seed orchards. *Forest Ecology and Management* 174:117-126.
- Kang K., Lindgren D. 1999. Fertility variation among clones of Korean pine (*Pinus koraiensis* S. et Z.) and its implications on seed orchards management. *Forest Genetics* 2: 183–192
- Kang K.S., Harju A.M., Lindgren D., Nikkanen T., Amquist C., (2001): Variation in effective

- population number of clones in seed orchards. *New Forests* 21:17-33.
- Kaya N., Isik K., 2009. Genetic identification of clones and the genetic structure of seed crops in a *Pinus brutia* seed orchard. *Turkish Journal of Agriculture and Forestry*. 34: 127–134.
- Kaya N., Isik K., Adams W. 2006. Mating system and pollen contamination in a *Pinus brutia* seed orchard. *New Forest* 31: 409–416. doi: 10.1007/s11056-005-0876-x.
- Konarzewska M., Spólnicka M., Sołtyzewski I., Berent J. 2006. Polimorfizm *locus* HUM-HUU w populacji polskiej – doniesienie wstępne. *Arch. Med. Sąd. Krym.* LVI: 99-102.
- Lewandowski A. 2006. Wykorzystanie izoenzymów jako markerów genetycznych. W: Sabor J. (red.) *Elementy genetyki i hodowli selekcyjnej drzew leśnych*. CILP 2006: 77-81.
- Marquardt P.E., Epperson B.K. 2004. Spatial and population genetic structure of microsatellites in white pine. *Mol. Ecol.* 13: 3305-3315.
- Nowakowska J.A. 2007. Zmienność genetyczna polskich wybranych populacji sosny zwyczajnej (*Pinus sylvestris* L.) na podstawie analiz polimorfizmu DNA. *Prace IBL, rozprawy i monografie, Sękocin Stary* 2007.
- Odrzykoski I. 2002. Badania nad zmiennością genetyczną kosodrzewiny (*Pinus mugo*) z wykorzystaniem markerów biochemicznych i molekularnych. *Wyd. Nauk. UAM*.
- Odrzykoski I. 2007. Weryfikacja zgodności genetycznej szczepów sosny zwyczajnej na terenie plantacji nasiennej 08-14-3-11-95A-m-00 (PN-34 C1) w Nadleśnictwie Zdrojowa Góra (RDLP Piła). Niepublikowany raport dla Nadleśnictwa Zdrojowa Góra.
- Van Oosterhout C, Hutchinson W.F., Wills D.P.M., Shipley P. 2004. MICRO-CHECKER – software for identifying and correcting genotyping errors in microsatellite data. *Molecular Ecology Notes* 4: 535-538.
- Paule L 1991. Clone identity and contamination in a Scots pine seed orchard. In: *Proceedings of the Meeting of the Nordic Group for Tree Breeding* (Ed. D Lindgren). Swedish University of Agricultural Sciences, Department of Forest Genetics and Plant Physiology Umea 10: 22–32.
- Peakall R., Smouse P. 2006. GENEALX 6: Genetic Analysis in Excel. Population genetic software for teaching and research. *Molecular Ecology Notes* 6: 288-295.
- Przybylski P. 2015. Czy na plantacjach nasiennych zawężamy zmienność genetyczną? Próba odpowiedzi na podstawie analiz mikrosatelitarnego DNA szczepów rosnących na plantacji nasiennej sosny zwyczajnej z Nadleśnictwa Susz. *Leśne Prace Badawcze* 76 (3): 240–249, doi: 10.1515-frp-2015-0023.
- Przybylski P., Kowalczyk J., Odrzykoski I., Matras J. 2019. Identifying alien genotypes and their consequences for genetic variation in clonal seed orchards of *Pinus sylvestris* L. *Dendrobiology* vol 81, 40-46.
- Slavov G.T., Howe G.T., Yakovlev I., Edwards K.J., Krutovskii K.V., Tuskan G.A., Carlson J.E., Strauss S.H., Adams W.T. 2004. Highly variable SSR markers in Douglas-fir: Mendelian inheritance and map locations. *Theor. Appl. Genet.* 108: 873-880.
- Soranzo N., Provan J., Powell W. (1998): Characterization of microsatellite loci in *Pinus sylvestris* L. *Molecular Ecology* 7: 1260-1261.
- Suchowera K., Chełmicki M. 2009. Wyniki weryfikacji zgodności genetycznej szczepów

- sosny zwyczajnej (*Pinus sylvestris* L.) na terenie plantacji nasiennej w Nadleśnictwie Zdrojowa Góra. Uniwersytet Rolniczy im. H. Kołłątaja w Krakowie, Wydział Leśny. Praca dyplomowa.
- Stoehr M, Webber J, & Woods W (2004) Protocol for rating seed orchard seedlots in British Columbia: quantifying genetic gain and diversity. *Forestry* 77(4):297-303. doi: 10.1093/forestry/77.4.297
- Taberlet P, Luikart G. 1999. Non-invasive genetic sampling and individual identification. *Biological Journal of the Linnean Society* 68, 4155, doi:10.1111/j.1095-8312.1999.tb01157.x.
- Trojankiewicz M., Burczyk J. 2005. Efektywna liczba klonów na plantacjach nasiennych sosny zwyczajnej (*Pinus sylvestris* L.) *Sylvan* 11: 50-58.
- Waits L.P., Luikart G., Taberlet P. 2001. Estimating the probability of identity among genotypes in natural populations: cautions and guidelines. *Molecular Ecology* 10, pp. 249-256.
- White E., Hunter J., Dubetz C., Brost R., Bratton A., Edes S., Sahota R. 2000. Microsatellite markers for individual tree genotyping: application in forest crime prosecutions. *Journal of Chemical Technology & Biotechnology* 75: 923-926.
- Wysocka J., Kapińska E., Cybulska L., Rebała K., Szczerkowska Z. 2008. Identyfikacja osobnicza w oparciu o analizę 11 polimorficznych *loci* DNA typu STR. Badania populacji Polski północnej z wykorzystaniem zestawu AmpFISTR® SEfiler™ kit. *Ann. Acad. Med. Gedan.* 38: 91-96.

137. Jahrgang (2020), Heft 2, S. 85-108

**Austrian Journal of
Forest Science**
Centralblatt
für das gesamte
Forstwesen

Estimating Biomass partitioning in *Mytilaria laosensis* Using Additive Models

Schätzung der Biomasseverteilung in *Mytilaria laosensis* unter Verwendung additiver Modelle

Guoming Qin¹, Rongsheng Li^{*}, Wentao Zou¹, Niu Yu¹, Jinchang Yang¹, Guangtian Yin¹, Zhihai Wang¹, Zhaoli Chen¹

Keywords: *allometric model; biomass allocation; SUR; Southeast China*

Schlüsselbegriffe: *Allometrisches Modell; Zuweisung von Biomasse; SUR; Südostchina*

Abstract

If the additivity of the biomass allometric equation is not taken into account, it can result in erroneous estimation of forest biomass. The aim of this study was to evaluate biomass allocation patterns within separate tree parts, and to develop additive allometric equations for *Mytilaria laosensis* in southeast China. For this study, 42 destructive sampled trees were used to develop allometric equations for total biomass. We estimated biomass allocation by calculating the biomass fraction of each component (stem, branches, roots and leaves). We examined the relationships between each biomass fraction and diameter at breast height, tree height and crown diameter as independent variables. The seemingly unrelated regressions method was used to fit the biomass into additive allometric equations. The stem had the largest proportion of biomass (70.44%), followed by roots (20.35%), and branches (7.17%), with the smallest proportion of biomass being in the leaves (2.04%). Stem, leaf, and branch

¹ Research Institute of Tropical Forestry, Chinese Academy of Forestry, Guangzhou 510520, China

^{*}Corresponding author: Rongsheng Li, fjrs@caf.ac.cn

biomass ratios increased with diameter at breast height, while a reverse trend was found for belowground biomass ratios. The additive biomass models showed a good model fit explaining 94–98% of variance. This study contributes to species-specific allometric equations and the knowledge of crown, aboveground, and total biomass, which is lacking for most subtropical forests. The allometric biomass model constructed in our study can be used to estimate the biomass and carbon pool of *Mytilaria laosensis* plantations in Southeast China.

Zusammenfassung

Wenn die Additivität in allometrischen Biomassefunktionen nicht berücksichtigt wird, kann dies zu fehlerhaften Schätzungen der Waldbiomasse führen. Das Ziel dieser Studie war es, die Allokationsmuster für Biomasse in einzelne Baumkompartimente zu evaluieren und additive allometrische Gleichungen für *Mytilaria laosensis* im Südosten Chinas zu entwickeln. Für diese Studie wurden 42 gefällte Bäume verwendet, um allometrische Gleichungen für die gesamte Biomasse zu entwickeln. Wir berechneten erst die Anteile von Stamm, Ästen, Wurzeln und Blättern. Wir untersuchten dann die Beziehungen zwischen Biomassefraktionen und Brusthöhendurchmesser, Baumhöhe und Kronendurchmesser als unabhängige Variablen. Die ‚seemingly unrelated regressions‘ Methode wurde verwendet, um die Biomasse mit additiven allometrischen Funktionen zu ermitteln. Der Stamm hatte den größten Anteil an Biomasse (70.44 %), gefolgt von Wurzeln (20.35 %) und Ästen (7.17 %) mit dem geringsten Anteil an Biomasse in den Blättern (2.04 %). Das Anteil von Stamm-, Blatt- und Astbiomasse nahm mit dem Durchmesser in Brusthöhe zu, wobei der Anteil der unterirdischen Biomasse mit Durchmesser abnimmt. Die additiven Biomassemodelle zeigten eine gute Modellperformance mit einer erklärten Varianz von 94–98 %. Unsere Baumart-spezifischen allometrischen Gleichungen tragen zum Wissen über Kronen-, ober- und unterirdische Biomasse subtropischer Wälder bei, die noch wenig untersucht wurde. Die in unserer Studie erstellten Funktionen können nun verwendet werden, um den Biomasse- und Kohlenstoffpool von *Mytilaria laosensis* Plantagen in China abzuschätzen.

1. Introduction

Forest biomass is an important indicator to evaluate forest ecosystem productivity (Bond-Lamberty et al. 2002), to quantify vegetation carbon pools, and to examine ecosystem structure and function (Garkoti et al. 2008; Overman et al. 1994). Forests dominate terrestrial biomes, and are in consequence important for the earth's biosphere, playing a key role in maintaining regional ecological environments, carbon balance, and mitigating global warming (Brown et al. 1999; Bayen et al. 2016).

This important role makes it imperative to estimate forest biomass accurately. Destructive biological sampling (Brown et al. 1997) involves felling of all trees within a certain area, followed by measuring the weight of each of their parts (Basuki et al.

2009). While this sampling method is most accurate, it is expensive, labor-intensive and time-consuming. Destructive sampling is thus suitable only for a small areas or with small sample sizes (Mensah et al. 2017). Combining non-destructive sampling and allometric biomass models is trade-off of accuracy and costs. The allometric equations permit estimating biomass at different scales and multiple time steps (Ter-Mikaelian and Korzukhin 1997). Allometric biomass models are essential for converting non-destructive obtained tree information, from ground-based investigation or remote sensing to biomass (Dimobe et al. 2018).

Different biomass estimation models have been established globally (Lambert et al. 2008; Jenkins et al. 2003). Several predictive variables, such as diameter at breast height (DBH), tree height, crown diameter (CD), crown area, or wood density have been considered in such models, depending on study objectives and the species of interest. DBH, irrespective which biomass is studied, is the most commonly used predictive variable in allometric equations, because its measurements are easy and accurate (Riofrío et al. 2015; Chen et al. 2017; Xiao et al. 2011). Many other allometric growth equations use tree height (Dimobe et al. 2018), CD (Kuyah et al. 2012; Schneider et al. 2011; Mäkelä and Albrektson 1992), or wood density (Basuki et al. 2009; Kalita et al. 2015) as additional predictive variables. The results from these studies show that combining different predictive variables can improve the model performance at different locations and tree species (Dimobe et al. 2018; Schneider et al. 2011; Yang et al. 2017; Sileshi 2014).

Until now, there have been a few studies based on the allometric growth equations that considered the biomass additivity of individual tree parts (Behling et al. 2019; Affleck et al. 2016). If the relationships between the individual tree parts are ignored in estimating biomass with a model, this may result in differences between the sum of the predicted values calculated from the separate biomass models for each component and the value predicted from the biomass model for the whole tree. Thus, the construction of additive biomass models has attracted the attention of many researchers (Affleck and Diéguez-Aranda 2016; Xu et al. 2015; Carvalho and Parresol 2003), in which the biomass model for each part of a tree must be an additive to satisfy the requirements for demonstrating logical relationships (Silenshi 2014). There are several methods that can ensure the additivity of such equations, including the adjusted proportion (AP) (Dong et al. 2014), generalized method of moments (GMM), and seemingly unrelated regression (SUR) (Tang et al. 2001; Parresol 2001). Of these, SUR has been widely used as it considers the correlation between the equations and ensures high efficiency of additivity (Riofrío et al. 2015; Bi et al. 2004).

Mytilaria laosensis Lecomte is a valuable broadleaved tree species mainly distributed in South China and Southeast Asia (Guo et al. 2006). It is well known for fast-growing high-yield plantations and has a broad biological adaptability to soil type and environmental condition (Huang et al. 2009). The *M. laosensis* wood has high quality due to moderate density and not easy to crack and it is therefore widely used as raw

material for high quality furniture and covering plywood (Liang et al. 2007). In addition, it also has strong carbon sink potential (Ming et al. 2014). Zheng et al. (2014) studied the carbon storage and distribution pattern of different indigenous species plantations system in subtropical China and found that *M. laosensis* had large carbon storage capacity. Consequently, *M. laosensis* is expected to become one of the main tree species used in afforestation in the subtropical forests in China (Liu et al. 2012). However, only a few allometric growth equations are available for measuring its above- and belowground biomass (Zhang 2016; Ming et al. 2012; Wu 2005), and no additive allometric model for *M. laosensis* has been developed. The lack of accurate species-specific allometric models may lead to inaccurate estimations of carbon stocks (Van Vinh et al. 2019; Mahmood et al. 2019). In addition, different management and geographical conditions also lead to differences in above- and belowground biomass allocation (Meng et al. 2019). The objective of this study was to develop additive allometric biomass models for *M. laosensis*.

2. Materials and Methods

2.1 Study Sites

The study was conducted in Xijiang Forestry Station, Yunfu City, Guangdong Province, southeast China (23°07'N, 111°51'E) (Figure 1). The site has south subtropical monsoon climate with annual average temperature of 21.5°C. The average annual frost-free period is about 315–340 days. The average precipitation is 1600–1700 mm per year with the wet season extending from April to September and the dry season from October to March. The understory shrub layer consists of *Microstegium vagans* (Nees ex Steud.), *Mimosa bimucronata* (DC.) Kuntze, and *Ilex asprella* (Hook. Et Arne.) Champ. Ex Benth. The studied plantation was established in early 2010 by planting 1-year-old seedlings, with an average seedling height of 0.6 m. The density of the studied plantation was 1667 trees per hectare, the survival rate was 97.1%, the average DBH was 15.23 cm, the average tree height was 16.41 m, and the basal area was 22.37 m² per hectare. The plantation has not been thinned.

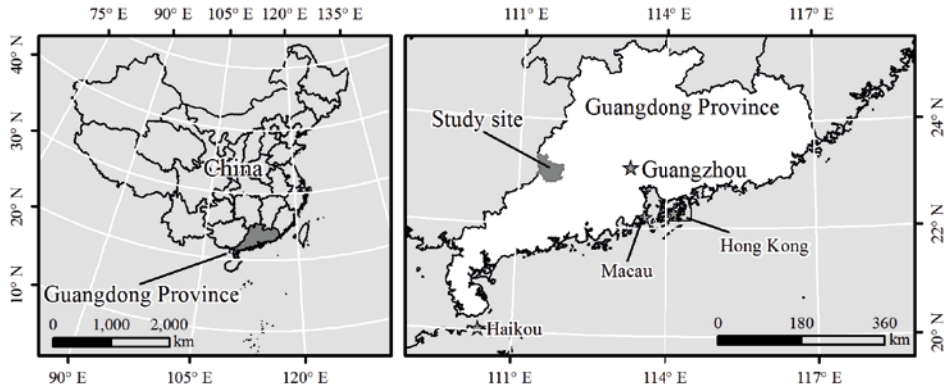


Figure 1: The Location of the study site.

Abbildung 1: Der Standort des Untersuchungsortes.

2.2 Biomass Data

In July 2018, six sampling plots (each 20 m × 30 m) were established at random locations in this *M. laosensis* plantation forest. Then we measured the diameter at breast height (DBH) using a diameter tape. We chose and excavated seven sample trees for biomass evaluation. The DBH of the sampled trees ranged from 10.5 cm to 21.5 cm, and the tree height from 14.1 m to 18.2 m (Table 1). The DBH of each tree was measured before being cutting the tree. Tree height, lowest living branch height, and crown diameter (CD) in four directions were recorded after felling.

Table 1: Range of diameter at breast height, tree height, crown diameter and biomass of sampled trees. (mean \pm standard deviation).

Tabelle 1: Durchmesserbereich in Brusthöhe, Baumhöhe, Kronendurchmesser und Biomasse der untersuchten Bäume. (Mittelwerte \pm Standardabweichung).

Diameter at breast height range (cm)	Tree height (m)	Crown diameter (m)	Biomass (kg)				Number of harvested tree
			Stem	Branch	Leaf	Root	
10—12	14.50 \pm 0.28	2.45 \pm 0.06	29.56 \pm 3.46	2.70 \pm 0.32	0.76 \pm 0.07	10.84 \pm 0.74	4
12—14	15.16 \pm 0.22	2.97 \pm 0.33	45.18 \pm 2.54	4.49 \pm 0.61	1.33 \pm 0.15	14.47 \pm 1.04	7
14—16	15.86 \pm 0.24	3.54 \pm 0.31	61.72 \pm 7.25	6.18 \pm 1.26	1.82 \pm 0.22	17.77 \pm 2.31	6
16—18	16.72 \pm 0.32	4.13 \pm 0.15	80.34 \pm 7.42	8.02 \pm 1.03	2.27 \pm 0.31	21.53 \pm 1.83	11
18—20	17.44 \pm 0.38	4.68 \pm 0.18	101.75 \pm 9.66	10.82 \pm 1.73	2.97 \pm 0.31	27.04 \pm 2.78	11
20—22	18.01 \pm 0.17	4.74 \pm 0.09	126.34 \pm 12.3	14.55 \pm 1.18	3.91 \pm 0.26	35.46 \pm 5.45	3

To measure stem biomass, stems were cut into 2 m long pieces, and the fresh weight of each segment was measured in the field. A thin disc was then cut from each piece to determine the weight with an accuracy of 0.5 g. The samples were then transported to the laboratory and dried to a constant weight in an oven at 75°C. From stem moisture content we calculated stem biomass. The tree crown was evenly vertically divided into three layers, and all branches, including leaves, were weighted in the field with a precision of 0.5 g. We separated leaves and wood for three selected branches and weighted wood and leaves separately and the ratio between leaves and branch mass were used to estimate leaf mass of the other branches. Finally, the samples (minimum 200 g) were taken back to the laboratory and dried to a constant mass in an oven at 75°C, after which the dry weight was measured, and the moisture content of each layer was calculated to obtain the biomass of branches and leaves (Ketterings et al. 2001).

Then we excavated a hole with radius of 1 m around each tree to a depth of 0.5 m and extracted the all root components including the broken roots. All roots were separated into thick roots (\geq 5 cm diameter), medium roots (2–5 cm diameter), fine roots (\leq 2 cm diameter) and stump. Representative samples (minimum 500 g) of each root fraction were weighed in the field. Then all samples were taken to the laboratory, dried to a constant weight, and the total belowground biomass was calculated (Wang 2006).

2.3 Data Analysis

The allocation of biomass to the stems, branches, leaves, and roots was estimated by calculating the ratio of the biomass of each part to total biomass. Statistical factors, such as arithmetic mean and standard deviation of total biomass (e.g., stem, bran-

ches, roots, and leaves) were calculated. The biomass portioning was used to test significance ($p < 0.05$). Additionally, the one-way ANOVA was used to test the differences between the biomass portions. The relationship between the explanatory variables (DBH, height, and CD) and the dependent variables (biomass stem, branch, leaf, and root) was evaluated using graphs to determine the abnormal values that might affect the fitted results. The allometric equations were created for the leaves, branches, roots, stems and total components depended on three different non-linear models with DBH, height (H) and CD as independent variables: equation (1), DBH as the only predictor variable; equation (2), DBH combined with tree height; and equation (3), DBH combined with tree height and CD as additional predictor variables. Logarithmic transformation was used to correct heteroscedasticity. The allometric models for the biomass of different parts (W_i) related to DBH, H and CD were established (Brown et al. 1989; Chave et al. 2005):

$$\ln(W_i) = \ln(\alpha_i) + \beta_i \cdot \ln(\text{DBH}) \quad \text{Eq.(1),}$$

$$\ln(W_i) = \ln(\alpha_i) + \beta_i \cdot \ln(\text{DBH}^2 \times H) \quad \text{Eq.(2),}$$

$$\ln(W_i) = \ln(\alpha_i) + \beta_i \cdot \ln(\text{DBH}^2 \times H) + \gamma_i \cdot \ln(\text{CD}) \quad \text{Eq.(3),}$$

The integration of DBH and tree height as a combined variable could solve the problem of collinearity and explain the changes in DBH at different heights (Dimobe et al. 2018). The SUR (Riofrío et al. 2015) fitting biomass model realized the additivity of the equation by constraining the equation parameters. This technique explained the correlation between regression residues, resulting in a small variance of the regression coefficients (Parresol 1999). The aggregated additive allometric equation satisfied the following conditions: (1) the sum of the biomass of individual part was equal to the total biomass; (2) the sum of the biomass of stem, branches, and leaves was equal to the aboveground biomass; and (3) the sum of branches and leaves was equal to the crown biomass. Estimation of three systems of equations were conducted by the SAS procedure of PROC model (SAS Institute Inc, Cary, NC, USA). For equation (1):

$$\ln(W_s) = \ln(\alpha_s) + \beta_s \cdot \ln(\text{DBH})$$

$$\ln(W_b) = \ln(\alpha_b) + \beta_b \cdot \ln(\text{DBH})$$

$$\ln(W_l) = \ln(\alpha_l) + \beta_l \cdot \ln(\text{DBH})$$

$$\ln(W_r) = \ln(\alpha_r) + \beta_r \cdot \ln(\text{DBH})$$

$$\ln(W_c) = \ln(\alpha_b \cdot \text{DBH}^{\beta_b} + \alpha_l \cdot \text{DBH}^{\beta_l})$$

$$\ln(W_a) = \ln(\alpha_s \cdot \text{DBH}^{\beta_s} + \alpha_b \cdot \text{DBH}^{\beta_b} + \alpha_l \cdot \text{DBH}^{\beta_l})$$

$$\ln(W_t) = \ln(\alpha_r \cdot \text{DBH}^{\beta_r} + \alpha_s \cdot \text{DBH}^{\beta_s} + \alpha_b \cdot \text{DBH}^{\beta_b} + \alpha_l \cdot \text{DBH}^{\beta_l})$$

Where W_s , W_b , W_l , W_r , W_c , W_a , W_t are stem, branch, leaf, root, crown, aboveground, and total biomass (kg), respectively; and α_i , β_i , and γ_i are the coefficients.

For equation (2):

$$\begin{aligned} \ln(W_s) &= \ln(\alpha_s) + \beta_s \cdot \ln(\text{DBH}^2 \times H) \\ \ln(W_b) &= \ln(\alpha_b) + \beta_b \cdot \ln(\text{DBH}^2 \times H) \\ \ln(W_l) &= \ln(\alpha_l) + \beta_l \cdot \ln(\text{DBH}^2 \times H) \\ \ln(W_r) &= \ln(\alpha_r) + \beta_r \cdot \ln(\text{DBH}^2 \times H) \\ \ln(W_c) &= \ln(\alpha_b \cdot (\text{DBH}^2 \times H)^{\beta_b} + \alpha_l \cdot (\text{DBH}^2 \times H)^{\beta_l}) \\ \ln(W_a) &= \ln(\alpha_s \cdot (\text{DBH}^2 \times H)^{\beta_s} + \alpha_b \cdot (\text{DBH}^2 \times H)^{\beta_b} + \alpha_l \cdot (\text{DBH}^2 \times H)^{\beta_l}) \\ \ln(W_t) &= \ln(\alpha_r \cdot (\text{DBH}^2 \times H)^{\beta_r} + \alpha_s \cdot (\text{DBH}^2 \times H)^{\beta_s} + \alpha_b \cdot (\text{DBH}^2 \times H)^{\beta_b} + \alpha_l \cdot (\text{DBH}^2 \times H)^{\beta_l}) \end{aligned}$$

For equation (3):

$$\begin{aligned} \ln(W_s) &= \ln(\alpha_s) + \beta_s \cdot \ln(\text{DBH}^2 \times H) + \gamma_s \cdot \ln(\text{CD}) \\ \ln(W_b) &= \ln(\alpha_b) + \beta_b \cdot \ln(\text{DBH}^2 \times H) + \gamma_b \cdot \ln(\text{CD}) \\ \ln(W_l) &= \ln(\alpha_l) + \beta_l \cdot \ln(\text{DBH}^2 \times H) + \gamma_l \cdot \ln(\text{CD}) \\ \ln(W_r) &= \ln(\alpha_r) + \beta_r \cdot \ln(\text{DBH}^2 \times H) + \gamma_r \cdot \ln(\text{CD}) \\ \ln(W_c) &= \ln(\alpha_b \cdot (\text{DBH}^2 \times H)^{\beta_b} \cdot (\text{CD})^{\gamma_b} + \alpha_l \cdot (\text{DBH}^2 \times H)^{\beta_l} \cdot (\text{CD})^{\gamma_l}) \\ \ln(W_a) &= \ln(\alpha_s \cdot (\text{DBH}^2 \times H)^{\beta_s} \cdot (\text{CD})^{\gamma_s} + \alpha_b \cdot (\text{DBH}^2 \times H)^{\beta_b} \cdot (\text{CD})^{\gamma_b} + \alpha_l \cdot (\text{DBH}^2 \times H)^{\beta_l} \cdot (\text{CD})^{\gamma_l}) \\ \ln(W_t) &= \ln(\alpha_r \cdot (\text{DBH}^2 \times H)^{\beta_r} \cdot (\text{CD})^{\gamma_r} + \alpha_s \cdot (\text{DBH}^2 \times H)^{\beta_s} \cdot (\text{CD})^{\gamma_s} + \alpha_b \cdot (\text{DBH}^2 \times H)^{\beta_b} \cdot (\text{CD})^{\gamma_b} + \alpha_l \cdot (\text{DBH}^2 \times H)^{\beta_l} \cdot (\text{CD})^{\gamma_l}) \end{aligned}$$

The use of logarithmic allometric equation may produce the systematic deviations of the response variable when converting back to the original scale (Ledermann and Neumann 2006; Eckmüllner 2006). To correct this bias, the correction factors (CF) of these equations were computed (Baskerville 1972; Sprugel 1983).

$$\text{CF} = \exp\left(\frac{\text{SEE}^2}{2}\right) \quad \text{Eq.(4)}$$

SEE is the standard error of the estimates. The model was evaluated by the following three goodness-of-fit statistical methods: root mean square error (RMSE), Akaike information criterion (AIC), and the adjusted coefficient of determination (Adj. R²) (Cai et al. 2013). The most suitable model was that with the lowest RMSE and AIC, and the highest Adj. R². A t-test was used to examine significant deviations between the observed and estimated values of the crown, aboveground, and total biomass, and graphical analyses between the predicted vs. observed values were carried out using the best additive allometric models.

$$\text{RMSE} = \sqrt{\frac{\sum_{i=1}^n (Y_i - \hat{Y}_i)^2}{n}} \quad \text{Eq.(5),}$$

$$\text{AIC} = n \ln(\text{SSR}) + 2(k+1) - n \ln(n) \quad \text{Eq.(6),}$$

$$\text{Adj. R}^2 = 1 - \left(1 - \frac{\sum_{i=1}^n (Y_i - \hat{Y}_i)^2}{\sum_{i=1}^n (Y_i - \bar{Y})^2}\right) \frac{n-1}{n-k} \quad \text{Eq.(7).}$$

Where Y_i is the observed value, \hat{Y}_i is the estimated biomass values based on models, \bar{Y}_i is the mean value of the biomass, n is the number of samples, and k is the number of parameters.

3. Results

3.1 Biomass Partitioning

The biomass of the different *M. laosensis* tree parts (stems, roots, branches, and leaves) were significantly different ($p < 0.001$). The stem accounted for the largest contribution to the total biomass at $70.44\% \pm 2.33$ (mean \pm SD), while the contributions of the belowground, branch, and leaf biomass were $20.35\% \pm 2.80$, $7.17\% \pm 0.84$, and $2.04\% \pm 0.18$, respectively. The proportion of stems, branches, and leaves biomass exhibited similar incremental trends with DBH (Figure 2). With increasing DBH from 10.5 to 21.5 cm, the proportion contributed by the stem to the total biomass increased from 65.85% to 75.60%, while that of the branches and leaves increased from 5.05% to 9.27% and 1.59% to 2.41%, respectively. In contrast, the proportion attributed to belowground biomass decreased from 26.39% to 18.15%.

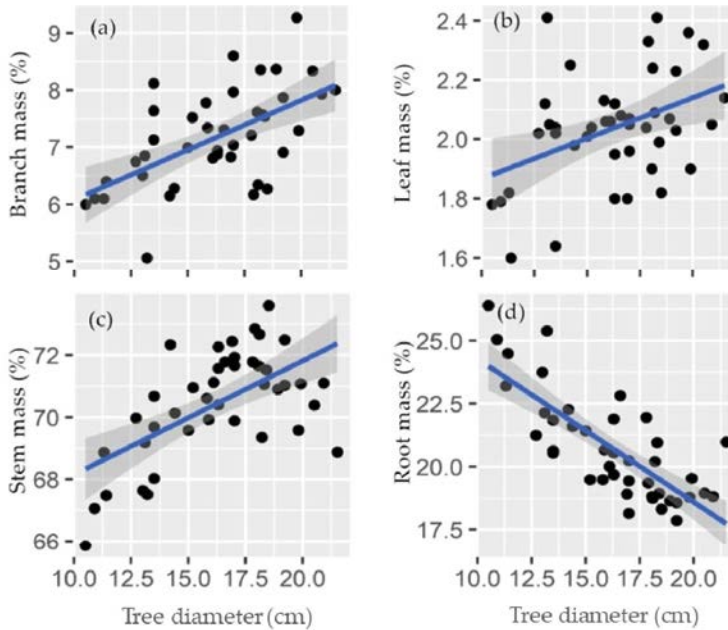


Figure 2: Partitioning of total biomass in relation to diameter of *M. laosensis*, percentage of (a) stem biomass, (b) leaf biomass, (c) branch biomass, (d) belowground biomass.

Abbildung 2: Verteilung der Gesamtbiomasse in Bezug auf den Durchmesser von *M. laosensis*, Prozentsatz von (a) Stamm biomasse, (b) Blatt biomasse, (c) Zweig biomasse, (d) unterirdische Biomasse.

3.2 Biomass Allometric Equations

The non-linearity trend in the observed values for tree height, crown, aboveground, and total biomass as a function of DBH is displayed in Figure 3. Our results showed model 1 with DBH as the only predictor, could effectively explain the biomass of individual part, with $R^2 > 94\%$ and $RMSE < 0.1$ (Table 2). The addition of tree height into the biomass model significantly improved the fit of some models, while the addition of CD only significantly improved the fit of the root biomass model. For leaf biomass, model 2 had a larger R^2 and smaller RMSE and AIC, and the addition of CD did not improve the fit of the model. For branch biomass, model 1 was a better fit. For stem biomass, each model had a similar fit, but model 2 showed a better fit with respect to R^2 , RMSE, and AIC. For root biomass, the addition of height and CD improved the overall fit of the model, and model 3 had a larger R^2 , and smaller RMSE and AIC.

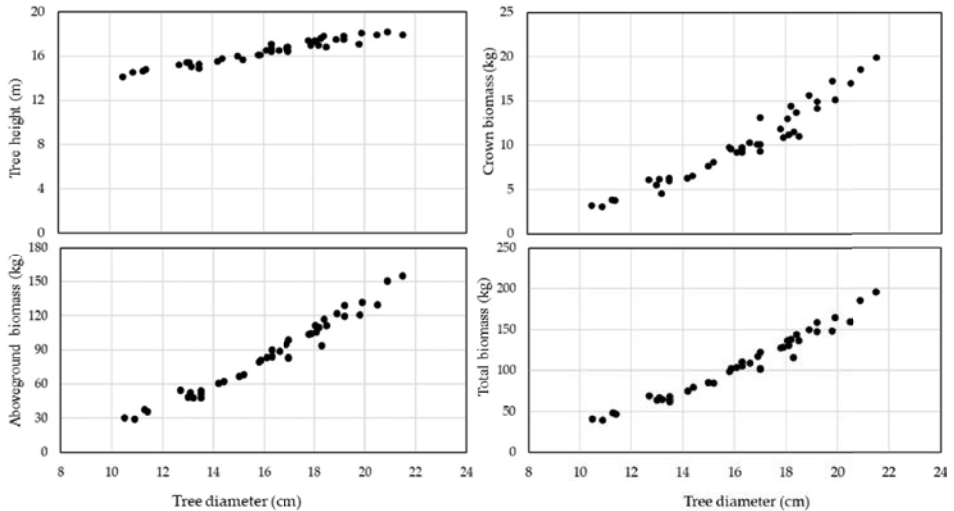


Figure 3: Relationships between DBH and (a) tree height, (b) crown biomass, (c) aboveground biomass, and (d) total biomass of *M. laosensis*.

Abbildung 3: Beziehungen zwischen DBH und (a) Baumhöhe, (b) Kronenbiomasse, (c) oberirdischer Biomasse und (d) Gesamtbiomasse von *M. laosensis*.

To estimate the biomass of *M. laosensis* more accurately, the optimal biomass model for an individual part was used to construct the multivariate additive biomass model (Table 2). The R^2 values for total biomass and the biomass of individual parts in the optimal additive biomass models were more than 95%, and the RMSE was relatively small (Table 3). The correction factors for the optimal equations were also listed (Table 3). The fit of the stem, aboveground, and whole plant biomass models was better (R^2 was relatively large and RMSE was relatively small) than that of the biomass models of leaves, branches, roots, and crowns (smaller R^2 and larger RMSE values). Figure 4 shows the linear 1:1 trend for the scatter plot of the observed and predicted crown, aboveground, and total biomass.

Table 2: Regression equations for estimation of leaf, branch, stem, and root biomass through seemingly unrelated regression in *M. laosensis*. α , β , and γ are the coefficients used in the model. DBH, diameter at breast height; H, tree height; CD, crown diameter; RMSE, root mean square error; AIC, Akaike information criterion; Adj. R^2 , adjusted coefficient of determination.

Tabelle 2: Regressionsgleichungen zur Schätzung der Biomasse von Blättern, Ästen, Stamm und Wurzeln durch seemingly unrelated regressions bei *M. laosensis*. α , β und γ sind die im Modell verwendeten Koeffizienten. DBH, Brusthöhendurchmesser; H, Baumhöhe; CD, Kronendurchmesser; RMSE, quadratischer Mittelwertfehler; AIC, Akaike-Informationskriterium; Adj. R^2 , angepasster Bestimmungskoeffizient.

Model	Predictors	Components	Regression coefficients			Performance criteria		
			$\ln(\alpha)$	β	γ	RMSE	AIC	Adj. R^2
1	DBH	Leaf	-6.02*** ± 0.22	2.43*** ± 0.08		0.093	-76.148	0.959
2	DBH**H	Leaf	-7.86*** ± 0.28	1.03*** ± 0.03		0.092	-76.614	0.959
3	DBH**H;CD	Leaf	-8.81*** ± 0.71	1.20*** ± 0.12	-0.36 ^{ns} ± 0.25	0.093	-76.56	0.955
1	DBH	Branch	-5.19*** ± 0.25	2.58*** ± 0.09		0.107	-64.913	0.952
2	DBH**H	Branch	-7.14*** ± 0.33	1.09*** ± 0.04		0.110	-62.408	0.950
3	DBH**H;CD	Branch	-6.69*** ± 0.86	1.01*** ± 0.15	0.17 ^{ns} ± 0.30	0.111	-60.754	0.948
1	DBH	Stem	-2.09*** ± 0.15	2.29*** ± 0.05		0.064	-108.021	0.978
2	DBH**H	Stem	-3.84*** ± 0.18	0.97*** ± 0.02		0.061	-111.397	0.980
3	DBH**H;CD	Stem	-3.77*** ± 0.48	0.96*** ± 0.08	0.02 ^{ns} ± 0.17	0.065	-109.418	0.977
1	DBH	Root	-1.91*** ± 0.19	1.77*** ± 0.07		0.083	-86.291	0.940
2	DBH**H	Root	-3.26*** ± 0.24	0.75*** ± 0.03		0.081	-88.372	0.943
3	DBH**H;CD	Root	-4.77*** ± 0.58	1.02*** ± 0.09	-0.57** ± 0.20	0.074	-94.167	0.952

*** Significance level: $p < 0.001$. ** Significance level: $p < 0.01$. The final selected models of each biomass part are in bold.

Table 3: Selected biomass equations simultaneously fitted through seemingly unrelated regression in *M. laosensis*. AGB, aboveground biomass; TGB, total biomass; DBH, diameter at breast height; H, height; CD, crown diameter; RMSE, root mean square error; AIC, Akaike information criterion; Adj. R^2 , adjusted coefficient of determination; CF, logarithmic correction factor.

Tabelle 3: Ausgewählte Biomassegleichungen, die gleichzeitig durch scheinbar nicht verwandte Regression bei *M. laosensis* angepasst wurden. AGB, oberirdische Biomasse; TGB, Gesamtbiomasse; DBH, Durchmesser in Brusthöhe; H, Höhe; CD, Kronendurchmesser; RMSE, quadratischer Mittelwertfehler; AIC, Akaike-Informationskriterium; Adj. R^2 , angepasster Bestimmungskoeffizient; CF, logarithmischer Korrekturfaktor.

Components	Biomass equations	RMSE	Adj. R^2	CF
Leaf	$\ln W_{li} = -7.86 + 1.03 \ln(\text{DBH}^2 \text{H})$	0.092	0.959	1.110
Branch	$\ln W_{br} = -5.19 + 2.58 \ln(\text{DBH})$	0.107	0.952	1.124
Stem	$\ln W_{st} = -3.84 + 0.97 \ln(\text{DBH}^2 \text{H})$	0.061	0.98	1.096
Root	$\ln W_{ro} = -4.77 + 1.02 \ln(\text{DBH}^2 \text{H}) - 0.52 \ln(\text{CD})$	0.074	0.952	1.061
Crown	$\ln W_{cr} = \ln(e^{-7.86} (\text{DBH}^2 \text{H})^{1.03} + e^{-5.19} (\text{DBH})^{2.58})$	0.087	0.972	
AGB	$\ln W_{ag} = \ln(e^{-3.84} (\text{DBH}^2 \text{H})^{0.97} + e^{-7.86} (\text{DBH}^2 \text{H})^{1.03} + e^{-5.19} (\text{DBH})^{2.58})$	0.058	0.981	
TGB	$\ln W_{tg} = \ln(e^{-4.77} (\text{DBH}^2 \text{H})^{1.02} (\text{CD})^{-0.52} + e^{-3.84} (\text{DBH}^2 \text{H})^{0.97} + e^{-7.86} (\text{DBH}^2 \text{H})^{1.03} + e^{-5.19} (\text{DBH})^{2.58})$	0.055	0.979	

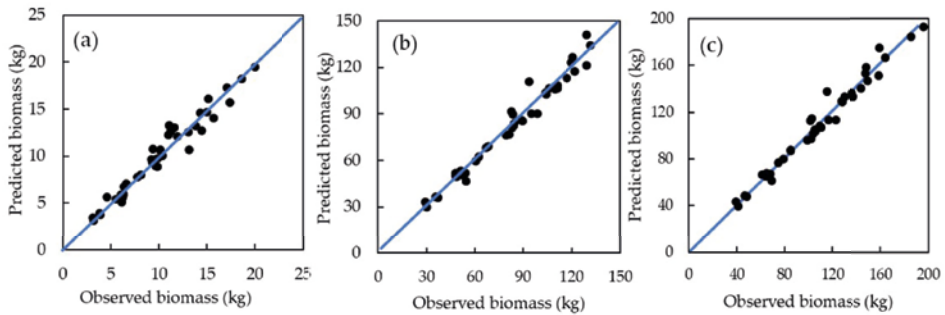


Figure 4: Scatterplots for the observed biomass and the predicted biomass of (a) crown, (b) aboveground, (c) total biomass of additive equations. Lines are 1:1 equivalence.

Abbildung 4: Streudiagramme für die beobachtete Biomasse und die vorhergesagte Biomasse von (a) Krone, (b) oberirdisch, (c) Gesamtbiomasse der additiven Gleichungen. Linien entsprechen 1:1.

4. Discussion

Biomass is a form of energy accumulated in the process of plant growth and development (Mensah et al. 2017; Dong et al. 2014). Plant species, age, and the external environment can change biomass distribution patterns in various parts of forest trees. Our results demonstrated that the stem accounted for the largest proportion of the total biomass (nearly 72%), followed by the roots (19.5%). Leaf biomass contributed the smallest amount to the total biomass, about 2%; this is similar to the proportion determined in other studies (Zhang 2016; Wu 2005). Our biomass results suggest that photosynthetic products in *M. laosensis* are primarily concentrated in the stem and roots. Biomass accumulation in the stem promotes large diameter wood in the tree species, while the well-developed root system promotes the absorption of water and nutrients, thereby supporting tree growth. In our study, the biomass proportion of the stem, branches, and leaves increased, and root biomass decreased with increasing diameter class. These results contradict those of previous studies on *M. laosensis*, and we speculated that this might be owing to the difference in growth periods of the studied tree species or the strategies. As a shade-intolerant tree species, *M. laosensis* competes in the initial growth stages for limited terrestrial resources, such as light. In forests, trees with more branch biomass have a competitive advantage, mainly through advantage in tree height and expansion of the crown resulting in shading of neighboring trees (Dimobe et al. 2018). Similar growth trends have also been found in a previous study with fast-growing *Eucalyptus* spp., which allocate more biomass in the stem compared with leaves and branches (Kuyah et al. 2012).

When constructing the biomass model, the sum of the biomass of individual part was equal to the total biomass (Dimobe et al. 2018; Behling et al. 2019; Meng et al. 2019).

When the correlation between the total biomass and that of individual part was taken into account, the fitting equations were required to be additive. Some of the published biomass equations are not-additive because they were estimated by ordinary least-squares regression (OLS) (Cai et al. 2013; Blujdea et al. 2012). The use of SUR to construct an additive allometric growth equation can however account for the correlation between the biomasses of individual part, resulting in more effective parameter estimation (Parresol 2011); SUR is not only able to determine the additivity of the equation, but also reduces the predicted interval of biomass estimation (Bi et al. 2004; Parresol 2001; Dong et al. 2015).

In the current study, a logarithmic transformation equation was used to estimate the relationship between biomass and explainable variables. When an estimated value was converted back to the original untransformed value, the expected biomass will still be underestimated. To correct this deviation, Baskerville (1972) and Sprugel (1983) proposed a correction factor (CF) method, which is often used to correct system errors. Consequently, the results of this study indicated that a few deviation were produced on the process of using logarithmic transformation to fit the biomass allometric equations. Some researchers believe that the correction is unnecessary, since the difference in biomass estimation can be considered negligible (Malimbwi et al. 1994). However, it is suggested to analyze each case individually to make sure the necessity of CF in biomass estimation.

Most studies on allometric models have been based on DBH to predict tree biomass (Xiang et al. 2016; Kusmana et al. 2018). In our study, the model containing DBH as the variable had an explanation rate of over 90% for stem, branch, leaf, and below-ground biomass variability. Consistent with previous studies (Dimobe et al. 2018; Van Vinh 2019; Xiang et al. 2016), the addition of tree height as an independent variable to the equation improved the fit of the equation. It has also been suggested that the estimation of biomass could be improved by combining wood density and CD as predictors (Chave et al. 2005; Ploton et al. 2016). In our study, however, the addition of CD as a predictor variable into the equation reduced root RMSE from 0.083 to 0.074, and slightly increased the fitting degree from 0.94 to 0.952, indicating a close relationship between the crown and belowground part (Kuyah et al. 2012; Harrington et al. 2003). Additionally, the crown height, a potential and efficient input variable in other studies (Ledermann and Neumann 2006; Repola 2009) can be studied in further research on this species.

To date, there have been few studies on the allometric growth equation regarding the biomass of *M. laosensis*, and only a few researchers (Zhang 2016; Ming et al. 2012; Wu 2005) from Guangxi and Fujian in China have studied *M. laosensis*. The published allometric growth equation for *M. laosensis* only uses DBH as predictor variables (Zhang 2016; Ming et al. 2012; Wu 2005). In our study, we added CD into the predictive variables of biomass for this species, but the fitting effect was not improved. We also compared the equations of this paper with other biomass allometric equations for

M. laosensis (Figure 5). For the same DBH, the models construct by Ming et al. (2012) and Wu (2005) gave higher total biomass values than our study. Ming et al. (2012) established an allometric growth equation for the biomass of 28-year-old *M. laosensis* in Guangxi using DBH and tree height as explanatory variables, with a sample size of 13 trees (DBH range of 17 cm to 31 cm, compared with the range in our study of only 10.5 cm to 21.5 cm). Paul et al. (2018) stated that a sample of fewer than 15 independent samples may give inaccurate results; however, Ming et al. (2012) used a sample size smaller 15. Therefore, the accuracy of equation previously published needs to be improved. Zhang (2016) studied the biomass of a 22-year-old *M. laosensis* plantation in the Fujian area of China, with a sample size of 15, but their sampling DBH range was not reported. However, it can be inferred from the comparison with the equations in this paper that the range of the DBH of the equation should be close to our paper. Wu et al. (2005) established biomass models for the branches, bark, leaves, and stems of 15-year-old *M. laosensis*, but they had a small sample size (only four), this may also result in the low accuracy. In their study, the individual branch and leaf biomass were estimated based on the basal diameter of the branches, and then the branch and leaf biomass of the whole tree was calculated. Compared with the method used in our study, the method used by Wu et al. (2005) was complex, the sample size was small, additivity was not taken into account, and the accuracy of model fit was low. In addition, the root sampling method may also cause a few discrepancies for biomass estimation in those studies. Excavation was used to determine the belowground biomass in this paper, which was the same way as Ming et al. (2012). Zhang (2016) studied the roots by collecting along a 1.2 m deep soil profile, which was divided into 6 layers of 20 cm sampling depth each. Wu (2005) estimated the root biomass by the root-shoot ratio of the forest communities. Currently, few studies have considered the correction for the loss of the roots on *M. laosensis* for instance using Goff's approach (2001). Furthermore, the discrepancies between the current studies of total biomass by comparing the biomass of single compartments (Supplementary Figure S1) were further explored and the results indicated that the discrepancy by Wu (2005) is mostly caused by branches and roots, while for Ming (2012) it is stem and roots, especially for larger diameters. For Zhang (2016), the discrepancy was mainly attributable to branches. In all, the differences in the estimated biomass between this study and other studies may be due to differences in sampling sites, the DBH ranges, sampling approach, number of samples, and management. The accuracy of the model increases with increasing sample size (Kusmama et al. 2018). There should be already enough material available to make a robust widely applicable biomass model for *M. laosensis*, at least for certain regions.

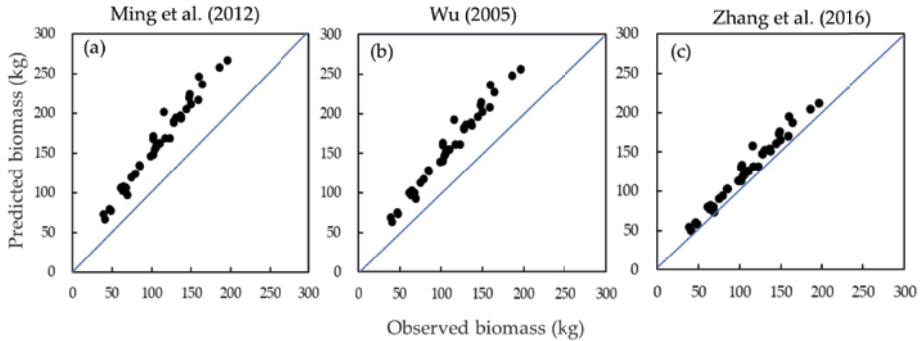


Figure 5: Scatterplots for the observed biomass and the predicted biomass of total biomass of (a) Ming et al (2012), (b) Zhang (2016), (c) Wu et al (2005). Lines are 1:1 equivalence.

Abbildung 5: Streudiagramme für die beobachtete Biomasse und die vorhergesagte Biomasse der Gesamtbiomasse von (a) Ming et al. (2012), (b) Zhang (2016), (c) Wu et al. (2005). Linien entsprechen 1: 1.

5. Conclusions

Mytilaria laosensis allocates more biomass in the woody parts, especially in stem, probably to confer a competitive advantage over its surrounding competitors. DBH is effective in estimating branch biomass; the introduction of the independent variable of tree height can improve the accuracy of determining leaf and stem biomass, while the addition of CD as a variable can improve the prediction of belowground biomass. The biomass model constructed in our study can be used to estimate the biomass and carbon pool of *M. laosensis* plantations from the same region and exhibiting similar stand properties (DBH, height, CD) as the studied stands. However, this newly constructed allometric model must be used cautiously in estimating the biomass of trees in other locations with different tree growth patterns and sizes.

Acknowledgements

This research is funded by Forestry Scientific and Technological Innovation Funds of Guangdong Province (2019KJCX004). The authors thank Haikun Wu for help with data collection. We also would like to thank Xuemei Yan and Weijun He for their help in data analysis and Chunsheng Wang for his comments on this article. Sincere thanks to the reviewers for their useful suggestions on earlier drafts of this paper.

References

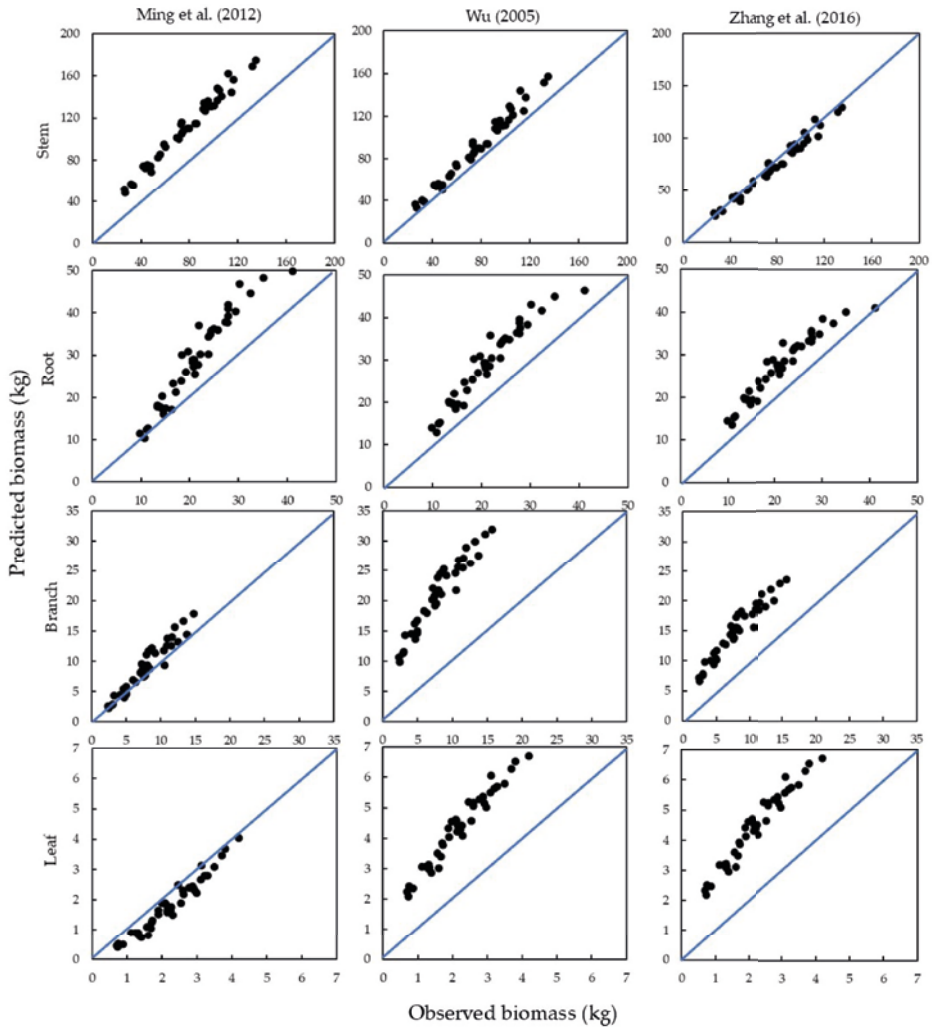
- Affleck, D.L.R. and Diéguez-Aranda, U. 2016 Additive nonlinear biomass equations: a likelihood-based approach. *Forest Science*, 62(2), 129-140.
- Baskerville, G.L., 1972 Use of logarithmic regression in the estimation of plant biomass. *Canadian Journal of Forest Research*, 2(1), 49-53.
- Basuki, T.M., Van Laake, P.E., Skidmore, A.K. and Hussin, Y.A. 2009 Allometric equations for estimating the above-ground biomass in tropical lowland Dipterocarp forests. *Forest Ecology and Management*, 257(8), 1684-1694.
- Bayen, P., Bognounou, F., Lykke, A.M., Ouédraogo, M. and Thiombiano, A. 2016 The use of biomass production and allometric models to estimate carbon sequestration of *Jatropha curcas* L. plantations in western Burkina Faso. *Environment, Development and Sustainability* 18(1), 143-156.
- Behling, A., Péllico-Netto S., Sanquetta, C.R., Corte, A.P., Simon, A.A. Rodrigues AL and Caron BO. 2019 Additive and non-additive biomass equations for Black Wattle. *Floresta e Ambiente* 26(4), e20170439.
- Bi, H., Turner, J. and Lambert, M.J. 2004 Additive biomass equations for native eucalypt forest trees of temperate Australia. *Trees* 18(4): 467-479.
- Blujdea, V.N.B., Pilli, R., Dutca, I., Ciuvat., L. and Abrudan, I.V. 2012 Allometric biomass equations for young broadleaved trees in plantations in Romania. *Forest Ecology and Management* 264, 172-184.
- Bond-Lamberty, B., Wang, C. and Gower, S.T. 2002 Aboveground and belowground biomass and sapwood area allometric equations for six boreal tree species of northern Manitoba. *Canadian Journal of Forest Research* 32(8), 1441-1450.
- Brown S, Gillespie A J R, Lugo A E. 1989 Biomass estimation methods for tropical forests with applications to forest inventory data. *Forest science* 35(4): 881-902.
- Brown, S. 1997 Estimating Biomass and Biomass Change of Tropical Forests, A Primer. (FAO Forestry Paper 134. Food and Agriculture Organization of the United Nations, Rome, 23.
- Brown, S.L., Schroeder, P. and Kern, J.S. 1999 Spatial distribution of biomass in forests of the eastern USA. *Forest Ecology and Management* 123(1), 81-90.
- Cai S, Kang X and Zhang L. 2013 Allometric models for aboveground biomass of ten tree species in northeast China. *Annals of Forest Research* 56(1), 105-122.
- Carvalho, J.P. and Parresol, B.R. 2003 Additivity in tree biomass components of Pyrenean oak (*Quercus pyrenaica* Willd.). *Forest Ecology and Management* 179(1-3), 269-276.
- Chave, J., Andalo, C., Brown, S., Cairns, M.A., Chambers, J.Q., Eamus, D., Fölster, H., Fromard, F., Higuchi, N., Kira, T., Lescure, J.P., Nelson, B.W., Ogawa, H., Puig, H., Riéra, B. and Yamakura, T. 2005 Tree allometry and improved estimation of carbon stocks and balance in tropical forests. *Oecologia* 145(1), 87-99.
- Chen, D., Huang, X., Zhang, S. and Sun, X. 2017 Biomass modeling of larch (*Larix* spp.) plantations in China based on the mixed model, dummy variable model, and Bayesian hierarchical model. *Forests* 8(8), 268.
- Dimobe, K., Mensah, S., Goetze, D., Ouédraogo, A., Kuyah, S., Porembski, S and Thiom-

- biano, A. (2018) Aboveground biomass partitioning and additive models for *Combreum glutinosum* and *Terminalia laxiflora* in West Africa. *Biomass and Bioenergy* 115, 151-159.
- Dong, L., Zhang, L., Li, F. 2014 A three-step proportional weighting system of nonlinear biomass equations. *Forest Science* 61(1), 35-45.
- Dong, L., Zhang, L., Li, F., 2015 Developing additive systems of biomass equations for nine hardwood species in Northeast China. *Trees* 29(4), 1149-1163.
- Eckmüllner O. 2006 Allometric relations to estimate needle and branch mass of Norway spruce and Scots pine in Austria. *Austrian Journal of Forest Science* 123(1-2): 7-15.
- Garkoti, S.C. 2008 Estimates of biomass and primary productivity in a high-altitude maple forest of the west central Himalayas. *Ecological Research* 23(1), 41-49.
- Goff, N.L., Ottorini, J.M. 2001 Root biomass and biomass increment in a beech (*Fagus sylvatica* L.) stand in North-East France. *Annals of Forest Science* 58,1-13.
- Guo, W.F., Cai, D.X., Jia, H.Y., Li, Y.X. and Lu, Z.F. 2006 Growth laws of *Mytilaria laosensis* plantation. *Forest Research* 19(5), 585-589. (in Chinese).
- Harrington, T.B., Dagley, C.M. and Edwards, M.B. 2003 Above-and belowground competition from longleaf pine plantations limits performance of reintroduced herbaceous species. *Forest Science* 49(5), 681-695.
- Huang, Z.T., Wang S.F., Jiang Y.M., Mo J.X. 2009 Exploitation and utilization prospects of eximious native tree species *Mytilaria laosensis*. *Journal of Guangxi Agriculture Science* 40(9), 1220-1223. (in Chinese).
- Jenkins, J.C., Chojnacky, D.C., Heath, L.S. and Birdsey, R.A. 2003 National-scale biomass estimators for United States tree species. *Forest Science* 49(1), 12-35.
- Kalita, R.M., Das, A.K. and Nath, A.J. 2015 Allometric equations for estimating above-and belowground biomass in Tea (*Camellia sinensis* (L.) O. Kuntze) agroforestry system of Barak Valley, Assam, northeast India. *Biomass and Bioenergy* 83, 42-49.
- Ketterings, Q.M., Coe, R., van Noordwijk, M. and Palm, C.A. 2001 Reducing uncertainty in the use of allometric biomass equations for predicting above-ground tree biomass in mixed secondary forests. *Forest Ecology and Management* 146(1-3), 199-209.
- Kusmana, C., Hidayat, T., Tiryana, T., Rusdiana, O. 2018 Allometric models for above-and below-ground biomass of *Sonneratia* spp. *Global Ecology and Conservation* 15, e00417.
- Kuyah, S., Muthuri, C., Jamnadass, R., Mwangi, P., Neufeldt, H., Dietz, J. 2012 Crown area allometries for estimation of aboveground tree biomass in agricultural landscapes of western Kenya. *Agroforestry Systems* 86(2), 267-277.
- Lambert, M.C., Ung, C.H., Raulier, F. 2005 Canadian national tree aboveground biomass equations. *Canadian Journal of Forest Research* 35(8), 1996-2018.
- Ledermann, T., Neumann, M. 2006 Biomass equations from data of old long-term experimental plots. *Austrian Journal of Forest Science* 123(1), 47-64.
- Liu, E., Wang, H. and Liu, S.R. 2012 Characteristics of carbon storage and sequestration in different age beech (*Castanopsis hystrix*) plantations in south subtropical area of China. *Chinese Journal of Applied Ecology* 23, 335-340 (in Chinese).

- Liang S.Q., Luo J.J., 2007 wood anatomical properties and their variations of *Mytilaria laosensis* plantations. *Journal of Beijing Forestry University* 29(3), 142-148.
- Mahmood, H., Siddique, M.R.H., Costello, L., Birigazzi, L., Abdullah, S.R., Henry, M., Siddiqui, B.N., Aziz, T., Ali, S., Al Mamun. A., Forhad, M.I.K, Akhter, M., Iqbal, Z. and Mondol, F.K. 2019 Allometric models for estimating biomass, carbon and nutrient stock in the Sal zone of Bangladesh. *iForest-Biogeosciences and Forestry* 12(1), 69-75.
- Malimbwi R E, Solberg B, Luoga E. 1994 Estimation of biomass and volume in miombo woodland at Kitulungalo Forest Reserve, Tanzania. *Journal of Tropical Forest Science* 7, 230-242.
- Mäkelä, A. and Albrektson, A. 1992 An analysis of the relationship between foliage biomass and crown surface area in *Pinus sylvestris* in Sweden. *Scandinavian Journal of Forest Research* 7(1-4), 297-307.
- Meng, S., Jia, Q., Liu, Q., Zhou, G., Wang, H. and Yu. J. 2019 Aboveground Biomass Allocation and Additive Allometric Models for Natural *Larix gmelinii* in the Western Daxing'anling Mountains, Northeastern China. *Forests* 10(2), 150.
- Mensah, S., Veldtman, R. and Seifert, T. 2017 Allometric models for height and aboveground biomass of dominant tree species in South African Mistbelt forests. *Southern Forests, A Journal of Forest Science* 79(1), 19-30.
- Ming, A., Jia H., Zhao, J., Tao, Y. and Li, Y. 2014 Above-and below-ground carbon stocks in an indigenous tree (*Mytilaria laosensis*) plantation chronosequence in subtropical China. *PLoS One* 9(10), e109730.
- Ming, A.G., Jia, H.Y., Tao, Y., Lu, L.H., Su, J.M. and Shi, Z.M. 2012 Biomass and its allocation in 28-year-old *Mytilaria laosensis* plantation in southwest Guangxi. *Chinese Journal of Ecology* 31(5), 1050-1056 (in Chinese).
- Overman, J.P., Witte, H.J. and Saldarriaga, J.G. 1994 Evaluation of regression models for above-ground biomass determination in Amazon rainforest. *Journal of tropical Ecology* 10(2), 207-218.
- Parresol, B.R. 1999 Assessing tree and stand biomass: a review with examples and critical comparisons. *Forest Science* 45(4), 573-593.
- Parresol, B.R. 2001 Additivity of nonlinear biomass equations. *Canadian Journal of Forest Research* 31(5), 865-878.
- Paul, K.I., Radtke, P.J., Roxburgh, S.H., Larmour, J., Waterworth, R., Butler, D., Brooksbank, K. and Ximenes, F. 2018 Validation of allometric biomass models: How to have confidence in the application of existing models. *Forest Ecology and Management* 412, 70-79.
- Ploton, P., Barbier, N., Momo, S.T., Réjou-Méchain, M., Boyemba Bosela, F., Chuyong, G.B., Dauby, G., Droissart, V., Fayolle, A., Goodman, R.C., Henry, M., Kamdem, N.G., Katembo Mukirania, J., Kenfack, D., Libalah, M., Ngomanda, A., Rossi, V., Sonké, B., Texier N., Thomas, D., Zebaze, D., Couteron, P., Berger, U. and Pélissier, R. 2016 Closing a gap in tropical forest biomass estimation: taking crown mass variation into account in pantropical allometries. *Biogeosciences* 13, 1571-1585.
- Repola, J. 2009 Biomass equation for Scots pine and Norway spruce in Finland. *Silva Fennica* 43(4), 625-647.
- Riofrío, J., Herrero, C., Grijalva, J. and Bravo, F. 2015 Aboveground tree additive biomass models in Ecuadorian highland agroforestry systems. *Biomass and Bioenergy* 80,

- 252-259. Schneider, R., Berninger, F., Ung, C.H., Mäkelä, A., Swift, D.E. and Zhang, S.Y. 2011 Within crown variation in the relationship between foliage biomass and sapwood area in jack pine. *Tree Physiology* 31(1), 22-29.
- Sileshi, G.W. 2014 A critical review of forest biomass estimation models, common mistakes and corrective measures. *Forest Ecology and Management* 329, 237-254.
- Sprugel, D.G. 1983 Correcting for bias in log-transformed allometric equations. *Ecology* 64(1), 209-210.
- Tang, S., Li, Y. and Wang, Y. 2001 Simultaneous equations, error-in-variable models, and model integration in systems ecology. *Ecological Modelling* 142(3), 285-294.
- Ter-Mikaelian, M.T. and Korzukhin, M.D. 1997 Biomass equations for sixty-five North American tree species. *Forest Ecology and Management* 97(1), 1-24.
- Van Vinh, T., Marchand, C., Linh, T.V., Vinh, D.D. and Allenbach, M. 2019 Allometric models to estimate above-ground biomass and carbon stocks in *Rhizophora apiculata* tropical managed mangrove forests (Southern Viet Nam). *Forest Ecology and Management* 434, 131-141.
- Wang, C. 2006 Biomass allometric equations for 10 co-occurring tree species in Chinese temperate forests. *Forest Ecology and Management* 222(1-3), 9-16.
- Wu, Q.Z. 2005 Study of *Mytilaria laosensis* plantation biomass. *Journal of Fujian Forestry Science and Technology* 32, 125-129 (in Chinese).
- Xiang, W., Zhou, J., Ouyang, S., Zhang, S., Lei, P., Li, J., Deng, X., Fang, X. and Forrester, D.I. 2016 Species-specific and general allometric equations for estimating tree biomass components of subtropical forests in southern China. *European Journal of Forest Research* 135(5), 963-979.
- Xiao, C.W. and Ceulemans, R. 2004 Allometric relationships for below-and above-ground biomass of young Scots pines. *Forest Ecology and Management* 203(1-3), 177-186.
- Xiao, X., White, E.P., Hooten, M.B. and Durham, S.L. 2011 On the use of log-transformation vs. nonlinear regression for analyzing biological power laws. *Ecology* 92(10), 1887-1894.
- Xu, Y., Zhang, J., Franklin, S.B., Liang, J., Ding, P., Luo, Y., Lu, Z., Bao, D. and Jiang, M. 2015 Improving allometry models to estimate the above-and belowground biomass of subtropical forest, China. *Ecosphere* 6(12), 1-15.
- Yang, X., Blagodatsky, S., Liu, F., Beckschaefer, P., Xu, J. and Cadisch, G. 2017 Rubber tree allometry, biomass partitioning and carbon stocks in mountainous landscapes of sub-tropical China. *Forest Ecology and Management* 404, 84-99.
- Zhang, H.M. 2016 Biomass of *Mytilaria laosensis* plantation on site of continuous Chinese fir (*Cunninghamia lanceolata*) monoculture. *Journal of Fujian Forestry Science and Technology* 43, 49-54 (in Chinese).
- Zheng, L., Cai, D.X., Lu L.H., M, A.G., Li C.Y. 2014 carbon pool of different species plantation ecosystems in lower subtropical area of China. *Journal of Central South University of Forestry and Technology* 34(12), 110-116 (in Chinese).
- Zianis, D., Xanthopoulos, G., Kalabokidis, K., Kazakis, G., Ghosn, D. and Roussou, O. 2011 Allometric equations for aboveground biomass estimation by size class for *Pinus brutia* Ten. trees growing in North and South Aegean Islands, Greece. *European Journal of Forest Research* 130(2), 145-160.

Supplementary Material



Appendix: Supplementary Figure S1.

Anhang: Supplementary Figure S1.

Diameter at breast height (cm)	Tree height (m)	Crown diameter (m)	Biomass (kg)			
			Leaf	Branch	Stem	Root
10.5	14.1	2.4	0.73	2.46	27	10.82
10.9	14.5	2.5	0.7	2.39	26.26	9.81
11.3	14.6	2.38	0.88	2.95	33.29	11.22
11.4	14.8	2.5	0.75	3.01	31.72	11.51
12.7	15.2	2.8	1.4	4.67	48.45	14.71
13	15.8	2.45	1.35	4.14	43.1	15.13
13.1	15.4	2.95	1.61	4.57	46.15	14.37
13.2	15	2.8	1.32	3.26	43.49	16.35
13.5	14.9	3.2	1.24	4.99	41.81	13.42
13.5	15.28	3.5	1.32	4.95	45.15	13.37
13.5	14.9	3.1	1.12	4.86	48.15	13.99
14.2	15.5	3.15	1.68	4.61	54.11	14.41
14.4	15.8	3.2	1.57	4.98	55.63	17.12
15	16.6	3.51	1.71	5.95	59.19	18.22
15.2	15.7	3.69	1.73	6.38	60.24	16.54
15.8	16.3	3.96	2.3	7.68	69.75	19.25
15.9	15.8	3.74	1.9	7.52	71.44	21.12
16.1	16.5	4.03	2.14	7.07	73.84	20.78
16.3	16.4	3.98	2.24	7.33	74.28	21.69
16.3	16.7	4.12	1.89	7.37	75.27	20.69
16.3	17.1	4.3	2.15	7.62	79.87	20.89
16.6	16.5	4.03	2.27	8.41	78.52	20.58
16.9	16.7	4.12	2.11	7.99	84.76	22.13
17	16.5	4.03	2.54	10.55	85.74	23.85
17	16.8	4.16	2.1	7.21	73.43	19.71
17	16.4	3.98	1.99	8.11	73.21	18.47
17.8	17.5	4.44	2.61	9.2	91.66	24.21
17.9	17	4.25	2.98	7.9	93.27	23.88
18.1	17.4	4.44	2.6	10.42	98.03	25.74
18.1	17.3	4.4	2.92	8.26	94.63	24.4
18.3	17.9	4.25	2.88	11.5	95.42	27.79
18.3	17.6	4.54	2.78	8.73	91.95	21.86
18.4	17.8	4.64	2.87	10.86	103.06	27.28
18.5	16.8	4.16	2.47	8.53	100.15	24.93
18.9	17.5	4.49	3.1	12.53	106.22	27.94
19.2	17.8	4.64	3.29	11.61	104.79	27.84
19.2	17.5	4.49	3.22	10.96	115.05	29.46
19.8	17.1	4.3	3.5	13.75	103.21	27.87
19.9	18.1	4.8	3.12	11.97	116.74	32.4
20.5	17.9	4.8	3.7	13.3	112.25	30.21
20.9	18.2	4.85	3.81	14.71	131.87	35.07
21.5	17.9	4.6	4.2	15.66	134.9	41.1

Appendix: Supplementary Figure S2.

Anhang: Supplementary Figure S2.

Other studies	Allometric Equations			
	Stem	Root	Branch	Leaf
Ming et al. (2012)	$W_s = 0.1740(D^2H)^{0.7661}$	$W_r = 0.0094(D^2H)^{0.9538}$	$W_{br} = 0.0002(D^2H)^{1.2696}$	$W_{lf} = 0.0002D^{3.2304}$
Wu (2005)	$W_s = 0.0344(D^2H)^{0.9340}$	$W_r = 0.0479(D^2H)^{0.7624}$	$W_{br} = 0.0586(D^2H)^{0.6985}$	$W_{lf} = 0.0123(D^2H)^{0.6984}$
Zhang et al. (2016)	$W_s = 0.0171(D^2H)^{0.9901}$	$W_r = 0.1017(D^2H)^{0.6653}$	$W_{br} = 0.0252(D^2H)^{0.7587}$	$W_{lf} = 0.0155(D^2H)^{0.6733}$

Appendix: Supplementary Figure S3.

Anhang: Supplementary Figure S3.

137. Jahrgang (2020), Heft 2, S. 109-132

**Austrian Journal of
Forest Science**

Centralblatt
für das gesamte
Forstwesen**Stoichiometric characteristics of ecological-economic forests in karst rocky desertification areas of southern China****Stöchiometrische Eigenschaften von verkarsteten Öko-ökonomischen Wäldern in Südchina**Yu Zhang¹, Kangning Xiong^{1*}, Yao Qin¹, Yanghua Yu¹, Tingling Li¹

Keywords: *karst; plantations; afforestation, biogeochemistry; litter, soil, Eucalyptus robusta, Cupressus funebris, Eriobotrya japonica, Zanthoxylum bungeanum, Juglans regia*

Schlüsselbegriffe: *Karst, Aufforstungen, Wiederbewaldung, Streu, Boden, Biogeochemie; Eucalyptus robusta, Cupressus funebris, Eriobotrya japonica, Zanthoxylum bungeanum, Juglans regia*

Abstract

Investigating the eco-stoichiometric characteristics of carbon (C), nitrogen (N), and phosphorus (P) in plants, leaf litter, and soil of revegetated forests in areas of karst rocky desertification can improve our understanding of nutrient cycling and stability of karst ecosystems. In this paper, we selected five forest types typical for South China karst regions to study the stoichiometry of C, N, and P, and their internal correlation with the "plant leaf-litter-soil continuum". The five forest types were Chinese weeping cypress (*Cupressus funebris* Endl.) mixed with Eucalyptus (*Eucalyptus robusta* Smith), loquat (*Eriobotrya japonica* (Thunb.) Lindl.), Chinese prickly ash (*Zanthoxylum bungeanum* Maxim.), walnut (*Juglans regia* Linn.), and teak (*Tectona grandis* Linn. f.). The average C, N, and P contents in the leaves of the five species were 481.66, 14.68,

¹ School of Karst Science, Guizhou Normal University / State Engineering Technology Institute for Karst Desertification Control, Guiyang, 550001, China

*Corresponding author: Kangning Xiong, hxcandzy@163.com

and 2.23 mg g⁻¹, respectively; in leaf litter 434.52, 9.22, and 1.70 mg g⁻¹, and in soil 36.74, 2.85, and 0.64 mg g⁻¹. The vegetation of the eco-economic forest in the karst area was low in N, rich in P, and had a relatively high C storage. The order of C:N ratios was leaf litter > plant leaf > soil for all forests, except for the teak forest. No statistically significant difference was observed in soil C: N ($P > 0.05$). N and P content in plant leaves was significantly positively correlated with that in leaf litter ($P < 0.05$), although the reabsorption rate of N and P was relatively low. The reabsorption rate may not be an important adaptation mechanism to plant nutrient limitation, but appears to be an intrinsic characteristic of the studied species. Productivity was not correlated with C, N, or P in plant, litter, and soil and was probably influenced by other factors than nutrient supply. The grade of rocky desertification strongly affected the C storage. For our study region we estimated a potential C sequestration in litter alone of 3748 t C (in decreasing order, the potential, mild, moderate, and severe rock desertification areas contributed 1220.40 t, 1566.87 t, 556.60 t, and 403.59 t). This study contributes to our understanding of nutrient uptake and utilization of nutrients by tree species in karst areas and provide a theoretical basis for vegetation restoration and reconstruction to control karst rocky desertification.

Zusammenfassung

Eine Untersuchung der stöchiometrischen Eigenschaften von Kohlenstoff (C), Stickstoff (N) und Phosphor (P) in Pflanzen, Streu und Böden von rekultivierten Wäldern in einem ökologisch fragilen, zum Karst verwüsteten, felsigen Gebiet ermöglicht ein besseres Verständnis deren Nährstoffkreisläufe. In dieser Studie haben wir fünf Waldtypen des südchinesischen Karst ausgewählt, Zypresse (*Cupressus funebris* Endl.) gemischt mit Eukalyptus (*Eucalyptus robusta* Smith), japanische Mispel (*Eriobotrya japonica* (Thunb.) Lindl.), Szechuan-Pfefferbaum (*Zanthoxylum bungeanum* Maxim.), Walnuss (*Juglans regia* Linn.) und Teak (*Tectona grandis* Linn. f.). Es zeigte sich, dass der durchschnittliche Gehalt von C, N und P in der Laubmasse der fünf Pflanzen 481.66, 14.68 und 2.23 mg g⁻¹ war, in der Laubstreu 434.52, 9.22, und 1.70 mg g⁻¹ und im Boden 36.74, 2.85 und 0.64 mg g⁻¹. Die Vegetation dieser Wälder war somit arm in N, reich an P und zeigte eine relativ hohe Kapazität für C-Speicherung. Das C:N Verhältnis war in der Reihenfolge Laubstreu > Pflanzenblatt > Boden, außer für den Teak Wald. Wir fanden keine statistische Signifikanz in den C:N-Verhältnissen in den Böden ($P > 0.05$). Der Gehalt von N und P in den Blättern war signifikant positiv korreliert mit C und N in der Laubstreu ($P < 0.05$). Die Reabsorptionsrate von N und P war relativ gering und offensichtlich ist die Reabsorptionsrate in einem Karst-Milieu kein wichtiger Mechanismus zur Anpassung an den Nährstoffbedarf von Pflanzen. Die Reabsorptionsrate scheint hingegen ein inhärentes Merkmal der untersuchten Baumarten zu sein. Produktivität hatte keinen Zusammenhang mit C-, N- und P-Gehalt und steht offensichtlich unter dem Einfluss anderer Faktoren. Die Kohlenstoffspeicherung wirdentscheidend vom Grad der Verkarstung beeinflusst. Schätzungen der potenziellen Kohlenstoffreserven in der Streu sind 3748 t für das Untersuchungsgebiet (in absteigender Reihenfolge potenzielle, milde, mäßige und schwere Verkarstung 1220.40

t, 1566.87 t, 556.60 t und 403.59 t). Diese Studie kann zu einem Verständnis von Nährstoffaufnahme in Aufforstungen in Karstgebieten beitragen. Außerdem liefert sie eine theoretische Basis für die Restoration und Rekonstruktion von Vegetationen zur Kontrolle von Verkarstungen.

1. Introduction

Ecological stoichiometry studies the interaction of various elements in ecosystems, mainly how the balance and interaction of carbon (C), nitrogen (N), and phosphorus (P), and other elements affect ecosystems and ecological processes (Sturner and Elser 2002). C, N, and P are essential elements for all living matter. Soil nutrient supply, plant nutrient requirements, self-regulation of nutrient requirement by plants, and nutrient return by litterfall and litter decomposition are accomplished through transformation of C, N, and P. Therefore, ecological stoichiometry is an important method for the study of chemical cycles in biological systems (Agren and Bosatta 1998; Shen et al. 2019).

There are differences in the stoichiometric characteristics of different climatic regions. Studies have shown that the productivity of temperate and boreal forests is mainly limited by N, while the productivity of tropical rainforests and subtropical evergreen forests is generally limited by P (Aerts and Chapin 2000; Aerts et al. 2003). These findings have been confirmed at a global scale; however, there is a sparsity of research on the stoichiometric characteristics of vegetation at a regional level and within various landform types. Currently, much research is conducted on the coupling of stoichiometric characteristics and environmental factors, mostly focusing on three ecosystems: forests, wetlands, and grasslands (Kerkhoof et al. 2006; Yan et al. 2010; Zhang et al. 2017; Ye et al. 2016; Zhao et al. 2016). Previous research focused more on stoichiometric characteristics of different successional stages, seasonal changes, vegetation types, different plant organs, and spatial variability such as latitude and longitude (Liu et al. 2010; Zhou et al. 2010; Wardle et al. 2004; Sun et al. 2018; Zhao et al. 2018; Wang et al. 2018). Stoichiometry studies have often focused on single components (soil or vegetation) or single plant organs (plant leaves or fine roots). Consequently, there are still many research gaps in the study of stoichiometry in terms of vegetation, litter, and soil as a whole system, particularly at a regional scale.

Karst rocky desertification is a process of land degradation caused by dissolution of soluble rocks such as limestone and dolomite. Human activities can promote karst rocky desertification by vegetation damage and soil erosion, which increase the speed by which rock is exposed, eventually leading to a decline in land productivity. Finally, the soil surface becomes dominated by bare rocks which is visually similar to a desert landscape (Yuan 1997). Karst landforms are frequent worldwide, particularly in Mediterranean Europe, south Australia, the Russian Ural mountains, Kentucky and Indiana in the United States, South China, and Cuba (Gao et al. 2003).

Consequently, many countries have paid attention to the effect of karst on soil formation and vegetation. In China, karst landforms are particularly widespread, covering an area of 1.24 million ha (approx. 13% of the total land mass of China). China's karst rocky desertification is mainly present in the southwest centered on the Guizhou Plateau, and it represents one of three major ecological problems in China (Xiong et al. 2012; Yuan and Zhang 2008; Yue et al. 2011). The main challenges caused by karst rocky desertification are its ecological fragility, low ecological carrying capacity, and slow recovery, which impairs the economic and social sustainable development of karst-affected regions. Unsuitable land use is the dominant reason for rocky karst desertification in the southwest karst region (Yuan 1997). Karst rocky desertification restricts plant growth, the establishment of secondary forests leading to stunted tree growth, and it is problematic both for regional socio-economic development and the healthy ecological functioning of ecosystems (Gra and Hetherington 2004). Therefore, to control karst rock desertification, the ecological and economic functions of ecosystems have to be balanced to ameliorate environmental conditions and improve ecosystem health. Studies have shown that afforestation of woody plants with high calcium and drought tolerance, and conservation of soil and water, are important for sustainable land management in karst regions (Zhang et al. 2019). Afforestation, which considers local conditions, may be an effective way to ecologically restore and control karst rocky desertification.

The ecosystems in southwest China karst are fragile and sensitive to environmental stress and disturbances (Xiong et al. 2016; Xiong et al. 2017). Since the 1990s, a large number of vegetation restoration projects have been carried out to control karst rocky desertification, and large-scale eco-economic forests have been planted. The ecological status of karst has been significantly improved since the development of these projects. To date, China has planted 5.5 million hectares of Chinese weeping cypress (*Cupressus funebris* Endl.), 4.5 million hectares of Eucalyptus (*Eucalyptus robusta* Smith), 13,000 hectares of loquat (*Eriobotrya japonica* (Thunb.) Lindl.), 833,300 hectares of Chinese prickly ash (*Zanthoxylum bungeanum* Maxim.), 440,000 hectares of walnut (*Juglans regia* Linn.) and 4,000 hectares of teak (*Tectona grandis* Linn. f.) (Xiong et al. 2002). However, studies on vegetation restoration in the control of karst rocky desertification have largely focused on grassland productivity and establishing economic forests (Xiong et al. 2002). There has been limited research on the mechanisms of degradation and the effect of adaptive rehabilitation technology such as afforestation. The interactions between plants, litter, and soil in these ecosystems are still unclear, which may potentially lead to continued degradation, and a decrease in productivity or failure of restoration projects.

The aims of this study were to investigate the stoichiometry of C, N, and P of leaf-litter-soil in eco-economic forests in karst rocky desertification areas. The objectives were:

1. to quantify nutrient cycling and nutrient absorption of five important ecoecono-

- mic forest types in SE China karst regions, and explore the relationship between nutrient cycling and productivity, and
2. to provide a theoretical basis for the restoration, reconstruction, and management of eco-economic forests in karst rocky desertification regions.

2. Material and Methods

2.1 Study region

South West China has eight provinces with karst formations, and our study region is located in Guizhou province (Fig. 1). The demonstration area of Guanling-Zhenfeng Huajiang for studying comprehensive treatments for karst rocky desertification is located in the southwest part of the Guizhou province (105°36'30"–105°46'30"E, 25°39'13"–25°41'00"N). Huajiang canyon of the Beipanjiang river is a typical karst valley area on the Guizhou Plateau. It has a subtropical monsoon climate (Fig. 1) with an annual average temperature of 18.4 °C, an annual average rainfall of 1100 mm, and the elevation ranges from 450 to 1450 m. The experimental plots used in this study are located at elevations from 526 to 1133 m, representing a wide elevation gradient, which may also cause differences in soil fertility and nutrients between the sites. The karst area accounts for 87.92% of the total demonstration area of 51.62 km², and the area of karst rocky desertification is 13.52 km² with potential, mild, moderate, and severe karst rocky desertification contributing to 3.32 km² (24.54%), 5.47 km² (40.48%), 2.42 km² (17.93%), and 2.31 km² (17.06%) of the area, respectively (Fig. 2). The dominant soil types are calcisols with discontinuous distribution and poor water-holding capacity, which are inadequate for agriculture or as pasture due to the shallow soil.

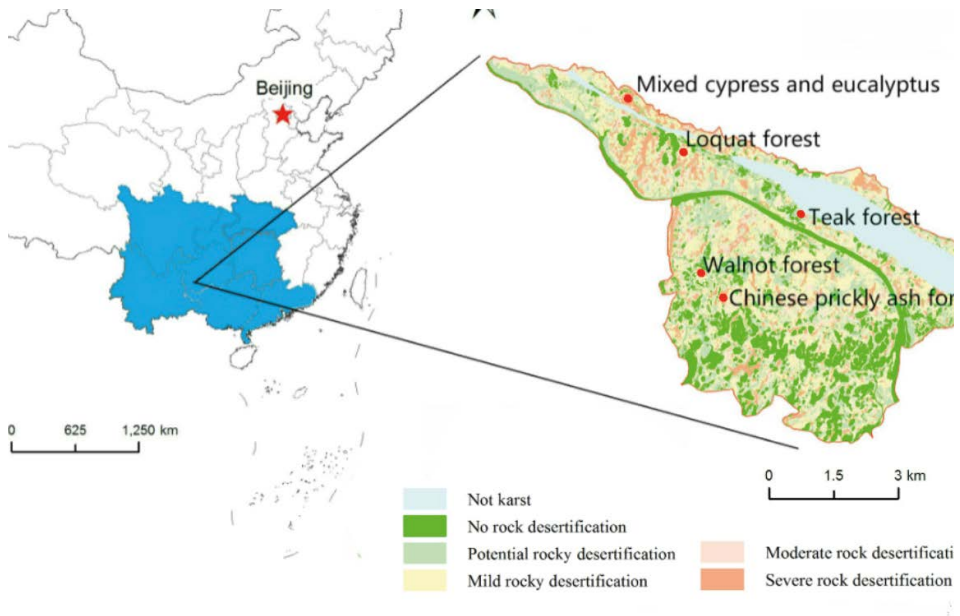


Figure 1: Location of study area for karst rocky desertification control in Guizhou in southeast China and the grades of desertification.

Abbildung 1: Lage des Untersuchungsgebietes in Guizhou, Südostchina, und die unterschiedliche Intensität der Verkarstung.

We studied five tree species, which are favoured for karst rocky desertification control: cypress (*Cupressus funebris* Endl.) mixed with eucalyptus (*Eucalyptus robusta* Smith), loquat (*Eriobotrya japonica* (Thunb.) Lindl.), Chinese prickly ash (*Zanthoxylum bungeanum* Maxim.), walnut (*Juglans regia* Linn.), and teak (*Tectona grandis* Linn. f.). The management of the forests is conducted under the guidance of the provincial government. The selected stands are about 20 years old. For the duration of the research, the stands received the same fertilizer treatment with a compound fertilizer applied in April and August at 45 kg per hectare. Trunk diameter was measured at 50 cm height in Chinese prickly ash, and at 1.3 m for other tree species. 5 m × 5 m subplots were established in three 30 m × 30 m plots, and the number of plants and their trunk diameters were measured in each plot. The number of plants and their diameters (basal area) per hectare were estimated by averaging the number of trees and diameter in the three plots. The basic characteristics are summarized in Table 1.

Table 1: Stand characteristics of the studied forests. KRD is kart rocky desertification.

Tabelle 1: Zusammenfassung der Bestandeseigenschaften der untersuchten Wälder. KRD ist der Verkarstungsgrad.

Forest type	Location	Altitude (m)	Grade of KRD	Slope (°)	Stem number (ha ⁻¹)	Average diameter (cm)	Basal area (m ² /ha)	Age (year)	Tree height (m)	Canopy cover (%)
Mixed cypress and eucalyptus	25° 42' 16" N 105° 37' 11" E	1133	Severe	18	800	11.68	9.50	24	11.28	88
Loquat	25° 41' 32" N 105° 37' 58" E	817	Moderate	7	400	11.89	4.56	18	9.34	80
Chinese prickly ash	25° 39' 23" N 105° 38' 35" E	773	Severe	15	600	5.64	1.68	20	2.03	68
Walnut	25° 39' 24" N 105° 38' 21" E	804	Mild	12	420	10.91	3.92	23	8.13	81
Teak	25° 40' 25" N 105° 39' 56" E	526	Potential	15	700	12.90	9.43	19	13.54	73

2.2 Field sample collection and pretreatment

Three plots of 30 m × 30 m were used for each of the five forest types. All field measurements were taken in late August 2017. Five to six plants with similar growth were randomly selected in the plots, and 1,000 g of healthy mature leaves (50% sun leaves, 50% shade leaves) from four directions of the canopy were collected, mixed, and dried in the lab at 105 °C for 15 min. Undecomposed and semi-decomposed litter was collected from multiple areas in four plots sized 1 m × 1 m, mixed and brought back to the lab. Tree branches, humus, and other debris in the litter layer were removed in order to analyze the relationship between plant leaves and leaf litter. All samples were dried at 65 °C in an oven until constant weight was reached. A subsample of the plant leaves and the leaf litter was pulverized into 0.1 mm powder with a shredder to determine the soil organic C, total N, and total P. Soil was collected from the root zones of three or four small plots along an "S" route at a depth of 0–10 cm (the actual soil depth was recorded, if the soil depth was less than 10 cm). After thorough mixing, about 1 kg of soil from each forest type was sampled by quartation and taken back to the lab. They were air-dried and separated from impurities such as animals, plant debris, and gravel. Then, the soil samples were ground with an agate pestle and mortar. After sieving through a 100-mesh nylon screen, the resulting samples were stored in plastic bags for the determination of chemical properties.



Figure 2: Study site for mixed cypress and eucalyptus.

Abbildung 2: Untersuchungsfläche mit Zypressen gemischt mit Eukalyptus.



Figure 3: Study site of walnut (left) and Chinese prickly ash (right).

Abbildung 3: Untersuchungsfläche mit Walnuss (links) und Szechuan-Pfefferbaum (rechts).

2.3 Elemental analysis

Organic C was measured using the modified Mebius method (Nelson et al. 1982). Total N was measured using the modified Kjeldahl wet digestion procedure (Gallaher et al. 1976) and a 2300 Kjelttec Analyzer Unit (FOSS, Sweden), and total P was measured using the molybdate-blue reaction (Bao 2000) with a UV-2450 spectrophotometer (Shimadzu Scientific Instruments, Japan). This method was used for plant leaves, litter, and soil.

2.4 Data processing and statistical analysis

The initial analysis and sorting of data were carried out with MS Excel 2010, and statistical analyses were performed by SPSS 20.0 (SPSS, Chicago, IL, USA) software. One-way ANOVA was employed to test the significance of the nutrient content in leaves, leaf litter, and soil, and their ratios (C:N, C:P, N:P). Least Significant Difference method was applied for multiple comparisons. Pearson correlation analysis was used to show the relationship of each component's ecological stoichiometry.

Litter and potential storage of soil carbon were calculated by carbon storage per unit area and the area of rocky desertification of different grades. Mixed cypress – eucalyptus and Chinese prickly ash both belong to severe rocky desertification areas, and their carbon storage per unit area was estimated as the average of the two. Soil depth was different in the severe karst rocky desertification compared to the other grades of desertification. The average thickness of the severe rocky desertification area was 5 cm, and 10 cm for other classes. The graphs were drawn with the program Origin8.6. The equation is as follows:

$$\text{SOC} = C \times D \times E \times \frac{1 - G}{10}$$

In the formula, SOC is the soil organic carbon storage (t ha^{-1}), C is the soil organic carbon content (g kg^{-1}), D is the soil bulk density (g cm^{-3}), E is the soil thickness (cm), G is the volume proportion of gravel with diameter $> 2 \text{ mm}$ (%).

$$\text{Potential C storage} = \text{C density} \times \text{Karst rocky desertification area}$$

Nutrient (N and P) reabsorption rate was calculated as the percentage of the difference in the nutrient content between plants and leaf litter and the nutrient content in plants, and it was calculated as previously described by Wang et al. (2011). The equation is as follows:

$$\text{N(P)Reabsorption rate(\%)} = \frac{\text{N(P)content in plants} - \text{N(P)content in litter}}{\text{N(P)content in plants}} \times 100\%$$

3. Results

3.1 The characteristics of C, N, and P in plant leaf-litter-soil

The standing leaf litter of mixed cypress and eucalyptus was 4.53 t ha⁻¹, for loquat 5.35 t ha⁻¹, Chinese prickly ash 3.48 t ha⁻¹, walnut 6.51 t ha⁻¹, and teak forest was 8.80 t ha⁻¹. The average contents of C, N, and P in leaves from the five plant communities were 481.66, 14.68, and 2.23 mg g⁻¹, respectively. The content in leaf litter was 434.52, 9.22, and 1.70 mg g⁻¹, which was 36.74, 2.85, and 0.64 mg g⁻¹ of soil, respectively. The content of C, N, and P in plant leaves was significantly different from those in soil in all five forests, and the order of the average C, N, and P content was plant leaves>litter>soil. In addition, significant differences were observed in N and P content in different plant communities (Table 2).

Table 2: Content of C, N, and P in plant, leaf litter, and soil from five communities (mg g⁻¹) (Mean ± standard error). Different capital letters in the same column indicate significant differences (P<0.05) between plant-litter-soil in same nutrient. Different lowercase letters in the same row indicate significant differences (P<0.05) among different species.

Tabelle 2: Gehalt von C, N, und P in Pflanzen, Laubstreu und Böden in fünf Gemeinden (mg g⁻¹) (Mean ± Standardfehler). Unterschiedliche Großbuchstaben in derselben Spalte zeigen signifikante Unterschiede (P<0.05) zwischen den Nährstoffen in den Pflanzen, Laubstreu und Böden an. Unterschiedliche Kleinbuchstaben in derselben Spalte weisen auf signifikante Unterschiede (P<0.05) zwischen unterschiedlichen Spezies.

Content	Item	Mixed cypress and eucalyptus	Loquat forest	Chinese prickly ash forest	Walnut forest	Teak forest
C (mg g ⁻¹)	plant	489.09±33.12 ^{aA}	483.24±18.18 ^{aA}	458.01±16.65 ^{aA}	503.80±17.57 ^{aA}	474.14±19.12 ^{aA}
	litter	441.04±6.68 ^{aA}	427.75±35.61 ^{aA}	433.76±4.99 ^{aA}	442.37±27.90 ^{aB}	427.70±0.34 ^{aA}
	soil	39.92±1.69 ^{aB}	26.02±1.91 ^{bB}	40.37±0.527 ^{aB}	9.57±0.38 ^{cC}	67.79±8.08 ^{dB}
N (mg g ⁻¹)	plant	9.89±0.08 ^{aA}	11.67±0.03 ^{bA}	22.46±0.20 ^{eA}	18.81±0.08 ^{dA}	10.59±0.15 ^{eA}
	litter	5.89±0.38 ^{aB}	8.81±0.36 ^{bB}	11.68±0.08 ^{eB}	13.20±0.47 ^{dB}	6.50±0.34 ^{aB}
	soil	3.92±0.75 ^{aC}	2.55±0.18 ^{bC}	3.82±0.15 ^{aC}	2.46±0.02 ^{bC}	1.49±0.09 ^{cC}
P (mg g ⁻¹)	plant	1.40±0.02 ^{aA}	1.23±0.08 ^{bA}	3.81±0.01 ^{eA}	2.69±0.01 ^{dA}	2.00±0.04 ^{eA}
	leaf	1.095±0.063 ^{aB}	1.10±0.02 ^{aAB}	3.04±0.08 ^{bB}	2.17±0.09 ^{bB}	1.07±0 ^{aB}
	soil	0.94±0.05 ^{aC}	0.98±0.03 ^{bB}	0.23±0.00 ^{cC}	0.90±0.01 ^{bC}	0.16±0.01 ^{dC}

3.2 The ecological stoichiometric ratio of C-N-P

The C:N ratio ranged from 20.39 to 49.48 of the leaf materials from five communities with an average of 36.58. In leaf litter, its range was 33.51–83.77 with an average of 54.54. In soil, it was 3.89–45.82 with an average of 16.20. The averages of C:P of leaf, leaf litter, and soil were 257.60, 334.88, and 134.59, respectively, which indicates that the differences were significant between leaf materials from different communities. The averages of N:P were 6.96, 6.10, and 7.09 in leaf, leaf litter, and soil. Thus, various communities varied in their stoichiometric ratios, and differentiation regularities were completely consistent, showing that C:N and C:P were higher than N:P. Except for teak forest, C:N ratios of leaf-litter-soil followed the pattern of litter>leaf>soil, and no significant difference of C:N was observed among soil samples ($P>0.05$) (Fig. 4).

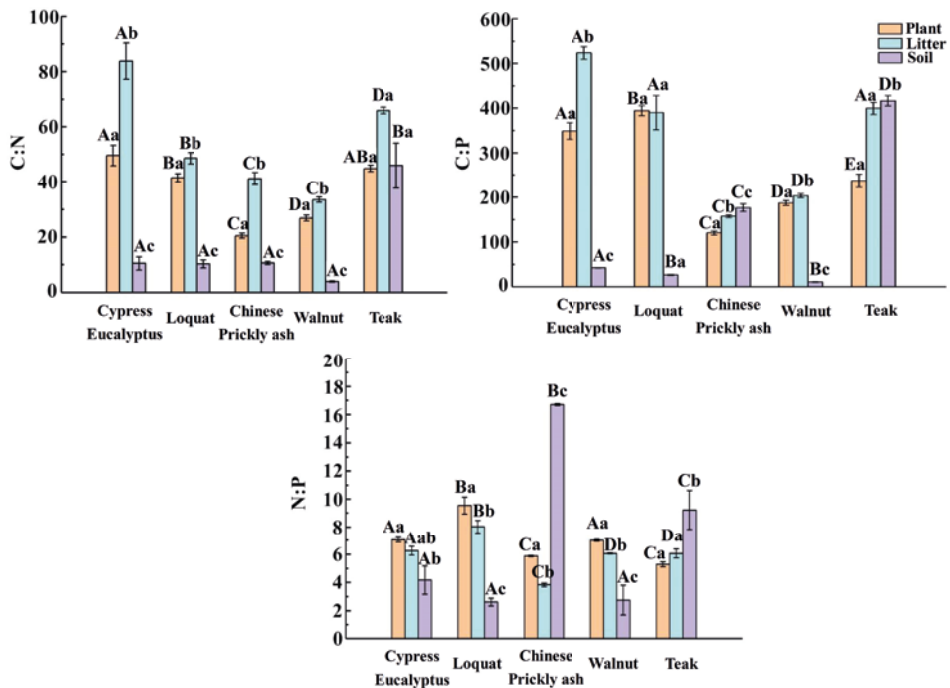


Figure 4: C:N, C:P, and N:P of leaves, leaf litter, and soil from five plant communities (Mean \pm standard error). Different capital letters indicate significant differences ($P<0.05$) among different species in the same component, different lowercase letters indicate significant differences ($P<0.05$) between plant - litter - soil.

Abbildung 4: C:N, C:P und N:P für Blätter, Laubstreu und Böden von fünf Pflanzengemeinschaften (Mean \pm SE). Unterschiedliche Großbuchstaben zeigen signifikante Unterschiede ($P<0.05$) zwischen unterschiedlichen Spezies, unterschiedliche Kleinbuchstaben signifikante Unterschiede ($P<0.05$) zwischen Pflanzen-Laubstreu-Böden.

3.3 Carbon and nutrient pools in afforestations in karst rocky desertification areas

Litter C storage in cypress and eucalyptus was 199.79 g m^{-2} ; loquat, 230.05 g m^{-2} ; Chinese prickly ash 149.64 g m^{-2} ; walnut 286.44 g m^{-2} , and teak 376.37 g m^{-2} . Average litter C for the entire demonstration area was 249.15 g m^{-2} . The estimated potential carbon reserves of litter in the potential, mild, moderate, and severe rock desertification areas were 1220.40 t, 1566.87 t, 556.60 t, and 403.59 t, respectively (sum 3748 t).

Carbon storage in the soil under the trees was 6980 g m^{-2} for teak, 2694 g m^{-2} for loquat, 973 g m^{-2} for walnut, 3730 g m^{-2} for Chinese prickly ash, and 1900 g m^{-2} for cypress and eucalyptus. They represent four different grades of rocky desertification areas. According to calculations, the potential carbon reserves of soil in the potential, mild, moderate, and severe rock desertification areas were 23172.47 t, 5302.64 t, 6520.00 t, and 4439.04 t, respectively (sum 39434 t). Soil carbon storage was thus 10.5 times higher than litter carbon.

Table 3: Carbon storage of litter and soil.

Tabelle 3: Kohlenstoffspeicherung von Streuschicht und Boden.

Karst rocky desertification	Area (km ²)	Litter carbon density (g m ⁻²)	Total litter carbon (t)	Soil depth (cm)	Bulk density (g cm ⁻³)	Volume of gravel > 2 mm (%)	SOC (g m ⁻²)	Total soil carbon (t)
Potential	3.32	376.37	1220.40	10	67.79	10	6980	23172.47
Mild	5.47	286.44	1566.87	10	26.02	14	973	5302.64
Moderate	2.42	230.05	556.60	10	9.57	12	2694	6520.00
Severe	2.31	174.72	403.59	5	40.145	15.5	2815	4439.04
All	13.52		3747.37					39434.15

3.4 The correlation of ecological stoichiometric characteristics

The correlation analysis of leaves, leaf litter, soil, and productivity (diameter of basal area) showed no correlation between C and tested elements. The N and P content

of plant material exhibited a significant correlation to N, P, C: N, and C:P in leaf litter ($P < 0.05$). The correlation between plant N and P and the stoichiometric ratio of plant and leaf litter was relatively significant, and a very close correlation was observed between living leaf material and leaf litter. Soil N exhibited an extremely significant positive correlation to C: N and C:P with a correlation coefficient of 0.889 and 0.890, respectively. In addition, soil P was significantly correlated to C:P and N:P in both plants and soil, suggesting that the soil element dynamic balance affects the storage characteristics of nutrient stoichiometry of leaf material. Productivity (basal area) showed no correlation with the tested elements ($P > 0.05$).

Table 4: The correlation between the ecological stoichiometric characteristics of plant-litter-soil. Yellow and blue indicate significant correlations at the $p < 0.05$ and 0.01 , respectively.

Tabelle 4: Korrelation zwischen den ökologisch-stöchiometrischen Eigenschaften der in Pflanzen-Laubstreu-Böden. Gelb und blau weist darauf hin, dass die Korrelation signifikant sind auf der $p < 0.05$ und $p < 0.01$.

Item		plant			litter			soil			plant			litter			soil			productivity basal area
		C	N	P	C	N	P	C	N	P	C:N	C:P	N:P	C:N	C:P	N:P	C:N	C:P	N:P	
plant	C	1																		
	N	-0.191	1																	
	P	-0.318	-0.931	1																
litter	C	0.23	0.104	0.49	1															
	N	0.116	0.889	0.702	0.193	1														
	P	-0.239	0.985	0.956	0.129	0.808	1													
soil	C	-0.013	0.306	0.243	0.258	0.097	0.406	1												
	N	-0.477	-0.399	-0.059	-0.267	-0.693	-0.299	-0.249	1											
	P	0.53	-0.289	-0.587	0.142	0.027	-0.357	0.201	-0.702	1										
plant	C:N	0.257	-0.984	-0.898	-0.066	-0.908	-0.947	-0.178	0.411	0.279	1									
	C:P	0.288	-0.831	-0.955	-0.024	-0.627	-0.846	-0.027	-0.05	0.655	0.813	1								
	N:P	0.227	-0.258	-0.575	0.053	0.038	-0.3341	0.079	-0.599	0.798	0.198	0.727	1							
litter	C:N	-0.049	-0.857	-0.664	-0.019	-0.967	-0.767	-0.026	0.637	0.019	0.892	0.565	-0.118	1						
	C:P	0.106	-0.987	-0.927	-0.05	-0.879	-0.976	-0.319	0.407	0.262	0.957	0.843	0.307	0.838	1					
	N:P	0.344	-0.583	-0.77	-0.057	-0.198	-0.697	-0.529	-0.251	0.549	0.481	0.748	0.753	0.096	0.618	1				
soil	C:N	-0.315	-0.445	-0.143	-0.303	-0.568	-0.412	-0.647	0.889	-0.664	0.402	-0.052	-0.541	0.501	0.445	0.03	1			
	C:P	-0.414	-0.149	0.181	-0.228	-0.37	-0.096	-0.5	0.89	-0.886	0.132	-0.337	-0.72	0.311	0.164	-0.235	0.93	1		
	N:P	-0.581	0.557	0.769	-0.059	0.162	0.652	0.267	0.48	-0.861	-0.504	-0.699	-0.648	-0.198	-0.519	-0.759	0.24	0.554	1	
productivity	basal area	0.363	0.3673	0.628	-0.194	0.067	0.624	0.572	-0.444	0.629	0.626	0.5124	-0.592	0.547	0.514	-0.345	0.519	0.487	0.624	1

3.5 The reabsorption rate of N and P in five tree communities

The reabsorption rates of N in the five plant communities ranged from 19.98% to 48.75% with an average of 36.30%, and its range was 5.88%–47.56% of P with an average of 23.61%. The highest reabsorption rate of N among the five species was observed in Chinese prickly ash forest, followed by cypress and eucalyptus, teak, loquat, and walnut. Teak exhibited the highest reabsorption rate of P, followed by cypress and eucalyptus, Chinese prickly ash, walnut, and loquat. Overall, teak showed a relatively high reabsorption rate of N and P, and the reabsorption rate of N was higher than that of P in all plant communities except for teak (Fig. 5).

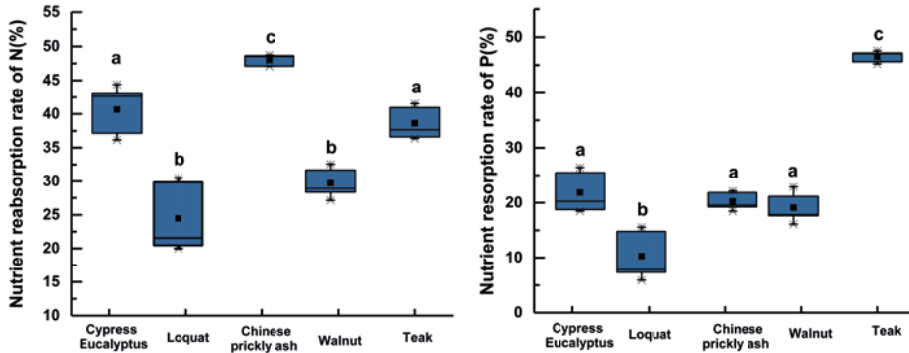


Figure 5: The reabsorption rate of C and P of five plant communities. Different lowercase letters indicate significant differences ($P < 0.05$). The box represents 95th and 5th percentile; line in the box is median; \star is maximum value; \times is minimum and \blacksquare is mean.

Abbildung 5: Die Reabsorptionsrate von C und P in fünf Pflanzengemeinschaften. Unterschiedliche Kleinbuchstaben weisen auf signifikante Unterschiede ($P < 0.05$) hin. Die Box ist 95% und 5% Perzentile, die horizontale Linie in der Bok ist der Median, \star ist der Maximalwert, \times ist das Minimum, und \blacksquare ist der Mittelwert.

4. Discussion

4.1 The content characteristics of C, N, and P of plant leaf-litter-soil

Our data demonstrated that the C, N, and P content of five economic tree species in the dry hot karst valley exhibited the order of plant leaf > litter > root soil. The C content in leaves was higher than that in leaf litter; this is because organic components such as crude fat, tannin, and soluble sugar decompose after leaf fall (Yang et al. 2007) resulting in a significant decrease in C content in leaf litter. It may also be related to the slower leaf growth rate and reduced photosynthesis prior to leaf fall. The average content of N and P in leaf litter was lower than that in leaves, the reason for which may be that partial nutrients are transferred to other components, reabsorbed, and reused. The decrease of N may also result from the utilization of N for photosynthesis, and the higher N utilization rate lowers the nitrogen level in leaf litter (Zhang et al. 2016); this result is consistent with a previous study by Bai et al. (2016), in which N and P content followed the order of leaf > litter > soil in three types of cultivated forests.

C is the structural element of plants (Xiang et al. 2006), while N and P are the main limiting elements that regulate plant growth in terrestrial ecosystems (Han et al. 2005). In this paper, the average C content in plant leaves was 481.66 mg g^{-1} higher than that reported by Wang et al. (2017) in the plants of natural secondary forest in the Loess Plateau (468.67 mg g^{-1}), and it was also higher than the average C content of 492 terrestrial plant leaves, which was 464 mg g^{-1} reported by Elser et al. (2000), in-

dicating a relatively strong C storage capacity in the ecoeconomic forest in the karst area. This may be determined by the sampling time that was right at the peak of the growth stage in our study, or by the availability of soil elements in sampling areas. The average N content in the leaves of the five plant communities was 14.68 mg g^{-1} , lower than that of the Loess Plateau 21.36 mg g^{-1} (Yang et al. 2014), the average of 753 terrestrial plants of China 18.6 mg g^{-1} (Han et al. 2005), and the average N content of plant leaves worldwide (20.09 mg g^{-1}) (Reich and Oleksyn 2004). Previous studies demonstrated that P content in terrestrial plants in China is lower than that on a global scale (Ren et al. 2007). In this paper, the average P content in the five plant communities was 2.23 mg g^{-1} , significantly higher than the global scale by 0.43 mg g^{-1} (Reich and Oleksyn 2004), and it was also higher than the average for terrestrial plants in China (0.77 mg g^{-1}) (Han et al. 2005). The N deficiency and P rich status of the ecoeconomic forest of karst is mainly due to the substantial bare rock, low vegetation coverage, enriched nutrition in the tree layer, lack of a symbiotic nitrogen fixation system, and low weathering of soil (Hedin 2004). In addition, high P can facilitate the metabolic rate to support the energy demand of macromolecule synthesis, and further protect vegetation against the harsh environment in karst areas (such as poor moisture retention capacity and soil nutrient loss).

Leaf litter plays an important role in forest ecosystems, which is an intrinsic component of nutrient cycling in forest ecosystems and the main source of soil organic matter. The average contents of C, N, and P in leaf litter of five plant communities were 434.52, 9.22, and 1.70 mg g^{-1} , respectively. It was lower than the global scale of N (10.9 mg g^{-1}), while higher than the global scale of P (0.90 mg g^{-1}) (Kang et al. 2010), indicating that leaf litter shows exactly the same characteristics as plants. The reason for such phenomena is that in artificial or secondary forests the dominant tree species and plant community structure are relatively simple and variation in leaves and leaf litter is limited.

Soil nutrient composition is a key factor affecting plant growth, and it plays important roles in maintaining biological and mineral metabolism, providing nutrients and other ecological processes (Bin et al. 2014). The average C, N, and P content in the top 0–10 cm soil layer of five plant communities in the karst area was 36.74, 2.85, and 0.64 mg g^{-1} , respectively, higher than those of forest ecosystems in hilly and gully regions of the Loess Plateau (23.21, 1.91, and 0.57 mg g^{-1}) (Zhao et al. 2017), higher than those of temperate grasslands of Inner Mongolia 0–10 cm soil layer (25.30, 1.70, 0.10 mg g^{-1}) (Yin et al. 2010), and also higher than the 0–20 cm soil layer of north China larch plantations by 13.01, 1.51, and 0.61 mg g^{-1} (Bai et al. 2015). Although the soil layer in the karst area is thin, the nutrient content in the surface soil is very high, the reasons for which may be that the humid and hot climate conditions in the southwest karst area are favorable to the growth of soil microorganisms and small animals, leading to a stronger capacity for "self-fertilization" than other areas (Zeng et al. 2015). Alternatively, it may be attributable to the release of nutrients to soil when a large amount of tree leaf litter, root residues, and secretions decompose together, which is consistent

with the study of Zhang et al. (2012) showing that soil nutrient characteristics in the tree layer are significantly higher than shrub, grassland, and bare land in karst areas.

4.2 The stoichiometric ratio of C, N, and P in plant-litter-soil-productivity and their correlation

C:N and C:P ratios of plants usually reflect the utilization efficiency of N and P in plants, and partially reflect the supply status of N and P in soil (Zeng et al. 2015). Because different pathways control the assimilation of C in photosynthesis and absorption of plant nutrients, C content is high with little variation in most plants, and C is usually not a limiting element for plant growth (Reich and Oleksyn 2004). In this study, C:N and C:P ratios of leaves were 36.57 and 257.60, respectively, higher than those of the global average level (22.50 and 232) (Elser et al. 2004), further suggesting that C:N and C:P ratios are relatively high in the dry hot valley area of karst rocky desertification, and suggests a relatively high utilization rate of N and P. Previous studies have demonstrated that plants exhibit a higher nutrient utilization rate in nutrient deficient conditions, which is a survival strategy for plants to adapt to low nutrient levels (Bowman 1994).

The N:P critical ratio of plant leaves can be regarded as an indicator to assess the nutrient supply status of the environment to plant growth (Aerts and Chapin 2000). The growth rate hypothesis argues that organisms accumulate large amounts of P into rRNA during high-speed growth so that ribosomes can rapidly synthesize large amounts of protein to accelerate growth rate (Elser et al. 2003). The average N:P ratio of the plant leaves in this study was 6.96, which was lower than that of 753 terrestrial plants of China (16.3) (Elser et al. 2004), lower than that of forest leaves in Dinghushan mountain (25.84) (Liu et al. 2010), and lower than that of plant leaves of different life types in north Tianshan mountain (17.36) (Xie et al. 2016). Studies have shown that when the N:P ratio is greater than 16, the ecosystem is restricted by P, the ratio less than 14 indicates that the ecosystem is restricted by N, and when it is between 14 and 16, the ecosystem is simultaneously limited by N and P or nutrients are so abundant that it is not limited (Koerselman and Meuleman 1996). According to the above definition, we found that the N:P ratio of five plants in the karst dry valley is lower than 14, indicating that it is mainly restricted by N and the application of N fertilizer can increase the biomass yield of vegetation. The reason is that in the management of plantation forests in the study area, the application of compound fertilizer is the main method, and the fertilization method is relatively extensive. In addition, the shallow soil layer and the surface-subsurface binary loss exacerbate the drought stress and lack the medium for nutrient dissolution and migration, leading to a lack of synergy between water and fertilizer supply, and low efficiency of nutrient use.

The average ratios of C:N and C:P in the leaf litter were 54.54 and 334.88, respectively, which were lower than the global scale (57.30 and 1175.60), as well as Changbai Mountain, Jilin (39.43 and 552.00) (Wang et al. 2011; McGroddy et al. 2004), indicating

the limited content of N and P in leaf litter of the karst area. A significant positive correlation was observed between N and P content of plant leaves and N and P content of leaf litter. It is possible that N and P contents of plant leaves are reduced due to nutrient reuse before leaf fall, but it is insufficient to change the relationship between N and P content in leaves. Thus, the N and P content of leaf litter was similar to that of living leaves, which is consistent with the study by Zhu et al. (2017).

Soil C:N is inversely proportional to the decomposition rate of organic matter and affects the mineralization rates of N and P, so it is a sensitive index to demonstrate variations in soil quality. The average C:N ratio of five plant communities in the hot dry valley of the karst area was 16.20, higher than that of the natural secondary forests in the Ziwuling area of the Loess Plateau (11.9), that of global forest (12.40), and that of grassland (11.80) (Cleveland and Liptzin 2017) at a depth of 0–10 cm. It indicates a high-level organic matter content, a low mineralization rate of N, as well as a strong retention potential of C and N in the study area, which is consistent with the study by Ye et al. (2016). Soil C:P is generally considered as an indicator of soil P mineralization ability, and it is also a marker to indicate P release from the organic matter in microbial mineralized soil or the potential of P absorption and fixation from the environment (Pang et al. 2018). High soil C:P can cause soil microorganisms to compete with plants for soil inorganic P, which is unfavorable for plant growth. On the contrary, low C:P can facilitate microbial decomposition of organic matter to release nutrients and increase the content of available P in soil, so it can also represent high P availability in soil. The average C:P of five vegetation types in the karst rocky desertification area was 134.59, higher than global forest (81.90) and grassland (64.30) (Ye et al. 2016), indicating that soil microorganisms competed with plants for soil inorganic P, which is not favorable to plant growth. N in soil mainly originates from the leaf litter and the deposition of atmospheric nitrogen (Liu et al. 2010), and N:P in soil indicates the supply status of soil nutrients during plant growth. Our study showed that the average soil N:P of five plots was $7.09 < 14$, suggesting N deficiency, which impedes vegetation growth. The reason for such low N:P is that N is enriched in the surface layer of soil due to uneven topography, the severe cave, and fissures in karst, and surface water leakage; N then moves through fissures to lower layers along with water (Li et al. 2006), resulting in N deficiency in the dry hot valley area in Southwest China with ample rainfall.

Some studies have shown that soil nutrient status limits productivity (Ning et al. 2006). However, similar results have not been obtained in this study. The results showed that there was no direct relationship between plant, litter, soil, and productivity. It may be affected by the heterogeneity of the rocky desertification environment, and other factors.

4.3 Carbon and nutrient pools in afforestations on karst rocky desertification

Studies showed that nutritional reserves of litter C in cypress and eucalyptus were 199.79 g m^{-2} ; in loquat were 230.05 g m^{-2} ; in Chinese prickly ash were 149.64 g m^{-2} ; in walnut were 286.44 g m^{-2} ; and in teak were 376.37 g m^{-2} . The average reserves of litter C in the entire demonstration area were 249.15 g m^{-2} . Teak litter had the highest carbon storage and the teak test plot was located in a potential rocky desertification area, with thick soil, low rock exposure rate, and high carbon storage per unit area. Cypress-eucalyptus and Chinese prickly ash grow in the area of severe rocky desertification, and the carbon storage per unit area is small. Loquat and walnut grow in moderate and mild rocky desertification areas, with moderate carbon reserves. It is obvious that the grade of rocky desertification affect the carbon storage of litter. From the current rock desertification control projects in the demonstration area, these five types of eco-economic forests are mainly used. Thus we can estimated the potential carbon reserves of litter in the potential, mild, moderate, severe rock desertification areas are 1220.40 t, 1566.87 t, 556.60 t, and 403.59 t, respectively.

Studies showed that the soil organic carbon densities of the four grades of desertification were quite different, which indicates that the soil of karst rocky desertification is scattered, the thickness of the rock exposed soil layer is obviously different, and the environmental spatial heterogeneity is large. The results were consistent with those of Zhang Zhenming et al. (2017). The average carbon storage of soil in four grades of rocky desertification area was 3.26 kg m^{-2} . It was smaller than the national average level (9.6 kg m^{-2}) (Zhao 2005), for the Loess Plateau (10.92 kg m^{-2}) (Xue et al. 2015), or the Sanjiang Plain (9.72 kg m^{-2}) (Mao et al. 2015). Due to the special dual hydrological structure, complex topography and landform in karst areas, the rock fracture structure causes a large amount of soil organic carbon loss.

4.4 The characteristics of the reabsorption rate for N and P

Nutrient reabsorption refers to the process of nutrient transfer from old tissues and organs to other fresh organs and it is an important component of the nutrient cycle, reflecting plants' ability to conserve, utilize nutrients, and to adapt to nutrient-poor environments. Our data showed that the N reabsorption ranged from 24.48% to 40.37% with an average of 36.27%, and the range of P reabsorption was 10.28%–46.52% with an average of 23.61% in the ecoeconomic forest of the hot dry valley in the karst area, which is significantly lower than those of 172 species of woody plants in East China 49.1% and 51.0%, respectively; Tang et al. (2013) and those of 199 species of woody plants worldwide (57.4% and 60.7%) respectively; Han et al. (2014). The low reabsorption rate in Han's study indicated that the contents of N and P were relatively abundant in the study area, which is inconsistent with the first result of N deficiency in our study. This is because vegetation can directly absorb and utilize effective nutrients, not total nutrients (Bai et al. 2015). In addition, microbial decomposition absorb some N and P from soil and leaf litter, thus affecting nutrient cycling.

Therefore, there can be high total N and P in root-soil with a high reabsorption rate, or low total N and P with a low re-absorption rate, indicating no correlation of the reabsorption rate of N and P with the availability of N and P in soil, which is similar to the previous study by McGroddy et al. (2004). High N and P transfer rates may be an inherent characteristic of species, but not an important adaptation mechanism of plants to N and P nutrient stress (Wang et al. 2018). Such results are consistent with Aerts et al. (2000), in which the conclusion that evergreen plants occupy more barren habitats and have higher nutrient reabsorption rates is not supported. Plants adapt to the environment mainly by absorbing nutrients from the root zone, and not by a capacity for reabsorption.

5. Conclusions

The vegetation of the ecoeconomic forest in the karst area was deficient in N, rich in P, and exhibited a relatively high capacity for C storage. The N and P content of leaf litter was similar to that of living leaves, so leaf litter possessed exactly the same characteristics as plants. There was no direct relationship between plant, litter, soil, and productivity. The grade of rocky desertification will affect the carbon storage of litter. Low carbon storage in karst rocky desertification areas. In general, the soil was limited by N, so appropriate application of N fertilizer could facilitate plant growth. Plants adapt to the environment mainly by absorbing nutrients from root soil, but not by reabsorption capability.

Acknowledgments

This research was funded by the Project of the National Key Research and Development Program of China in the 13th Five-year Plan Period: Ecological Industry Model and Integrated Technology Demonstration of the Karst Plateau-Gorge Rocky Desertification Control (2016YFC0502607); The Key Project of the Science and Technology Program of Guizhou Province: Model and Technology demonstration for from the karst desertification control (No.5411 2017 Qiankehe Pingtai Rencai).

References

- Aerts R, Chapin FS. 2000. The mineral nutrition of wild plants revisited: a re-evaluation of processes and patterns. *J Plant Ecol* 30: 1-67.
- Aerts R, De Caluwe H, Beltman B. 2003. Is the relation between nutrient supply and biodiversity CO₂ limited by the type of nutrient limitation. *Oikos* 101:489-498.
- Agren GI, Bosatta E. 1998. *Theoretical Ecosystem Ecology: Understanding Element Cycles*. Cambridge University Press, Cambridge, UK. 234.
- Bai XF, Xu FL, Wang WL, Zhao YF, Wang LL, Sun PY. 2015. Ecological stoichiometry of soil carbon, nitrogen and phosphorus in a *Larix principis-rupprechtii* plantation. *Sci Soil and Water Conserv* 13: 68-75.
- Bai XJ, Zeng QC, An SS, Zhang HX, Wang BY. 2016. Ecological stoichiometry character-

- ristics of leaf-litter-soil in different plantations on the Loess Plateau, China. *Chin. J. App. Ecol* 27: 3823-3830.
- Bao SD. 2000. Soil agrochemical analysis. Beijing: China Agriculture Press.
- Bin ZJ, Wang JJ, Zhang WP, Xu DH, Cheng XH, Li KJ, Cao DH. 2014. Effect of N addition on ecological stoichiometric characteristics in six dominant plant species of alpine meadow on the Qinghai-Xizang Plateau. China. *Chin J Plan Ecolo* 38:231-237.
- Bowman WD. 1994. Accumulation and use of nitrogen and phosphorus following fertilization in two alpine tundra communities. *Oikos* 70: 261-270.
- Cleveland CC, Liptzin D. 2017. C:N:P stoichiometry in soil: Is there a "Redfield ratio" for the microbial biomass. *Biogeochemistry* 85: 235-252.
- Elser JJ, Acharya K, Kyle M, Cotner J, Makino W, Markow T, Watts T, Hobbie S, Fagan W, Schade J, Hood J, Sterner RW. 2003. Growth rate-stoichiometry couplings in diverse biota. *Ecol Lett* 6: 936-943.
- Elser JJ, Fagan WF, Denno RF, Dobberfuhl DR, Folarin A, Huberty A, Interlandi S, Kilham SS, McCauley E, Schulz KL, Siemann EH, Sterner RW. 2000. Nutritional constraints in terrestrial and freshwater food webs. *Nature* 408: 578-580.
- Gao GL, Deng ZM, Xiong KN, Su XL. 2003. The call and hope of karst. Guizhou science and technology press, Gui Yang, Chinese, 1-3.
- Gallaher RN, Weldon CO, Boswell FC. 1976. A semi-automated procedure for total nitrogen in plant and soil samples. *Soil Science Society of America Journal* 40: 887-889.
- Gra YJE, Hetherington AM. 2004. Plant development: YODA the stomatal switch. *Current Biology* 14: 488-490.
- Han WX, Fang JY, Guo DL, Zhang Y. 2005. Leaf N and P stoichiometry across 753 terrestrial plant species in China. *New Phytol* 168: 377-385.
- Han WX, Tang LY, Chen YH, Fang JY. 2014. Relationship between the relative limitation and resorption efficiency of nitrogen vs phosphorus in woody plants. *Plos One* 9. doi:10.1371/journal.pone.0083366.
- Hedin LO. 2004 Global organization of terrestrial plant-nutrient interactions. *PNAS* 101:10849-10850.
- Kang HZ, Xin ZJ, Berg B, Burgess PJ, Liu QL, Liu ZC, Li ZH, Liu CJ. 2010. Global pattern of leaf litter nitrogen and phosphorus in woody plants. *Ann Forest Sci* 67: 811-811.
- Kerkhoff AJ, Fagan WF, Elser JJ, Enquist BJ. 2006. Phylogenetic and growth and growth from variation in the scaling of nitrogen and phosphorus in the seed plants. *The American Naturalist* 168: E103-E122.
- Koerselman W, Meuleman AFM. 1996. The vegetation N:P ratio: A new tool to detect the nature of nutrient limitation. *J App Ecol* 33: 141-150.
- Li YB, Shao JA, Wang SJ, Wei CF. 2006. A Conceptual Analysis of Karst Ecosystem Fragility. *Prog Geogr* 25 :1-8.
- Liu XZ, Zhou GY, Zhang DQ, Liu SZ, Chu GW, Yan JH. 2010. N and P stoichiometry of plant and soil in lower subtropical forest successional series in southern China. *Chin J Plan Ecolo* 34: 64-71.
- McGroddy ME., Daufresne T, Hedin LO. 2004. Scaling of C:N:P Stoichiometry in forests

- worldwide: implication of terrestrial Redfield-type ratios. *Ecology* 85: 2390-2401.
- Mao DH, Wang ZM, Li L. 2015. Soil organic carbon in the San Jiang Plain of China: Storage distribution and controlling factors. *Biogeosciences* 12: 1635-1645.
- Nelson DW, Sommers LE. 1982. Total carbon, organic carbon, and organic matter. In *Methods of soil analysis*. Madison: American Society of Agronomy and Soil Science Society of American.
- Ning ZY, Li YL, Yang HL, Zhang ZQ, Zhang JP. 2019. Stoichiometry and effects of carbon, nitrogen, and phosphorus in soil of desertified grasslands on community productivity and species diversity. *Acta Ecol. Sin* 39: 3537-3546.
- Pang DB, Wang GZ, Li GJ, Sun YL, Liu YG, Zhou JX. 2018. Ecological stoichiometric characteristics of two typical plantations in the karst ecosystem of southwestern China. *Forests* 9: 2-14.
- Reich PB, Oleksyn J. 2004. Global patterns of plant leaf N and P in relation to temperature and latitude. *PNAS* 101:11001-11006.
- Ren SJ, Yu GR, Tao B, Wang SQ. 2007. Leaf nitrogen and phosphorus stoichiometry across 654 terrestrial plant species in NSTEC. *Chin. J. Envir. Sci* 28: 2665-2673.
- Shen FF, Wu JP, Fan HB, Liu WF, Guo XM, Duan HL, Hu L, Lei XM, Wei XH. 2019. Soil N:P and C:P ratio regulate the responses of soil microbial community composition and enzyme activities in a long-term nitrogen loaded Chinese fir forest. *Plant Soil* 436:91-107.
- Sterner RW, Elser JJ. 2002. *Ecological Stoichiometry: The Biology of Elements from Molecules to the Biosphere*. Princeton: Princeton University Press.
- Sun SX, Yun XJ, Wu XH, Wei ZJ, Jiang C, Liu WT. 2018. Seasonal variations of ecological stoichiometry characteristics of major plant populations in desert steppe. *Ecol Environ* 27: 47-54.
- Tang LY, Han WX, Chen YH, Fang JY. 2013. Resorption proficiency and efficiency of leaf nutrients in woody plants in eastern China. *J Plant Ecol* 6: 408-417.
- Wang BR, Zeng QC, An SS, Zhang HX, Bai XJ. 2017. C:N:P stoichiometry characteristics of plants-litter-soils in two kind types of natural secondary forest on the Ziwuling region of the Loess Plateau. *Acta Ecol. Sin* 37: 5461-5473.
- Wang JY, Wang SQ, Li RL, Yan JH, Sha LQ, Han SJ. 2011. C:N:P stoichiometric characteristics of four forest types' dominant tree species in China. *Chin J Plan Ecolo* 35: 587-595.
- Wang L, Yu YH, Xing RR, Qin SY. 2018. Ecological stoichiometry characteristics of carbon, nitrogen, and potassium of different economic tree species in the karst frigid and arid area. *Acta Ecol. Sin* 38: 5393-5403.
- Wardle DA, Walker LR, Bardgett RD. 2004. Ecosystem properties and forest decline in contrasting long-term chronosequences. *Science* 305: 509-513.
- Xiang WH, Huang ZH, Yan WD, Tian DL, Lei PF. 2006. Review on coupling of interactive functions between carbon and nitrogen cycles in forest ecosystems. *Acta Ecol. Sin* 26: 2365-2372.
- Xie J, Chang SL, Zhang YT, Wang HJ, Song CC, He P, Sun XJ. 2016. Plant and soil ecological stoichiometry with vertical zonality on the northern slope of the middle Tianshan Mountains. *Acta Ecol. Sin* 36: 4363-4372.

- Xiong KN, Li P, Zhou ZF, An YL, Lv T, Lan AJ. 2002. Study on remote sensing – GIS model of karst rocky desertification. Geological press, Beijing, Chinese, 66-68.
- Xiong KN, Chi YK, Shen XY. 2017. Research on photosynthetic leguminous forage in the karst rocky desertification regions of southwestern China. *Pol. J. Environ. Stud* 26: 2319-2329.
- Xiong KN, Li J, Long MZ. 2012. Feature of Soil and Water Loss and Key Issues in Demonstration Areas for Combating Karst Rocky Desertification. *Acta Geogr Sin* 67: 878-888.
- Xiong KN, Zhu DY, Peng T, Yu LF, Xue JF, Li P. 2016. Study on ecological industry technology and demonstration for karst rocky desertification control of the Karst Plateau-Gorge. *Acta Ecol. Sin* 36: 7109-7113.
- Xue ZJ, Ma LS, An SS, Wang WZ. 2015. Soil organic carbon density and stock at the catchment scale of a hilly region of the loess plateau. *Acta Ecol. Sin* 35:2917-2925.
- Yan ER, Wang XH, Guo M, Zhong Q, Zhou W. 2010. C:N:P stoichiometry across evergreen broad-leaved forests, evergreen coniferous forests and deciduous broad-leaved forests in the Tiantong region, Zhejiang Province, eastern China. *Chin J Plan Ecolo* 34: 48-57.
- Yang JJ, Zhang XR, Ma LS, Chen YN, Dang TH, An SS. 2014. Ecological stoichiometric relationships between components of robinia pseudoacacia forest in loess plateau. *Acta Pedol. Sin* 51:133-142.
- Yang ZJ, Zeng J, Xue DP, Li SJ, Lu J. 2007. The processes and dominant factors of forest litter decomposition: A review. *Ecol. & Environ* 16: 649-654.
- Ye C, Pu YL, Zhang SR, Wang GY, Wang AB, Wang D, Jia YX, Xu XX. 2016. Ecological stoichiometry characteristics and storage of soil carbon, nitrogen and phosphorus during the wetland degradation process. *J. Soil Water Conserv* 30: 181-192.
- Yin XR, Ling CZ, Wang LX, Wang W, Liu ZL, Liu XP. 2010. Ecological stoichiometry of plant nutrients at different restoration succession stages in typical steppe of Inner Mongolia, China. *Chin J Plan Ecolo* 34: 39-47.
- Yuan DX. 1997. Rock desertification in the subtropical karst of south China. *Z. Geomorph. N. F.* 108:81-90.
- Yuan DX, Zhang C. 2008. Karst Dynamics Theory in China and its Practice. *ACTA GEOGRAPHICA SINICA* 29: 355-365.
- Yue YM, Wang KL, Zhang B, Liu B, Chen HS, Zhang MY. 2011. Uncertainty of Remotely Sensed Extraction of Information of Karst Rocky Desertification. *Adv Earth Sci* 26: 266-274.
- Zeng ZX, Wang KL, Liu XL, Zeng FP, Song TQ, Peng WX, Zhang H, Du H. 2015. Stoichiometric characteristics of plants, litter and soils in karst plant communities of Northwest Guangxi. *Chin J Plan Ecolo* 39: 682-693.
- Zhang JP, Pan GX. 2012. Characteristics of soil nutrients and biochemical properties under different vegetation communities in karst area. *J. Soil Water Conserv* 26: 77-84.
- Zhang QF, Xie JS, Chen NS, Chen T, Lv MK, Zhang H, Yang YS. 2017. Effects of ecological restoration on stoichiometric characteristics and nutrient resorption efficiency of *Pinus massoniana* foliage. *Acta Ecol. Sin* 37: 267-276.

- Zhang WJ, Liu XD, Jin M, Zhang XL, Che ZX, Jing WM, Wang SL, Niu Y, Qi P, Li WJ. 2016. Ecological stoichiometric characteristics of carbon, nitrogen and phosphorus in leaf-litter-soil system of *Picea Grassifolia* Forest in the Qilian Mountains. *Acta Pedol. Sin* 53 : 477-489.
- Zhang Y, Xiong KN, Yu YH , Xu M, Cheng W, Tan DJ. 2019. Daily variations of soil respiration among three types of non-wood forest in karst rocky desertification areas, Southern China. *Journal of Central South University of Forestry & Technology* 39: 92-99.
- Zhao SY, Li JT, Sun XK, Zeng DH, Hu YL. 2018. Responses of soil and plant stoichiometric characteristics along rainfall gradients in Mongolian pine plantations in native and introduced regions. *Acta Ecol. Sin* 38 :1-8.
- Zhao XD, Zeng QC, An SS, Fang Y, Ma RT. 2016. Ecological stoichiometric characteristics of grassland soils and plant roots relative to enclosure history on the Loess Plateau. *Acta Pedo. Sin* 53: 1541-1551.
- Zhao YP, Cao Y, Chen YM, Peng SZ. 2017. Ecological stoichiometry in a forest ecosystem in the hilly-gully area of the Loess Plateau. *Acta Ecol. Sin* 37: 5451-5460.
- Zhou P, Geng Y, Ma WH, He JS. 2010. Linkage of functional traits among plant organs in the dominant species of the Inner Mongolia grassland. *Chin J Plan Ecolo* 34: 7-16.
- Zhu WK, Chen SX, Wang ZC, Xu YX, Zhang LL, Du AP. 2017. Ecological stoichiometric characteristics of carbon, nitrogen and phosphorus in litter and soil of *Eucalyptus urophylla* × *E. Grandis* plantation at different forest ages. *J. Trop. & Subtrop. Bot* 25:127-135.
- Zhao QG. 2005. Study on evolution of organic carbon stock in agricultural soils of China: facing the challenge of global change and food security. *Prog. Geogr* 20: 384-393.
- Zhang ZM, Zhou YC, Huang XF, Tian X. 2017. Spatial heterogeneity and distribution characteristics of soil organic carbon density and soil organic carbon storage in a small karst watershed. *J. Soil Water Conserv.* 2:184-190.

137. Jahrgang (2020), Heft 2, S. 133-160

**Austrian Journal of
Forest Science**

Centralblatt
für das gesamte
Forstwesen**Individual-based modelling for predicting height and biomass of juveniles
of *Shorea robusta*****Einzelbaumbasierte Modellierung zur Abschätzung der Höhe und
Biomasse von Jungbäumen von *Shorea robusta***Shes Kanta Bhandari¹*, Bir Bahadur Khanal Chhetri¹**Keywords:** *Allometry, tree growth, Nepal, community forestry, Wood density, regeneration***Schlüsselbegriffe:** *Allometrie, Waldwachstum, Nepal, Soziale Waldbewirtschaftung, Holzdichte, Verjüngung***Abstract**

Shorea robusta is one of the most widespread timber species in the forests of southern Nepal. Large parts of *Shorea robusta* forests of Nepal were degraded in the recent past due to policy conflict between the government and local users. After the introduction of community forestry, these forests have been regenerating gradually and the proportion of juvenile individuals in the forest is now very high. In the absence of biomass models of juvenile individuals, almost all forest inventories are neglecting the contribution of juvenile individuals in total carbon sequestration and storage. To close this knowledge gap, we developed a height and biomass prediction model for juvenile *Shorea robusta* in Nepal using an individual-based modelling approach. The models were calibrated with data from 110 destructively sampled trees and validated with 45 trees. We tested different model forms to select the best suited height and biomass prediction model. Once the best model form was selected, we

¹ Institute of Forestry, Tribhuvan University, Nepal

*Corresponding author: Shes Kanta Bhandari, shesu15@yahoo.com

calculated several models using different combination of predictor variables (i.e. tree diameter, tree height and wood density). Linear form (coefficient of determination R^2 0.80) for height and power form (R^2 0.89) for biomass prediction were selected as the best model forms. Product of diameter squared and height (R^2 0.91) and product of wood density, diameter squared and height (R^2 0.94) for the density-dependent model were the best predictors for biomass model. Due to different input data the predicted biomass by the models of this study differed substantially from biomass predictions using previously developed models of *Shorea robusta*. Thus, site- and size-specific models are required for accurate predictions of biomass and height of Juvenile of *Shorea robusta*. The model introduced here is site-specific and its application should be limited to conditions similar to this study.

Zusammenfassung

Shorea robusta ist eine weit verbreitete Baumart in den Wäldern im südlichen Nepal. Große Teile des *Shorea robusta* Waldes in Nepal wurden in der jüngsten Vergangenheit aufgrund politischer Konflikte zwischen der Regierung und lokalen Nutzern degradiert. Nach Einführung der kommunalen Forstwirtschaft haben sich diese Wälder allmählich verjüngt und der Anteil an Jungbäumen ist jetzt sehr hoch. Weil geeignete Modelle zur Vorhersage des Biomassezuwachses von Jungbäumen fehlen, vernachlässigen derzeit fast alle Waldinventuren den Beitrag der Jungbäume zur Kohlenstoffspeicherung. Um diese Wissenslücke zu schließen, haben wir ein auf Einzelbäumen basierendes Modell zur Schätzung der Wuchshöhe und Biomasse von jungen *Shorea robusta* aus Nepal entwickelt. Die Modelle wurden mit 110 destruktiv beprobten Jungbäumen kalibriert und 45 Bäumen validiert. Wir testeten verschiedene Varianten der Modelle, um das beste Modell zur Vorhersage von Wuchshöhe und Biomasse zu finden. Nachdem die beste Variante des Vorhersagemodells ausgewählt worden war, wurden mehrere Modelle mit unterschiedlichen Kombinationen der Prädiktorvariablen (Durchmesser, Baumhöhe und Holzdicke) entwickelt. Die beste Modellvariante war eine lineare Funktion (R^2 0.80) für die Höhe und eine Potenzfunktion (R^2 0.89) für die Biomasse. Das Produkt aus Höhe und Durchmesser zum Quadrat (R^2 0.91) und das Produkt aus Holzdicke, Höhe und Durchmesser zum Quadrat (R^2 0.94) waren die besten Modelle für die Biomasse. Die Modelle dieser Studie ergeben deutlich unterschiedliche Biomasse von *Shorea robusta* als die zuvor entwickelten Modelle. Es zeigt sich somit, dass standort- und größenabhängige Modelle wichtig sind für eine genaue Abschätzung der Biomasse von *Shorea robusta*. Unser Modell ist standortspezifisch und seine Anwendung sollte daher auf Bestände beschränkt werden, die den dieser Studie zugrunde liegenden ähnlich sind.

1. Introduction

Forest biomass is relevant for both forest productivity and climate change (Berndes et al., 2016; Kilpelainen et al., 2014). Regarding forest productivity, more biomass results in a higher yield, while regarding climate change, more biomass has a positive role in

minimizing the impact of climate change through sequestering a higher amount of atmospheric carbon dioxide (Chen et al., 2017). Accurate estimation of forest biomass is thus very important. Forest biomass consists of aboveground and belowground biomass (Nonini and Fiala, 2019). Empirical measurements of belowground biomass are time-consuming, costly and difficult, therefore, belowground biomass is often estimated using a constant proportion of aboveground biomass (Zhao et al., 2019; Addo-Danso et al., 2016). This study focusses on aboveground biomass at individual tree level. Aboveground biomass is measured using the direct or the indirect method. In the direct method, individual trees are felled destructively and weighed (Devi and Yadava, 2009; Ravindranath and Ostwald, 2008; Chung-Wang and Ceulemans, 2004). The direct method is more accurate, however, requires a large amount of time and resources (De Gier, 2003). The direct method is often used to develop allometric equations (i.e., an indirect method) that can be applied on larger areas and whole forests (Shrestha et al., 2018; Sharma et al., 2017; Navar, 2009; Segura and Kanninen, 2005). The indirect method estimates biomass without felling the individual trees and thus can be applied to larger forest areas. The indirect method can employ the shape, size (diameter, height), wood density in the form of allometric equations to predicted biomass (Ravindranath and Ostwald, 2008; Montes et al., 2000; Brown et al., 1989).

Allometric models establish a quantitative relationship between two or more variables (Klingenberg, 2016). The variable, that is more difficult to assess, is used as the dependent variable, while variables, that are easy to measure, are used as predictor variables. The allometric relationship is developed based on the accurate and detailed measurement on a small sample of typical individuals which are assumed to hold true for other individuals of a similar size and nature from the similar population. The application of allometric relationship enables estimation and prediction of different variables of individual trees and forest (Altanzagas et al., 2019; Daba and Soromessa, 2019). In published allometric models, tree height is predicted from stem diameter (Sharma, 2009; Huang et al., 1992) and biomass is predicted from stem diameter (Chapagain et al., 2014; Ong et al., 2004; Clough et al., 1997), stem diameter and height (Chapagain et al., 2014; Subedi and Sharma, 2012), stem diameter, height and wood density (Shrestha et al., 2018; Sharma et al., 2017). Most of the available biomass models were developed using data from large trees (Shrestha et al., 2018; Sharma et al., 2017; Nam et al., 2016; Huy et al., 2016; Clough et al., 2016; Chave et al., 2014; Paul et al., 2013; Blujdea et al., 2012; Subedi and Sharma, 2012; Navar, 2009; Chave et al., 2005; Tamrakar, 2000). Contribution of large-sized trees to biomass and carbon storage is high, but the contribution of juvenile (defined as a plant ≥ 30 cm in height and < 5 cm in diameter at 10 cm above ground surface) individuals is not negligible. Juvenile individuals can contribute around 5% biomass in forest depending on successional stage (Francis, 2000). Juveniles do not only contain biomass and carbon, but are also an important indicator of sustainability of forest management, reducing soil erosion and a predictor variable in analysing neighbourhood competition (Ter-Mikaelian and Parker, 2000). Despite their importance, few studies have focussed on juvenile trees. Chaturvedi et al. (2012) developed the multispecies bio-

mass model for 47 dry tropical woody species at the juvenile stage. Chapagain et al. (2014) developed allometric biomass models to estimate juvenile biomass of three tropical tree species (*Shorea robusta*, *Acacia catechu* and *Terminalia tomentosa*). BK et al. (2019) developed the allometric biomass model for juveniles of *Rhododendron arboreum* from the temperate region of Nepal.

Shorea robusta (C.F. Gaertn.) (family Dipterocarpaceae) is a large tree reaching 30-50 m height and 3-3.5 m diameter at breast height (dbh) (Chitale and Behera, 2012; Jackson, 1994). It is found across Nepal, India, Bangladesh and Myanmar (Gautam and Devoe, 2006; Stainton, 1972). In Nepal, it grows from 120 m to 1200 m elevation, but is more common at elevation lower than 800 m (Sah, 2000; Jackson, 1994). The contribution of *Shorea robusta* in total standing volume in Nepal is 19.28% (31.76 m³/ha) with a stem number of 65 trees per hectare (≥ 10 cm dbh), covering 15.27% of forest area (DFRS, 2015). These most recent estimate of standing volume, stem number and coverage of *Shorea robusta* are lower than the numbers reported in DFRS (1999). The different parts of *Shorea robusta* trees have been extensively used such as the stem as timber, construction material and fuelwood (Jackson, 1994), the leaves as fodder (Kibria et al., 1994) and dining plates (Kora, 2019), the resin as medicine of dysentery and gonorrhoea (Joshi, 2003).

Most of the *Shorea robusta* forest of Nepal was degraded in the recent past due to policy conflict between the government and local users (Sah, 2000; Land Resources Mapping Project, 1986). But after the introduction of community forestry system, these forests have been rejuvenated gradually (Paudel and Sah, 2015) and the proportion of the juvenile plants is high. Ample research in community forest (CF) of Nepal has demonstrated the positive impact of CF on forest conservation and regeneration (Bhattarai and Conway, 2008) and local livelihoods (Chhetri et al., 2012). Indeed, this positive effect has also raised the attention for estimating the biomass of juvenile plants to promote ecological sustainability in CF of Nepal. CF, one of the most successful participatory forestry programs implemented in Nepal, is joint venture of government and local user for conservation, protection, management and utilization for forest resources (Aryal et al., 2019; Nuberg, et al. 2019; Luintel et al., 2018). In Kankali CF (study area of this study), the average stand density of the CF is 7687 ha⁻¹ whereas stand density with trees >10 cm dbh is 572 ha⁻¹ and trees <10 cm dbh is 7115 ha⁻¹. The biomass and carbon measurement guideline of Nepal has recommended the allometric equation of Tamrakar (2000) ($\log \text{biomass} = a + b \log (\text{dbh})$) to estimate the biomass/carbon of plants having dbh <5 cm, although this equation was developed using few data from small-sized trees. This equation includes a large number of data from large sized trees and a small number of data from small sized trees. In the case of *Shorea robusta*, the equation was developed using the data ranging from 3 cm to 20 cm dbh (Tamrakar, 2000). Biomass and carbon estimation from the equation of Tamrakar (2000) might induce significant errors in the case of small-sized plants. Another model for estimation of juvenile biomass of three tropical tree species including *Shorea robusta* is developed by Chapagain et al. (2014) for western Nepal. The

model of Chapagain et al. (2014) was developed using the data from the three CFs in Bardiya district (28.3102° N and 81.4279° E) of province number five of Nepal (Figure 1). Even though, the study area of Chapagain et al. (2014) and the study area of this study lies on southern Nepal, the climate, physiography, stand density, site quality and human disturbance differs. The average annual precipitation of Bardiya district is 1118 mm (Chapagain et al., 2014) while the average annual precipitation of Chitwan district (study area of this study) is 1916 mm (DFO Chitwan, 2017). The altitudinal range of Bardiya district is 138 to 1279 m above mean sea level (Chapagain et al. 2014), while the altitudinal range of Chitwan district is 100 to 815 m above mean sea level. A model developed for a specific site may not be suitable for another site with different climate, physiography, stand density, site quality and human disturbance.

To minimize the error in biomass and carbon estimation, species-specific and size-specific equations including juvenile individual is required. Therefore this study aimed to develop allometric equation to predict height and biomass for juveniles of *Shorea robusta*. To achieve this aim, we selected the best form of the model out of several available height and biomass prediction models. In the case of biomass model, we further improved the model using the different combination of predictor variables. We further categorized the developed models into wood density-independent and wood density-dependent, to make our models easier applicable depending on the availability of predictor variables. We validated these developed models using a subset of data which was not used in the model development. We also compared our biomass models with the previously developed biomass models of *Shorea robusta*.

2. Materials and Methods

2.1 Study Area

The study was conducted in Kankali CF of Khairahani Municipality of Chitwan district Nepal (27.5291° N, 84.3542° E) (Figure 1). The forest coverage in the district is 63.25% (DFRS, 2015) and the 14.94% forest of the district is managed by 87 community forest user groups (CFUGs) in the form of CF including 43,313 households (DOF, 2017). The altitude of the district ranges from 100 m to 815 m above mean sea level. The average minimum and maximum temperature is 9.4 °C in January and 33.7 °C in June and average annual rainfall is 1916 mm (DFO Chitwan, 2017). The studied forest is 760 ha in area and has been managed by local CFUG since 1995. The CFUG is implementing different forest management activities like weeding, cleaning, climber cutting, pruning, thinning and other selective cutting. The forest type is natural and mixed in composition with *Shorea robusta* as dominant species. *Terminalia belerica*, *Terminalia tomentosa* and *Terminalia chebula* are other associate species of the forest. According to the operational plan, the CF has good quality stands and crown coverage is more than 65%. A part of this forest had been studied for carbon sequestration and a mo-

nitary value of carbon credit had been paid through a REDD+ pilot project in Nepal funded by a Norwegian development aid agency (NORAD) (Saito-Jensen et al., 2014).

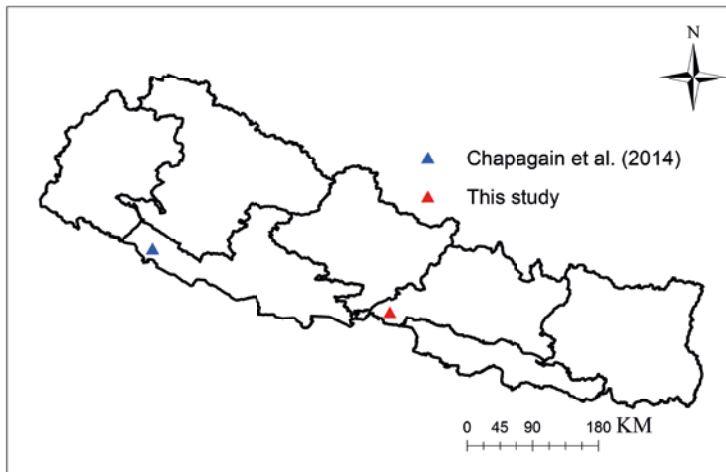


Figure 1: Map of Nepal showing the location of this study and the study site of Chapagain et al. (2014).

Abbildung 1: Karte von Nepal, die das Untersuchungsgebiet dieser Studie und das Untersuchungsgebiet der Studie von Chapagain et al. (2014) zeigt.

2.2 Sampling and Measurement

The operational plan of the CF was used to detect the variation in the size of the individuals of *Shorea robusta* (Operational Plan, 2019). 155 individual juveniles were selected purposively from the whole study area to represent existing variation of the site conditions, stand density, tree size (Chapagain et al., 2014; Adinugroho and Sidiyasa, 2006; Dorado et al., 2006; Edwards Jr et al., 2006). The individuals with a broken top, abnormal stem, diseased, dead and dying were excluded from measurement. We collected data on measured parameters (diameter, height, stem volume, total fresh weight of stem, branches and leaves, sample fresh weight of stem, branch and leaves) and derived parameters (total dry weight of stem, branch and leaves and wood density). Vernier Calliper (precision 1 mm) was used to measure the diameter of each juvenile at 10 cm above the ground level by following the method of Chapagain et al. (2014) and BK et al. (2019). Hereafter the diameter is referred as D . Then, the juvenile individual was felled by hand saw. Total height (H) was measured from base to tip of the juvenile using linear tape (precision 1 mm). A separate weight of stem, leaves and branches were recorded (precision 0.1 gram). At least 100 gram (g) of stem, lea-

ves and branches were weighed and placed in a labelled bag and transported to the laboratory as sample for oven dry weight. If a part (stem or branch or leaves) of the juvenile individual was less than 100 g, whole part was used for drying the samples. The fresh volume of the stem sample was determined using the principle of water displacement (BK et al., 2019; Shrestha et al., 2018; Chapagain et al., 2014; Chaturvedi and Khanna, 2011). The samples (leaves, branches, stem separately) were dried on an oven at 90°C till the constant weight was achieved to determine the dry weight of the sample. The weight of the samples was first recorded after 24 hours and then repeated at the interval of 12 hours. The wood density (ρ) was determined as the ratio of the dry weight of stem sample and its fresh volume (Equation 1). The total dry weight of leaves, branches and stem was determined using the ratio of dry weight and fresh weight of samples of leaves, branches and stem respectively. The total dry biomass of each juvenile individuals was calculated by adding the dry biomass of leaves, branches and stem. The descriptive statistics of the data used for modelling is given in Table 1.

$$\text{Wood density } (\rho) = \frac{\text{oven dry weight of sample}}{\text{fresh volume of sample}} \quad 1$$

Table 1: Descriptive statistics of the variables used for modelling the juvenile aboveground biomass of *Shorea robusta*.

Tabelle 1: Zusammenfassung der *Shorea robusta* Jungbäume, die für die Modellierung der oberirdischen Biomasse verwendet wurden.

Diameter class (cm)	Variables	Mean \pm Standard deviation (range)
0-1	Diameter (cm)	0.502 \pm 0.172 (0.2-0.91)
	Height (m)	0.79 \pm 0.29 (0.33-1.49)
	Wood density (g cm ⁻³)	0.29 \pm 0.08 (0.05-0.47)
	Biomass (g)	15.10 \pm 11.58 (1.30-45.33)
	Number	40
1-2	Diameter (cm)	1.39 \pm 0.28 (1.00-1.97)
	Height (cm)	1.53 \pm 0.35 (0.91-2.62)
	Wood density (g cm ⁻³)	0.38 \pm 0.07 (0.20-0.53)
	Biomass (g)	91.59 \pm 50.08 (33.66-259.69)
	Number	38
2-3	Diameter (cm)	2.52 \pm 0.28 (2.09-2.94)
	Height (cm)	2.10 \pm 0.56 (1.25-4.07)
	Wood density (g cm ⁻³)	0.46 \pm 0.11 (0.30-0.71)
	Biomass (g)	354.14 \pm 164.11 (129.23-918.14)
	Number	26
3-4	Diameter (cm)	3.51 \pm 0.27 (3.09-3.96)
	Height (cm)	3.16 \pm 0.73 (1.88-4.77)
	Wood density (g cm ⁻³)	0.49 \pm 0.07 (0.38-0.64)
	Biomass (g)	875.83 \pm 432.66 (403.12-2005.19)
	Number	23
4-5	Diameter (cm)	4.48 \pm 0.30 (4.02-4.96)
	Height (cm)	3.63 \pm 0.86 (2.11-5.55)
	Wood density (g cm ⁻³)	0.49 \pm 0.09 (0.25-0.68)
	Biomass (g)	1563.33 \pm 518.14 (883.61-2630.12)
	Number	28
Total 0-5	Diameter (cm)	2.22 \pm 1.48 (0.20-4.96)
	Height (cm)	2.06 \pm 1.19 (0.09-5.55)
	Wood density (g cm ⁻³)	0.41 \pm 0.11 (0.05-0.71)
	Biomass (g)	499.06 \pm 643.18 (1.30-2630.12)
	Number	155

2.3 Modelling approach

We fitted different forms of models including linear, logarithmic, inverse, quadratic, power, sigmoid and exponential (Table 2) to our data to select the best height and biomass prediction models. For height prediction, we fitted the models with height

as the dependent variable and diameter as the predictor variable. For biomass prediction, we fitted the models with biomass as the dependent variable and diameter as the predictor variable. The parameters and fit statistics for each model were estimated in R using the `lm`, `nls` and `nlsLM` function in the `minpack.lm` package (R Core Team, 2017), and evaluated using different criteria including significance of estimated parameters (at 5% level of significance); coefficient of determination (R^2 ; higher values indicate better models); root mean squared error (RMSE; lower values indicate better models) (Montgomery et al., 2001); and Akaike Information Criterion (AIC; lower values indicate better models) (Akaike, 1972; Burnham and Anderson, 2002). Distribution of residuals was also considered in selecting the best model.

*Table 2: Different forms of models and their equations used in height and aboveground biomass modelling of juveniles of *Shorea robusta* (Y is dependent variable and X is predictor variable).*

Tabelle 2: Modellformen und Gleichungen, die bei der Modellierung der Wuchshöhe und der oberirdischen Biomasse von Jungbäumen der *Shorea robusta* verwendet wurden (Y ist abhängige Variable und X Prädiktorvariable).

Model form	Equation
Linear	$Y = \alpha_1 + \alpha_2 X + \varepsilon_{ij}$
Logarithmic	$Y = \alpha_1 + \alpha_2 \log(X) + \varepsilon_{ij}$
Inverse	$Y = \alpha_1 + \frac{\alpha_2}{X} + \varepsilon_{ij}$
Quadratic	$Y = \alpha_1 + \alpha_2 X + \alpha_3 X^2 + \varepsilon_{ij}$
Power	$Y = \alpha_1 X^{\alpha_2} + \varepsilon_{ij}$
Sigmoidal	$Y = \exp\left(\alpha_1 + \frac{\alpha_2}{X}\right) + \varepsilon_{ij}$
Exponential	$Y = \alpha_1 \exp(\alpha_2 X) + \varepsilon_{ij}$

Once the best form of biomass model was selected, a different combination of predictor variables was used in that form of biomass model. The different combinations of predictor variables used were diameter alone (D), product of diameter and height (DH), product of square of diameter and height (D²H), product of wood density, diameter and height (ρ DH) and product of wood density, square of diameter and height

(ρD^2H) (BK et al., 2019; Shrestha et al., 2018; Chapagain et al., 2014).

2.4 Validation

The whole data ($n = 155$) was split into calibration data ($n = 110$) and validation data ($n = 45$). The validation data was used in the best-selected model to analyse the model performance. We estimated the correlation coefficients between the predicted values and observed value of validation data. Correlation coefficient was categorized as very high (>0.9), high ($0.7-0.9$), moderate ($0.5-0.7$), low ($0.3-0.5$) and negligible ($0-0.3$) (Mukaka, 2012). Plots of predicted versus observed values were also generated to evaluate whether the model prediction is similar to observed data or not. Furthermore, we used a paired sample t-test to test whether there was a significant difference between observed and predicted values at 5% level of significance.

2.5 Comparison of validated models with previously developed biomass models

We compared our biomass models with two categories of previously developed biomass models. The first category of models was biomass prediction models of juvenile individuals of *Shorea robusta*. Chapagain et al. (2014) had developed eight biomass models for juvenile individuals of three tropical tree species including *Shorea robusta* in Nepal. We compared our models (based on D , D^2H and ρD^2H) with three models of Chapagain et al. (2014) (Equation 2, 3 and 4) which predicts the biomass of *Shorea robusta* based on D , D^2H and ρD^2H .

$$\text{Biomass (g)} = 71.9320 D^{(1.6991+0.0585 D)} \quad 2$$

$$\text{Biomass (g)} = \exp(4.1580 (D^2H)^{0.1380}) \quad 3$$

$$\text{Biomass (g)} = \exp(4.4790 (\rho D^2H)^{0.1322}) \quad 4$$

Where D is diameter (cm) measured at 10 cm above the ground level, H is total height (m) and ρ is wood density (g cm^{-3}).

The second category of models were biomass prediction models of large sized trees of *Shorea robusta*. Sharma and Pukkala (1990) (Equation 5, 6), Tamrakar (2000) (Equation 7) and Subedi (2017) (Equation 8, 9) had developed biomass models for *Shorea robusta* in Nepal. These models were based on dbh (cm) and/or height (m) of the *Shorea robusta*, however, our models were based on diameter at 10 cm above the ground level and height. We developed a simple power function model to predict the dbh from the diameter at 10 cm above the ground level (Equation 10).

$$\ln(\text{Volume}) = -2.4554 + 1.9026 \ln dbh + 0.8352 \ln height \quad 5$$

$$\text{Biomass (Kg)} = \text{Volume} * 880 \quad 6$$

$$\ln(\text{biomass}) = a + b \ln(dbh) \quad 7$$

$$\ln(\text{Volume}) = -8.04674 + 2.26641 \ln dbh \quad 8$$

$$\text{Biomass (Kg)} = \text{Volume} * 880 \quad 9$$

$$dbh = 0.7031 D^{0.9527} \quad 10$$

Where dbh is diameter at breast height at 1.3 m above ground (cm) and D is diameter (cm) at 10 cm above the ground level.

For comparison, we predicted the biomass using the models of Chapagain et al. (2014), Sharma and Pukkala (1990), Tamrakar (2000), Subedi (2017) and the models developed in this study. Then we plotted the predicted biomass against the predictor variables (Figure 5). Paired sample t-test was used to test whether the predicted biomass by the model of this study and other previously developed models was same. Correlation coefficient (r) was used to evaluate the relationship between the models developed in this study and each of the previously developed models.

3. Results

The result showed that the stem, leaf and branch biomass of juvenile individual covers 83%, 11% and 6% of total biomass respectively. Leaf and branch biomass of juvenile covers 12% and 7% of total stem biomass. Similarly, branch biomass of juvenile covers 57% of leaf biomass.

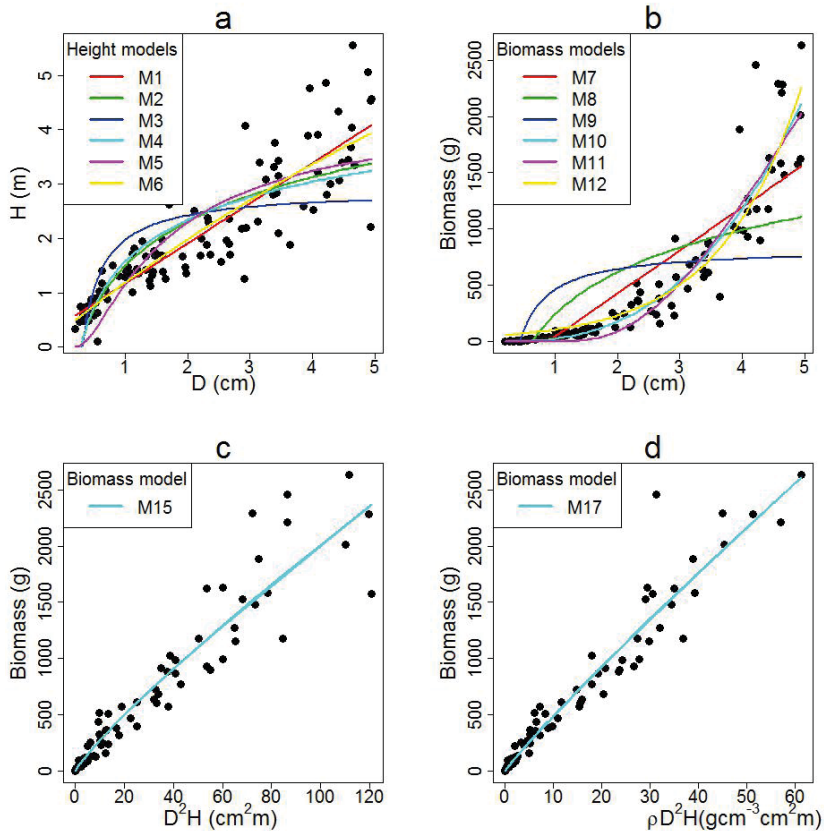


Figure 2: Model predictions of *Shorea robusta*; (a) tested tree height models, (b) tested aboveground biomass models, (c) best performing biomass model using diameter at 10 cm above ground (D) and tree height (H) and (d) best performing biomass model using D , H , and wood density (ρ).

Abbildung 2: Modellschätzungen von *Shorea robusta*; (a) getestete Baumhöhen-Modelle, (b) getestete Biomasse-Modelle, (c) bestes Biomasse-Modell unter Verwendung des Durchmessers 10 cm über dem Boden (D) und der Baumhöhe (H) und (d) bestes Biomasse-Modell unter Verwendung von D , H und Holzdicke (ρ).

3.1 Model for height prediction

All model parameters were significant at a 95% confidence interval except one parameter of the quadratic form of the model ($p = 0.59$), which we excluded from further analysis. The inverse form of the model only described 49% of the variation in total height with highest RMSE and AIC than other models (Table 3). Logarithmic form of model overestimated the height for smaller juveniles and underestimated for larger juveniles, however, the sigmoidal model underestimated the height for smaller ju-

veniles and overestimated the height of larger juveniles (Figure 2a). The exponential model overestimates the height for smaller juveniles (Figure 2a). Linear and power form of the model described more than 80% of the variation in total height. Furthermore, the linear and power form of the model produced smaller RMSE and AIC than other models. Out of the remaining two models, the linear model described higher variability in height with a lower RMSE and AIC than the power model (Table 3). Figure 3a showed negligible curvature and outliers while plotting the unstandardized residuals against the predicted height. The absence of curvature and outlier in the linear model suggests the absence of local bias. Thus, we selected the linear model (M1, Table 3) for predicting height from the diameter, though the difference of fit statistics between the linear model and power model was very small.

Table 3: Tested height models with equation and coefficients, their respective coefficient of determination R^2 , root mean square error (RMSE) and Akaike's Information Criterion (AIC) used diameter for juvenile *Shorea robusta*. H is tree height and D tree diameter 10 cm above ground.

Tabelle 3: Getestete Baumhöhen-Modelle, deren Gleichungen und Koeffizienten mit jeweiligen Bestimmtheitsmaß R^2 , RMSE und AIC unter Verwendung des Durchmessers von *Shorea robusta* Jungbäumen (H ist die Höhe und D der Stammdurchmesser).

	Model form	Equation	R^2	RMSE	AIC
M1	Linear	$H = 0.42 + 0.73 D$	0.80	0.53	178.95
M2	Logarithmic	$H = 1.49 + 1.17 \log D$	0.72	0.64	219.02
M3	Inverse	$H = 2.88 - \frac{0.91}{D}$	0.49	0.87	284.48
M4	Power	$H = 1.17 D^{0.75}$	0.80	0.54	182.13
M5	Sigmoidal	$H = \exp\left(1.51 - \frac{1.37}{D}\right)$	0.70	0.66	224.82
M6	Exponential	$H = 0.88 \exp(0.32 D)$	0.78	0.56	190.50

3.2 Model for biomass prediction

We employed similar criteria like height prediction model to select the best biomass prediction model. The parameter estimates of the quadratic model were non-significant ($p = 0.06$) at a 95% confidence interval and therefore excluded from further processing. The inverse and logarithmic models describe low variability in biomass of

juveniles (Table 4). Linear model overestimated the biomass for smaller juveniles and underestimated for larger juveniles (Figure 2b). The sigmoid model underestimated and exponential model overestimated the biomass for smaller juveniles (Figure 2b). The power model described higher variability in biomass of juveniles with minimum RMSE and AIC than other models (Table 4). Thus, power model was selected for predicting biomass of juveniles, though the difference in fit statistics among the power, sigmoid and exponential models was very small.

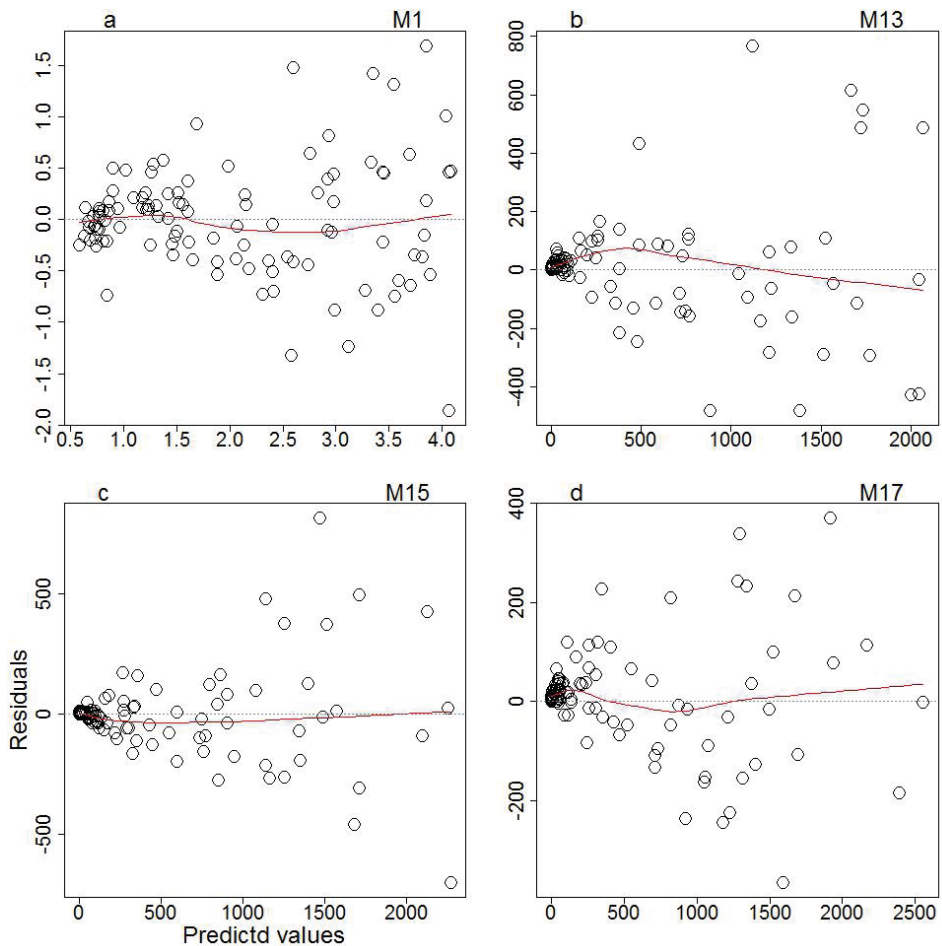


Figure 3: Distribution of residuals for four selected models for *Shorea robusta*, M1 predicts tree height, M13, M15 and M17 predicts aboveground biomass.

Abbildung 3: Verteilung der Residuen für vier ausgewählte Modelle für *Shorea robusta*, M1 prognostiziert die Baumhöhe, M13, M15 und M17 prognostizieren die oberirdische Biomasse.

Table 4: Tested biomass models with equation and coefficients, their respective coefficient of determination R^2 , root mean square error (RMSE) and Akaike's Information Criterion (AIC) used diameter for juvenile *Shorea robusta*. B is tree biomass and D tree diameter 10 cm above ground.

Tabelle 4: Getestete Biomasse-Modelle, deren Gleichungen und Koeffizienten mit jeweiligen Bestimmtheitsmaß R^2 , RMSE und AIC unter Verwendung des Durchmessers von *Shorea robusta* Jungbäumen (B ist die Biomasse und D der Stammdurchmesser).

	Model form	Equation	R^2	RMSE	AIC
M7	Linear	$B = -338.02 + 382.81 D$	0.77	305.81	1560.91
M8	Logarithmic	$B = 242.31 + 541.31 \log D$	0.54	434.91	1638.70
M9	Inverse	$B = 827.51 - \frac{364.75}{D}$	0.28	550.14	1688.93
M10	Power	$B = 26.89 D^{2.72}$	0.89	214.71	1483.81
M11	Sigmoidal	$B = \exp\left(9.70 - \frac{10.34}{D}\right)$	0.88	221.58	1490.68
M12	Exponential	$B = 50.53 \exp(0.76 D)$	0.88	222.70	1491.78

We also examined the power form of the model using a different combination of predictor variables to optimize the predictive capacity of the model (Table 5). The estimated parameters for five different categories of the power model were significant. In density-independent categories, the model with D^2H demonstrates the highest R^2 , lowest RMSE and AIC than others. On the other hand, the model with ρD^2H as predictor variable demonstrates the best fit (highest R^2 , lowest RMSE and AIC) in the group of density-dependent models (Table 5). The unstandardized residuals against the fitted values with a smooth superimposed curve for power model of biomass prediction (M13, M15 and M17) is presented in Figure 3b,c,d. Here we examined for evidence of curvature and outliers. The graph of power model (M13, M15 and M17) showed minimum error in M17 with negligible curvature and outliers. The absence of curvature in these models suggests the absence of local bias in the model. Overall, the model (M17) with the inclusion of wood density in the predictor variable (ρD^2H) best described the variations in biomass of juveniles of *Shorea robusta*. The curve of the model M15 and M17 overlaid on the observed data showed a good match to the data (Figure 2c, d).

Table 5: Variables and the estimated coefficients used for biomass models of juveniles of Shorea robusta in power form with their respective R^2 , RMSE and AIC (D is stem diameter, H height and ρ wood density).

Tabelle 5: Variablen und die geschätzten Parameter der Biomasse-Modelle von Jungbäumen der *Shorea robusta* der Potenzform mit jeweiligen R^2 , RMSE und AIC (D ist der Stammdurchmesser, H Höhe und ρ Holzdicke).

	Variables	a	b	R^2	RMSE	AIC	Rank
M13	D	26.89	2.72	0.89	214.71	1483.81	V
M14	DH	52.72	1.18	0.90	205.02	1473.75	IV
M15	D^2H	37.50	0.86	0.91	184.44	1450.69	III
M16	ρDH	119.84	1.21	0.92	176.59	1441.20	II
M17	ρD^2H	60.05	0.91	0.94	148.84	1403.94	I

3.3 Validation

By using the generated models for prediction of height (M1, Table 3) and biomass (M13, M15 and M17, Table 5), we executed prediction runs based on the validation dataset. The correlation coefficients between observed and predicted height was high ($r = 0.87$) (Figure 4a) and between observed and predicted biomass was very high ($r = 0.91$ to 0.97) (Figure 4b, c, d). The paired sample t-test showed that the observed and predicted values of height (Figure 4a) and biomass (Figure 4b, c, d) did not differ statistically ($p > 0.05$).

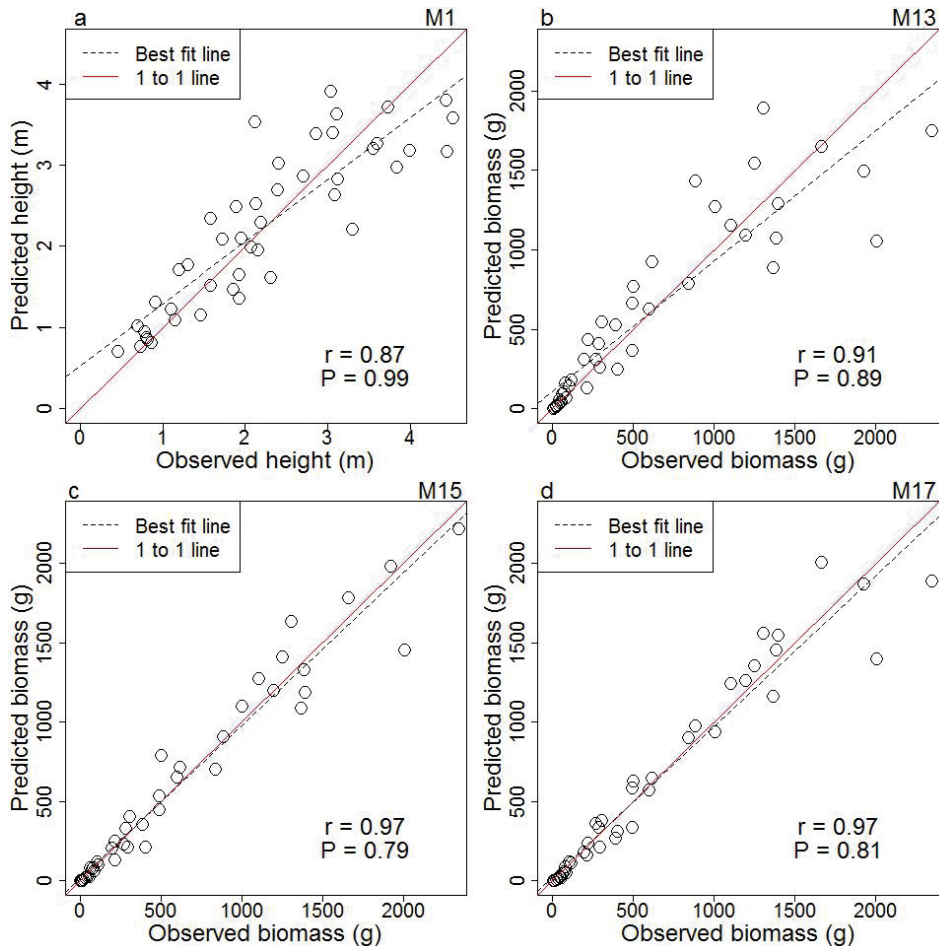


Figure 4: Relationships of observed and predicted values of four selected models of *Shorea robusta* (r = correlation coefficient and p = p -value); (a) model M1 predicts height from diameter; (b) model M13 aboveground biomass based on diameter only; (c) model M15 predicts biomass prediction model using product of diameter square and height; (d) model M17 predicts biomass prediction model from product of wood density, diameter squared and height.

Abbildung 4: Zusammenhang zwischen beobachteten und geschätzten Werten ausgewählter Modelle von *Shorea robusta* (r = Korrelationskoeffizient und p = p -Wert); (a) M1 Modell berechnet Höhen mit Durchmesser; (b) M13 Modell berechnet Biomasse ausschließlich mit Durchmesser; (c) M15 Modell berechnet Biomasse aus dem Produkt von Höhe und Durchmesser zum Quadrat; (d) M17 Modell berechnet Biomasse aus dem Produkt von Holzdicke, Höhe und Durchmesser zum Quadrat.

3.4 Comparison of validated models with previously developed biomass models

Juvenile biomass predicted by the model of this study (M13, M15 and M17) and the previous models of Sharma and Pukkala (1990), Tamrakar (2000), Chapagain et al. (2014) and Subedi (2017) showed a higher degree of positive correlation ($r = 0.97$ to 0.99). The predicted biomass by the model of this study (M13, M15 and M17) was significantly different ($p < 0.05$) with the predicted biomass of each of the previous models except one model of Chapagain et al. (2014) which is based on D ($p = 0.08$) (Equation 2).

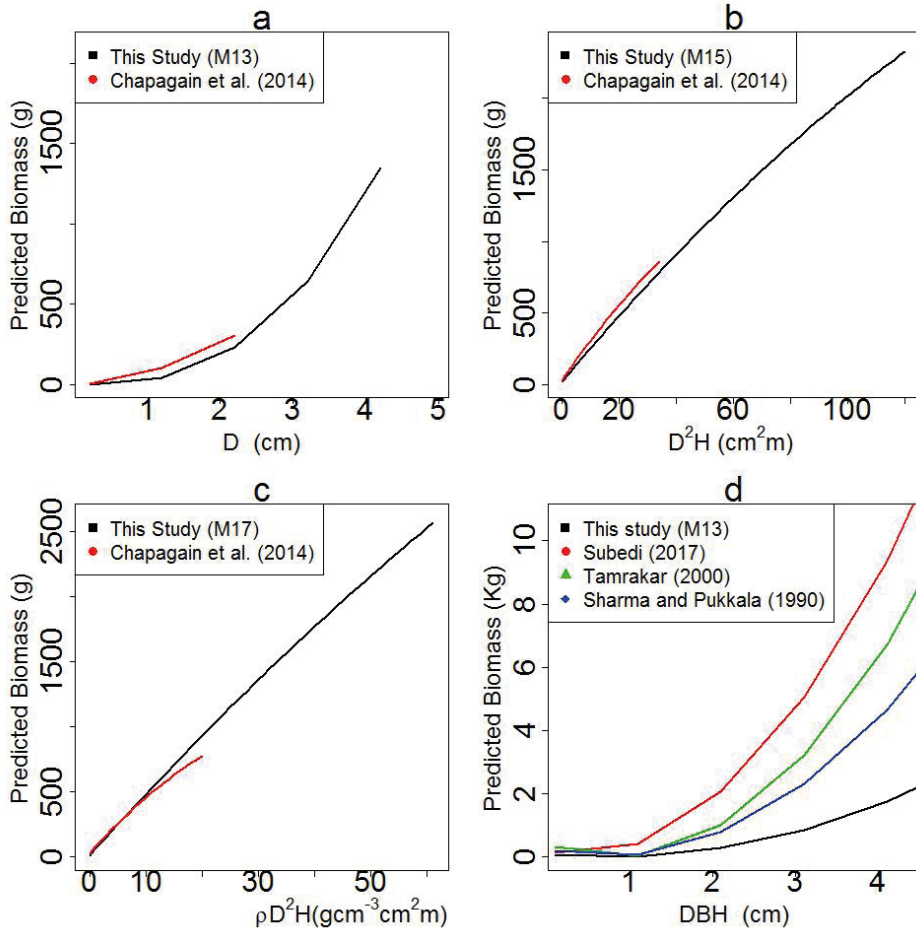


Figure 5: Comparison of the models introduced in this study with published models of *Shorea robusta* with different combinations of predictor variables (D , D^2H , ρD^2H , dbh) (a) biomass models based on diameter 10 cm above ground (D) only; (b) biomass models based on product of diameter squared and height only; (c) biomass models based on product of wood density, diameter squared and height; (d) biomass model based on diameter at breast height (dbh) (M13 has power form using the predicted dbh in cm and biomass in kg).

Abbildung 5: Vergleich unserer Modelle mit früheren Modellen der *Shorea robusta* mit verschiedenen Kombinationen von Prädiktorvariablen (D , D^2H , ρD^2H , dbh) (a) Biomasse-Modelle, die nur Durchmesser (D) verwenden; (b) Biomasse-Modelle, die auf dem Produkt von Höhe und Durchmesser zum Quadrat basieren; (c) Biomasse-Modelle, die auf dem Produkt von Holzdicke, Durchmesser zum Quadrat und Höhe basieren; (d) Biomasse-Modelle, die den Durchmesser in Brusthöhe (dbh) verwenden (Modell M13 ist die Potenzfunktion mit geschätztem dbh in cm und Biomasse in kg).

4. Discussion

This study showed the best performance of a liner model (M1) in diameter-height allometry. This result is inconsistent with the results of Sharma (2009) and Thapa et al. (2013), who reported a non-linear relationship in diameter-height allometry. As the growth in diameter and height is linear in nature during the juvenile stage of individual trees, the linear function may have explained a higher amount of variation in height. As the individual tree increases in age, the growth in height speed up until the individual trees reached the middle stage (Chaturvedi and Khanna, 2011), however, there will be less growth in diameter. As the individual trees reach the middle stage, the height growth tends to decrease and diameter growth tends to increase. The different rates of growth of individual tree at different stages of life introduced a non-linear relationship between diameter and height. The non-linear relationship of diameter-height allometry in large-sized individual trees has been well established (Deng et al., 2019; Ng'andwe et al., 2019; Subedi et al., 2018; Khadka et al., 2015).

Similar to studies (BK et al., 2019; Kebede and Soromessa, 2018; Sharma et al., 2017; Shrestha et al., 2018; Pastor et al., 1984), we found a simple power function as the best form of the model to predict the aboveground biomass of juvenile individual of *Shorea robusta*. Biomass of individual trees correlates non-linearly with individual tree variables, however, the form of non-linearity differs with species, stand density, site index, geographic regions and climate (Luo, 2020; Xing et al., 2019; Nam et al., 2016; Chave et al., 2014; Chapagain et al., 2014; Chave et al., 2005).

Biomass of individual trees is the sum of the biomass of stem, branches and foliage, however, a major portion of the biomass is contributed by stem of the individual trees (Ketterings et al., 2001). Therefore a number of biomass prediction models have found diameter as the best predictor variable (Pastor et al., 1984), which is not consistent with the result of this study. We found weakest performance while using diameter alone (M13) in the biomass prediction model (Table 5) compared to the models which uses diameter, height and wood density. As individual juveniles having the same stem diameter may vary in height, they may also vary in biomass. Therefore, the model with diameter and height as the predictor variables explained more variation in biomass. We observed this in our study as the model M14 and M15 performed better than model M13 which is consistent with many other studies (Xing et al., 2019; Kebede and Soromessa, 2018; Shrestha et al., 2018; Nam et al., 2016). As the individual juveniles having the same stem diameter and height may vary in wood density, they may also vary in biomass. Therefore, the model with diameter, height and wood density as the predictor variables explained more variation in biomass (Shrestha et al., 2018; Alvarez et al., 2012; Chaturvedi et al., 2012). This was also proved in our study as the model M16 and M17 performed better than model M13, M14 and M15. The model M17 performed best from the group of density-dependent models. The wood density does not improve the model always for example, Chapagain et al. (2014) found that the model with diameter and height better than the model with

diameter, height and wood density. We tested slenderness coefficient as predictor variable, however, it did not improve the model. Our models which were developed using ordinary least square regression showed a good fit to the data, however, there is still possibility of improving these models using mixed effect modelling approach. We could not use mixed effect modelling approach because the data were collected only at one time using individual juveniles selected purposively.

Model validation is one of the important step in the development of models as it increases the credibility and confidence about the predictive capacity of the models (Soares et al., 1995; Vanclay and Skovsgaard, 1997). A high ($r=0.87$) to very high ($r=0.97$) correlation coefficients between observed and predicted values suggested that our models are well validated (Figure 4). This validation was further supported by non-significant difference at a 95% confidence interval in paired sample t-test. It shows that the models selected in this study are capable to predict as accurately as field-measured biomass.

Biomass predicted by model of this study (M13) and Chapagain et al. (2014) using D as predictor variable (Equation 2) did not differ significantly, however, the biomass predicted by the model of this study (M15, M17) and Chapagain et al. (2014) using D^2H and ρD^2H as predictor variables (Equation 3, 4) differed significantly. The reason behind this difference may be the high variation in height and wood density of the juveniles that are growing in two different geographical areas thus, differences in the stand density, site quality, topography and climate. The average and range values of height and wood density of juveniles used in this study was higher than those used in Chapagain et al. (2014). The differences in predicted biomass was small for smaller juveniles, however, difference increased with an increase in values of predictor variable (Figure 5b, c).

As expected, the predicted biomass by our model (M13) and predicted biomass by previous models of Sharma and Pukkala (1990), Tamrakar (2000) and Subedi (2017) showed a significant difference ($p<0.05$) (Figure 5d). Two reasons may explain these differences. The first reason may be the differences in the size of the trees used in the model development. Our study used juvenile individuals of *Shorea robusta* ($D = 0.20$ cm to 4.96 cm) while Sharma and Pukkala used larger sized individuals of *Shorea robusta* ($dbh = 12.70$ cm to 144.50 cm). The dbh of *Shorea robusta* trees used in the model of Subedi (2017) ranged between 30.10 cm to 108.50 cm. The second reason may be the extent of area covered during sample data collection. The data for Sharma and Pukkala (1990) was collected from the whole range of distribution of *Shorea robusta* whereas the data for Subedi (2017) was collected from two districts (Kailali and Kanchanpur) of far western Nepal. The data for the present study was collected from the one community forest of Chitwan district of central Nepal.

As the altitudinal, climatic and species variation is very high in Nepalese forest, a universal model for all size, site and species is not suitable. The model developed from

the data of large sized individual may not predict the biomass of small sized individual and the model developed from one site of the country may not be suitable in another site. Therefore, new models that are size specific, site specific and species specific are required for accurate prediction of individual tree biomass.

Data collected using destructive sampling method were used to develop the models and the number of juvenile individuals used ($n=155$) in this study was larger than those used in other studies (BK et al., 2019; Shrestha et al., 2018; Subedi and Sharma, 2012; Sharma, 2011) which ranged from 27 to 66 individuals. Data from smaller number of sampled trees have also performed good results in biomass model development if they have been collected from destructively sampled trees representing potential sources of variation. The large-sized individual showed relatively high residuals, however, the overall distribution of residual was random (Figure 3). Similar trend of residuals have also been observed by Bk et al. (2019). The absence of systematic trend or bias in the residuals also confirms the higher degree of precision in our models. The precision of the model have also been proved from the validation of the models (Figure 4). The models developed in this study are applicable to a variety of predictor variables. For example, the biomass model is applicable if only the diameter is available, or diameter and height is available or diameter, height and wood density is available. The models with wood density provide higher precision, however, require more resources and time to determine wood density.

The direct application of the models developed in this study is to predict and estimate the height and biomass of juvenile individual of *Shorea robusta*. These models may help to minimize the lack of biomass models for the juvenile stage which has caused a substantial underestimation of the total biomass and carbon in forests. The models may contribute to adding the economic value of carbon trading from juvenile individuals. Prediction and estimation of biomass of juvenile individuals are used in quantification of forest fuels, assessing the potential of young stands as a fibre source and indicating net primary production (Wagner and Ter-Mikaelian, 1999). The juvenile individual biomass may be used as a response variable in evaluating the impact of neighbourhood competition (Ter-Mikaelian and Parker, 2000). In addition to these applications, juvenile individuals play an important role in balancing forest ecosystems.

5. Conclusions

Among several forms of the model tested, a linear form for height prediction and power form for biomass prediction performed better than other forms of the model. Different combinations of predictor variables further improved the biomass model. Product of square of diameter and height ($R^2 = 0.91$) for density-independent and product of wood density, square of diameter and height ($R^2 = 0.94$) for density-dependent model showed the strongest fit statistics and smaller variations of the residuals. The developed models were well validated as the correlation coefficients between

observed and predicted values ranged from high (0.87) to very high (0.97) and the difference between observed and predicted values was non-significant. As the predicted biomass by the models of this study differed significantly with the predicted biomass by the previously developed models of *Shorea robusta*, site and size specific models are required for accurate prediction of biomass of *Shorea robusta*. Future research is recommended from a wider geographical area including the variables that describes site quality, stand density, growth stage, climate and species distribution to make the model more applicable in wider areas.

Funding

This study was funded by Nepal Academy of Science and Technology.

Conflict of Interest

The authors declare that they have no conflict of interest.

Author contribution

The first author designed a research concept, carried out data collection, developed models and drafted the manuscript. The second author played a coordinating role in model development, manuscript writing and edited the manuscript thoroughly.

Acknowledgements

The authors express their gratitude to the user of the Kankali CF. The authors also thank to field research crew members: Prakash Adhikari and Makkhan Gurung. The authors also thank the Institute of Forestry, Pokhara Campus Pokhara, for allowing to use its laboratory. The authors are thankful to two anonymous reviewers for their constructive comments and suggestions.

6. References

- Addo-Danso, S.D., Prescott, C.E., Smith, A.R. 2016. Methods for estimating root biomass and production in forest and woodland ecosystem carbon studies: A review. *Forest Ecology and Management* 359:332-351.
- Adinugroho, W.C.D., Sidiyasa, K. 2006. Biomass estimation model of above-ground mahogany (*Swietenia macrophylla*) tree. *Jurnal Penelitian Hutan dan Konservasi Alam* 3(1):103-117.
- Akaike, H. 1972. A new look at statistical model identification. *IEEE Trans Automatic Control* Ac-19(6):716-723.
- Altanzagas, B., Luo, Y., Altansukh, B., Dorjsuren, C., Fang, J., Hu, H. 2019. Allometric

- equations for estimating the above-ground biomass of five forest tree species in Khangai, Mongolia. *Forests* 10(8). doi:10.3390/f10080661.
- Alvarez, E., Duque, A., Saldarriaga, J., Cabrera, K., de las Salas, G., del Valle, I., Lema, A., Moreno, F., Orrego, S., Rodríguez, L. 2012. Tree aboveground biomass allometries for carbon stocks estimation in the natural forests of Colombia. *Forest Ecology and Management* 267:297-308. <https://doi.org/10.1016/j.foreco.2011.12.013>.
- Aryal, K., Laudary, H.K., Ojha, H.R. 2019. To what extent is Nepal's community forestry contributing to the sustainable development goals? an institutional interaction perspective. *International Journal of Sustainable Development and World Ecology*. 27:28-39, DOI:10.1080/13504509.2019.1627681.
- Berndes, G., Abt, B., Asikainen, A., Cowie, A., Dale, V., Egnell, G., Lindner, M., Marelli, L., Paré, D., Pingoud, K., Yeh, S. 2016. Forest biomass, carbon neutrality and climate change mitigation. *European Forest Institute*, p 29.
- Bhattarai, K., Convey, D. 2008. Evaluating land use dynamics and forest cover change in Nepal's Bara district (1973-2003). *Human Ecology* 36:81-95.
- BK, R.B., Sharma, R.P., Bhandari, S.K. 2019. A generalized aboveground biomass model for juvenile individuals of *Rhododendron arboreum* (SM.) in Nepal. *CERNE* 25(2):19-130.
- Blujdea, V.N.B., Pilli, R., Dutca, I., Ciuvat, L., Abrudan, I.V. 2012. Allometric biomass equations for young broadleaved trees in plantations in Romania. *Forest Ecology and Management* 264:172-184.
- Brown, S., Gillespie, A.J.R., Lugo, A.E. 1989. Biomass estimation for tropical forests with applications to forest inventory data. *Forest Science* 35(4):881-902.
- Burnham, K.P., Anderson, D.R. 2002. *Model selection and inference: a practical information-theoretic approach*. Springer-Verlag, New York, USA.
- Chapagain, T., Sharma, R.P., Bhandari, S.K. 2014. Modelling above-ground biomass for three tropical tree species at their juvenile stage. *Forest Science and Technology* 10(2):51-60.
- Chaturvedi, A.N., Khanna, L.S. 2011. *Forest mensuration and biometry*. Khanna Bandhu, Dehradun.
- Chaturvedi, R.K., Raghubanshi, A.S., Singh, J.S. 2012. Biomass estimation of dry tropical woody species at juvenile stage. *The Scientific World Journal*, doi:10.1100/2012/790219.
- Chave, J., Andalo, C., Brown, S., Cairns, M.A., Chambers, J.Q., Eamus, D., Folster, H., Fromard, F., Higuchi, N., Kira, T., Lescure, J-P, Nelson, B.W., Ogawa, H., Puig, H., Riera, B., Yamakura, T. 2005. Tree allometry and improved estimation of carbon stocks and balance in tropical forests. *Oecologia* 145(1):87-99.
- Chave, J., Réjou-Méchain, M., Búrquez, A., Chidumayo, E., Colgan, M.S., Delitti, W.B.C., Duque, A., Eid, T., Fearnside, P.M., Goodman, R.C., Henry, M., Martínez-Yrizar, A., Mugasha, W.A., Muller-Landau, H.C., Mencuccini, M., Nelson, B.W., Ngomanda, A., Nogueira, E.M., Ortiz-Malavassi, E., Péliissier, R., Ploton, P., Ryan, C.M., Saldarriaga, J.G., Vieilledent, G. 2014. Improved allometric models to estimate the above-ground biomass of tropical trees. *Global Change Biology* 20:3177-3190. doi:10.1111/gcb.12629.
- Chen, S., Komiyama, A., Kato, S., Cao, R., Yoshitake, S., Ohtsuka, T. 2017. Stand dynamics

- and biomass increment in a lucidophyllous forest over a 28-year period in central Japan. *Forests* 8. doi:10.3390/f8100397.
- Chhetri, B.B.K., Lund, J.F., Nielsen, Ø.J. 2012. The public finance potential of community forestry in Nepal. *Ecological Economics* 73(1):113-121.
- Chitale, V.S., Behera, M.D. 2012. Can the distribution of sal (*Shorea robusta* Gaertn. f.) shift in the north-eastern direction in India due to changing climate? *Current Science* 102(8):1126-1135.
- Chung-Wang, X., Ceulemans, R. 2004. Allometric relationships for below-and above-ground biomass of young Scot pines. *Forest Ecology and Management* 203:177-186.
- Clough, B.F., Dixon, P., Dalhaus, O. 1997. Allometric relationships for estimating biomass in multi-stemmed mangrove trees. *Australian Journal of Botany* 45:1023-1031.
- Daba, D.E., Soromessa, T. 2019. Allometric equations for aboveground biomass estimation of *Diospyros abyssinica* (Hiern) F. white tree species. *Ecosystem Health and Sustainability* 5(1):86-97. doi:10.1080/20964129.2019.1591169.
- De Gier, A. 2003. A new approach to woody biomass assessment in woodlands and shrublands. In: ROY PS (eds.) *Geoinformatics for Tropical Ecosystems*. Asia Association of Remote Sensing, Dehradun, India, Pp 161-198.
- Deng, C., Zhang, S., Lu, Y., Froese, R.E., Ming, A., Li, Q. 2019. Thinning effects on tree height diameter allometry of masson pine (*Pinus massoniana* Lamb.). *Forests* doi:10.3390/f10121129.
- Devi, L.S., Yadava, P.S. 2009. Above-ground biomass and net primary production of semi-evergreen tropical forest of Manipur, North-Eastern India. *Journal of Forestry Research* 20:151-155.
- DFO Chitwan. 2017. Annual progress report of Chitwan district. District forest office, Chitwan Nepal.
- DFRS. 1999. Forest Resources of Nepal. Department of Forest Research and Survey, Ministry of Forest and Soil Conservation, HMG/ FINIDA, Report, Kathmandu, Nepal, p 33.
- DFRS. 2015. State of Nepal's Forest. Forest Resource Assessment (FRA) Nepal, Department of Forest Research and Survey (DFRS), Kathmandu, Nepal, p 73.
- DOF. 2017. Community forestry database. Community forestry division, Department of Forest (DoF), Ministry of forest and soil conservation, Government of Nepal, Kathmanu, Nepal.
- Dorado, F.C., Dieguez-Aranda, U., Anta, M.B., Rodriguez, M.S., von Gadow, K. 2006. A generalized height-diameter model including random components for radiata pine plantations in north-western Spain. *Forest Ecology and Management* 229(1-3):202-213.
- Edwards, Jr. T.C., Cutler, D.R., Zimmermann, N.E., Geiser, L., Moisen, G.G. 2006. Effects of sample survey design on the accuracy of classification tree models in species distribution models. *Ecological Modelling* 199(2):132-141.
- Francis JK. 2000. Estimating biomass and carbon content of saplings in Puerto Rican secondary forests. *Caribbean Journal of Science* 36(3-4):346-350.
- Gautam, K.H., Devoe, N.N.. 2006. Ecological and anthropogenic niches of sal (*Shorea*

- robusta* Gaertn. f.) forest and prospects for multiple-product forest management-a review. *Forestry: An International Journal of Forest Research* 79(1):81-101. <https://doi.org/10.1093/forestry/cpi063>.
- Huang, S., Titus, S.J., Wiens, D.P. 1992. Comparison of nonlinear height-diameter functions for major Alberta tree species. *Canadian Journal of Forest Research* 22:1297-1304.
- Huy, B., Paudel, K.P., Kralicek, K., Hung, N.D., Khoa, P.V., Phuong, V.T., Temesgen, H. 2016. Allometric equations for estimating tree aboveground biomass in tropical dipterocarp forests of Vietnam. *Forest* 7(8). <https://doi:10.3390/f7080180>.
- Jackson, J.K. 1994. *Manual of afforestation in Nepal*. Forest research and survey centre, Kathmandu, Nepal. P 824.
- Joshi, K. 2003. Leaf flavonoid patterns and ethnobotany of *Shorea robusta* Gaertn. (Dipterocarpaceae). *Proceedings of International Conference on Women, Science & Technology for Poverty Alleviation* (Pp. 101-107). WIST, Kathmandu, Nepal.
- Kebede, B., Soromessa, T. 2018. Allometric equations for aboveground biomass estimation of *Olea europaea* L. subsp. *cuspidata* in Mana Angetu Forest. *Ecosystem Health and Sustainability* 4(1):1-12.
- Ketterings, Q.M., Coe, R., van Noordwijk, M., Ambagau, Y., Palm, C.A. 2001. Reducing uncertainty in the use of allometric biomass equations for predicting above-ground tree biomass in mixed secondary forests. *Forest Ecology and Management* 146(1-3):199-209.
- Khadka, A., Subedi, T., Ghimire, M., Dhakal, B.P., Parikka, H. 2015. Diameter-height models for the Terai tree species. *Banko Jankari* 25(1):50-54.
- Kibria, S. S., Nahar, T.N., Mia, M.N. 1994. Tree leaves as alternative feed resource for Black Bengal goats under stall-fed conditions. *Small Ruminant Research* 13:217-222.
- Kilpelainen, A., Torssonen, P., Strandman, H., Kellomaki, S., Asikainen, A., Peltola, H. 2014. Net climate impacts of forest biomass production and utilization in managed boreal forests. *Global Change Biology Bioenergy* 8:307-316.
- Klingenberg, C.P. 2016. Size, shape, and form: concepts of allometry in geometric morphometrics. *Development genes and evolutions* 226:113-137. doi: 10.1007/s00427-016-0539-2.
- Kora, A.J. 2019. Leaves as dining plates, food wraps and food packing material: importance of renewable resources in Indian culture. *Bulletin of the National Research Centre* 43. <https://doi.org/10.1186/s42269-019-0231-6>.
- Land Resources Mapping Project. 1986. *Agriculture/ Forestry Report, Land Resources Mapping Project (LRMP)*. His Majesty Government of Nepal, Kathmandu, Nepal.
- Luintel, H., Bluffstone, R.A., Scheller, R.M. 2018. The effects of the Nepal community forestry program on biodiversity conservation and carbon storage. *PLoS ONE*. 13(6): e0199526. <https://doi.org/10.1371/journal.pone.0199526>.
- Luo, Y., Wang, X., Ouyang, Z., Lu, F., Feng, L., Tao, J. 2020. A review of biomass equations for China's tree species. *Earth System Science Data* 12:21-40.
- Montès, N., Gauquelin, T., Badri, W., Bertaudiere, V., Zaoui, E.H. 2000. A non-destructive method for estimating above-ground forest biomass in threatened woodlands. *Forest Ecology and Management* 130:37-46.

- Montgomery, D.C., Peck, E.A., Vining, G.G. 2001. Introduction to linear regression analysis. Wiley, New York, USA. P 641.
- Mukaka, M.M. 2012. Statistics corner: A guide to appropriate use of correlation coefficient in medical research. *Malawi Medical Journal* 24(3):69-71.
- Nam, V.T., Kuijk, M.V., Anten, N.P.R. 2016. Allometric equations for aboveground and belowground biomass estimations in an evergreen forest in Vietnam. *PLoS ONE* 11(6). e0156827. doi:10.1371/journal.pone.0156827.
- Navar, J. 2009. Allometric equations for tree species and carbon stocks for forests of north-western Mexico. *Forest Ecology and Management* 257(2):427-434.
- Ng'andwe, P., Chungu, D., Yambayamba, A.M., Chilambwe, A. 2019. Modelling the height-diameter relationship of planted *Pinus kesiya* in Zambia. *Forest Ecology and Management* 447:1-11.
- Nonini, L., Fiala, M. 2019. Estimation of carbon storage of forest biomass for voluntary carbon markets: preliminary results. *Journal of Forestry Research*. <https://doi.org/10.1007/s11676-019-01074-w>.
- Nuberg, I.K., Shrestha, K.K., Bartlett, A.G. 2019. Pathways to forest wealth in Nepal. *Australian Forestry* 82:106-120.
- Ong, J.E., Gong, W.K., Wong, C.H. 2004. Allometry and partitioning of the mangrove, *Rhizophora apiculata*. *Forest Ecology and Management* 188:395-408.
- Operational Plan. 2019. Operational plan of Kankali community forest. Kankali Community Forest, Chitwan, Nepal, p 72.
- Pastor, J., Aber, J.D., Melillo, J.M. 1984. Biomass prediction using generalized allometric regression for some northeast tree species. *Forest Ecology and Management* 7:265-274.
- Paudel, S., Sah, J.P. 2015. Effects of different management practices on stand composition and species diversity in subtropical forests in Nepal: implications of community participation in biodiversity conservation. *Journal of Sustainable Forestry* 34:738-760.
- Paul, K.I., Roxburgh, S.H., England, J.R., Ritson, P., Hobbs, T., Brooksbank, K., Raison, J., Larmour, J.S., Murphy, S., Norris, J., Neumann, C., Lewis, T., Jonson, J., Carter, J.L., McArthur, G., Barton, C. 2013. Development and testing of allometric equations for estimating above-ground biomass of mixed-species environmental plantings *Forest Ecology and Management* 310:483-494.
- Ravindranath, N.H., Ostwald, M. 2008. Methods for estimating above-ground biomass. In: Ravindranath NH, Ostwald M (eds) *Carbon inventory methods: handbook for greenhouse gas inventory, carbon mitigation and round wood production projects*. Springer, Dordrecht, Netherlands, Pp 113-114.
- R Core Team. 2017. R: A Language and Environment for Statistical Computing.
- Sah, S.P. 2000. Management options for sal forests (*Shorea robusta* Gaertn.) in the Nepal Terai. *Selbyana* 21:112-117.
- Saito-Jensen, M., Rutt, R.L., Chhetri, B.B.K. 2014. Social and environmental tensions-affirmative measures under REDD+ carbon payment initiative. *Human Ecology* 42(5):683-694.
- Segura, M., Kanninen, M. 2005. Allometric models for tree volume and total aboveg-

- round biomass in a tropical humid forest in Costa Rica. *Biotropica* 37(1):2-8.
- Sharma, E.R., Pukkala, T. 1990. Volume and biomass prediction equations of forest trees of Nepal. Forest survey and statistical division, Ministry of forest and soil conservation, Kathmandu, Nepal.
- Sharma, R.P. 2009. Modelling height diameter relationship for Chir pine trees. *Banko Jankari* 19(2):3-9.
- Sharma, R.P. 2011. Allometric models for total-tree and component-tree biomass of *Alnus nepalensis* D. Don in Nepal. *Indian Forester* 137(12):1386-1390.
- Sharma, R.P., Bhandari, S.K., BK, R.B. 2017. Allometric bark biomass model for *Daphne bholua* in mid-hill of Nepal. *Mountain Research and Development* 37(2):206-215.
- Shrestha, D.B., Sharma, R.P., Bhandari, S.K. 2018. Individual tree aboveground biomass for *Castanopsis indica* in the mid-hills of Nepal. *Agroforestry Systems* 92(6):1611-1623. doi: 10.1007/s10457-017-0109-2.
- Soares, P., Tome, M., Skovsgaard, J.P., Vanclay, J.K. 1995. Evaluating a growth model for forest management using continuous forest inventory data. *Forest Ecology and Management* 71(3):251-265.
- Stainton, J.D.A. 1972. Forests of Nepal. John Murray, London, P 181.
- Subedi, M.R., Oli, B.N., Shrestha, S., Chhin, S. 2018. Height-diameter modelling of *Cinnamomum tamala* grown in natural forest in Mid-Hill of Nepal. *International Journal of Forest Research*. <https://doi.org/10.1155/2018/6583948>.
- Subedi, M.R., Sharma, R.P. 2012. Allometric biomass models for bark of *Cinnamomum tamala* in mid-hill of Nepal. *Biomass and Bioenergy* 47:44-49.
- Subedi, T. 2017. Volume models for Sal (*Shorea robusta* Gaertn.) in far-western Terai of Nepal. *Banko Jankari* 27(2):3-11.
- Tamrakar, P.R. 2000. Biomass and volume tables with species description for community forest management. MoFSC, NARMSAP-TISC, Kathmandu.
- Ter-Mikaelian, M.T., Parker, W.C. 2000. Estimating biomass of white spruce seedlings with vertical photo imagery. *New Forests* 20(2):145-162.
- Thapa, T.B., Upadhyaya, C.P., Timilsina, Y.P., Bhandari, S.K., Puri, L. 2013. Predicting total height from diameter using nonlinear models in *Pinus roxburghii*. *Nepal Journal of Science and Technology* 14(1):147-152.
- Vanclay, J.K., Skovsgaard, J.P. 1997. Evaluating forest growth models. *Ecological Modelling* 98(1):1-12.
- Wagner, R.G., Ter-Mikaelian, M.T. 1999. Comparison of biomass component equations for four species of northern coniferous tree seedlings. *Annals of Forest Science* 56(3):193-199.
- Xing, D., Bergerib, J.A.C., Solarik, K.A., Tomm, B., Macdonald, S.E., Spence, J.R., He, F. 2019. Challenges in estimating forest biomass: use of allometric equations for three boreal tree species. *Canadian Journal of Forest Research* 49:1613-1622.
- Zhao, H., Li, Z., Zhou, G., Qiu, Z., Wu, Z. 2019. Site-Specific Allometric Models for prediction of above and belowground biomass of subtropical forests in Guangzhou, Southern China. *Forests* 10, 862. doi:10.3390/f10100862.

Guidelines for publication

1. Only original, unpublished work is accepted.
2. Manuscripts must be written double-spaced, one sided and ready for printing. For literature quotations, use the name of the author and year (in parentheses) in the text, and arrange the list at the end of the work alphabetically.
3. Original contributions should be arranged as follows: 1) Title of the manuscript in German and English; 2) by: Given names and surname of the author(s); 3) Key words: 3-6 terms; 4) Summary (English and German - Zusammenfassung); text of the article, literature, address of the author (the authors). 5) An explanatory capture text in English and German should be given for all tables and Figures.
4. All figures must be provided in electronic form and as a printed copy (photos on good paper) using a separate sheet. The text for the Figures must be on a separate sheet, and sequentially numbered.
5. After the review process, and the final approval by the editor in chief the author(s) receives galley proofs for final minor corrections. Only setting (typing) errors can be corrected at this stage.
6. Each author of an original article receives 20 off prints free of charge. Further copies can be ordered at the author(s) expense.

Richtlinien zur Veröffentlichung

1. Es werden nur Originalarbeiten angenommen.
2. Die Manuskripte müssen druckreif zweizeilig geschrieben sein; jedes Blatt nur einseitig beschreiben! Literaturzitate sind im Text mit dem Namen des Autors und in Klammern beigefügter Jahreszahl anzuführen und am Ende der Arbeit alphabetisch geordnet zusammenzustellen.
3. Die Gliederung der Originalbeiträge ist wie folgt zu gestalten: 1) Titel der Arbeit in Deutsch und Englisch; 2) von: Vor- und Zuname des Autors (der Autoren) Oxfordklassifikation; 3) Schlagwörter: 3-6 Begriffe, Key words: 3-6; 4) Zusammenfassung, Summary, Text, Literatur, Anschrift des Verfasser (der Verfasser). 5) Den Tabellen, Übersichten und Abbildungen ist ein erklärender Text in deutscher und in englischer Sprache beizufügen.
4. Die Vorlagen für die Abbildungen sind in reproduktionsfähigem Zustand (Fotos auf Hochglanzpapier) auf besonderen Blättern einzusenden, ebenso sind die Erklärungen der Abbildungen auf einem getrennten Blatt, fortlaufend nummeriert, beizuschließen.
5. Von den Arbeiten erhält der Autor Korrekturabzüge. In den Korrekturbogen dürfen nur mehr Satzfehler berichtigt werden.
6. Jeder Autor einer Originalarbeit erhält kostenlos 20 Sonderdrucke. Darüber hinaus benötigte Sonderdrucke müssen bei der Rücksendung der Korrekturabzüge bestellt werden. Die Kosten hierfür sind vorher beim Verlag zu erfragen.

Please send your manuscript (3 copies) to:

Manuskriptsendungen in dreifacher Ausführung sind erbeten an:

Univ.-Prof. Dr. Hubert Hasenauer

Centralblatt für das gesamte Forstwesen

Institut für Waldbau,

Peter-Jordan-Straße 82,

A-1190 Wien.

